

INTERRELATIONSHIPS BETWEEN INTRANARIAL PRESSURE AND
BIOSONAR CLICKS IN BOTTLENOSE DOLPHINS (*Tursiops truncatus*)

A Dissertation

by

WESLEY ROYCE ELSBERRY

Submitted to the Office of Graduate Studies of
Texas A&M University
in partial fulfillment of the requirements for the degree of

DOCTOR OF PHILOSOPHY

August 2003

Major Subject: Wildlife and Fisheries Sciences

INTERRELATIONSHIPS BETWEEN INTRANARIAL PRESSURE AND
BIOSONAR CLICKS IN BOTTLENOSE DOLPHINS (*Tursiops truncatus*)

A Dissertation

by

WESLEY ROYCE ELSBERRY

Submitted to Texas A&M University
in partial fulfillment of the requirements
for the degree of

DOCTOR OF PHILOSOPHY

Approved as to style and content by:

William E. Evans
(Chair of Committee)

Sam H. Ridgway
(Member)

William H. Neill
(Member)

Randall W. Davis
(Member)

Daniel S. Levine
(Member)

Ted W. Cranford
(Member)

Robert D. Brown
(Head of Department)

August 2003

Major Subject: Wildlife and Fisheries Sciences

ABSTRACT

Interrelationships Between Intranarial Pressure and
Biosonar Clicks in Bottlenose Dolphins (*Tursiops truncatus*). (August 2003)

Wesley Royce Elsberry, B.S., University of Florida;

M.S.C.S., University of Texas at Arlington

Chair of Advisory Committee: Dr. William E. Evans

Recent advances in technology permitted the first simultaneous digital recording of intranarial pressure and on-axis acoustic data from bottlenose dolphins during a biosonar target recognition task. Analysis of pressurization events in the intranarial space quantifies and supports earlier work, confirming that intranarial pressure is increased when whistle vocalizations are emitted. The results show complex relationships between various properties of the biosonar click to the intranarial pressure difference at the time it was generated. The intranarial pressure that drives the production of clicks is not the primary determinant of many of the acoustic properties of those clicks. A simple piston-cylinder physical model coupled with a sound production model of clicks produced at the monkey-lips/dorsal bursae complex yields an estimate of mechanical work for individual pressurization events. Individual pressurization events are typically associated with a single click train. Mechanical work for an average pressurization event is estimated at 10 Joules.

ACKNOWLEDGMENTS

I acknowledge the aid and assistance of many colleagues in the performance of the researches reported here and also in the production of this manuscript. Ted Cranford provided the opportunity for data collection involving both acoustic and physiological measures, and generously provided much assistance in discussion and review of the contents of this work. The actual data collection occurred under the sponsorship of the Office of Naval Research. Robert Gisiner provided funding to Ted Cranford for the project (ONR awards N66001-00-M-0497 & N00014-01-1-0683). Sam Ridgway, Don Carder, and William Van Bonn provided dolphins and expertise from the U. S. Navy Marine Mammal Program. The dolphins were trained for catheter acceptance and echolocation tasks by Tricia Kamolnick and Jennifer Carr. A number of people performed necessary tasks during the data collection phase, including Ted Cranford, Diane J. Blackwood, and Devon Bozliniski. Mark Todd provided video support and computer consultation during the data collection. Further assistance during the data reduction and analysis phase was provided by Ted Cranford, Devon Bozliniski, and Emily Decker. Jeanette Ridgway proofread the manuscript and provided suggestions on style.

I am indebted to John Heyning, and Dave Janiger of the Los Angeles County Museum of Natural History, who graciously provided access to prepared specimens for morphologic measurements necessary to my analysis.

I owe a debt of gratitude to the various organizations that have helped support my graduate studies and research with financial aid. These include the Regents of Texas A&M University, the Texas Institute of Oceanography, and the Texas Board of Higher Education for scholarships and research fellowships. The Department of Marine Sciences at Texas A&M University at Galveston provided me with a teaching

assistantship. Without their support throughout my time at Texas A&M University, this research would not have been possible.

Throughout my graduate studies at Texas A&M, William E. Evans has provided encouragement, support, and advice.

I also owe a debt to all my committee members, who have given their time and energy in providing valuable advice and commentary.

TABLE OF CONTENTS

CHAPTER		Page
I	INTRODUCTION	1
	A. Relevant anatomy	2
	B. An overview of dolphin biosonar research	5
II	MEASURING INTRANARIAL PRESSURE DURING BIOSONAR	12
	A. Introduction	12
	B. Methods	15
	1. Biosonar task training	16
	2. Data acquisition software	18
	3. Calibration of equipment	19
	C. Results	25
	D. Discussion	39
	E. Conclusion	44
III	DIGITAL SIGNAL PROCESSING FOR ODONTOCETE BIOSONAR	45
	A. Introduction	45
	B. Sampling	45
	C. Analysis	48
	1. Time-domain characteristics of clicks	49
	2. Frequency domain characteristics of clicks	51
	D. Conclusion	56
IV	BIOSONAR CLICK CHARACTERISTICS	57
	A. Introduction	57
	1. Ensonds in bottlenose dolphins	57
	2. Determination of the duration of a click	58
	B. Methods	63
	1. Automated classification of clicks	67
	C. Results	67
	1. Time-domain characteristics	68
	2. Frequency-domain characteristics	84
	3. Intranarial pressure treated as an independent variable	93

CHAPTER	Page
4. Click duration treated as an independent variable . . .	105
5. Radiated acoustic power treated as an independent variable	123
6. Classification of clicks	138
D. Discussion	138
1. Click duration	140
2. Peak-to-peak amplitude	141
3. Bimodality	142
4. Classification	144
5. Interrelationships with intranarial pressure	149
E. Conclusion	151
 V	
BIOENERGETICS OF INDIVIDUAL BIOSONAR CLICK TRAINS	153
A. Introduction	153
1. Overview of research on dolphin sound production . .	156
2. Experimental work involving pressure measurements .	158
3. Metabolic estimation of biosonar cost	159
4. Necessity of pressure data to produce estimates	160
B. Methods	161
1. Calculations of work and power based on model	162
C. Results	164
1. Computed tomography	165
D. Discussion	168
1. Physics of click production and energy	168
2. Time scales	170
3. Work and depth	171
4. Model-based estimation relies upon assumptions of model	172
5. Clicks and whistles in context	173
E. Conclusion	174
 VI	
CONCLUSION	176
A. Measurement of intranarial pressure and biosonar signals .	176
B. Biosonar click characteristics	176
C. Bioenergetics of individual pressurization events	178
 REFERENCES	179
 VITA	188

LIST OF TABLES

TABLE		Page
I	Physical characteristics of subjects.	16
II	Biosonar target recognition response matrix by subject and stimulus.	18
III	Observed and expected frequencies of target and response for BRT.	28
IV	Cell chi squares for target and response for BRT.	29
V	Observed and expected frequencies of target and response for BUS.	29
VI	Cell chi squares for target and response for BUS.	30
VII	Observed and expected frequencies of target and response for SAY.	31
VIII	Cell chi squares for target and response for SAY.	31
IX	Descriptive statistics for complete pressurization events.	32
X	Descriptive statistics of peak-to-peak source amplitudes (in dB re 1 μ Pascal).	69
XI	Descriptive statistics for click duration (in μ s).	72
XII	Descriptive statistics for energy flux density (dB re 1 μ Pa ² s).	75
XIII	Descriptive statistics for radiated acoustic power (dB re 1 watt).	78
XIV	Descriptive statistics for intranarial pressure difference (kPa).	81
XV	Descriptive statistics for peak frequency (kHz).	84
XVI	Descriptive statistics for dominant frequency (kHz).	87
XVII	Descriptive statistics for -3 dB bandwidth.	90
XVIII	Linear regression results for radiated acoustic power (dB re 1 watt) vs. intranarial pressure difference (kPa).	93

TABLE	Page
XIX	Linear regression results for peak frequency (kHz) vs. intranarial pressure difference (kPa). 96
XX	Linear regression results for dominant frequency (kHz) vs. intranarial pressure difference (kPa). 99
XXI	Linear regression results for -3 dB bandwidth (kHz) vs. intranarial pressure difference (kPa). 102
XXII	Linear regression results for peak-to-peak source level (dB re 1 μ Pa) vs. click duration (μ s). 105
XXIII	Second order polynomial regression results for peak-to-peak source level (dB re 1 μ Pa) vs. click duration (μ s). 105
XXIV	Linear regression results for energy flux density (dB re 1 μ Pa ² s) vs. click duration (μ s). 108
XXV	Second order polynomial regression results for energy flux density (dB re 1 μ Pa ² s) vs. click duration (μ s). 108
XXVI	Linear regression results for radiated acoustic power (dB re 1 watt) vs. click duration (μ s). 111
XXVII	Second order polynomial regression results for radiated acoustic power (dB re 1 watt) vs. click duration (μ s). 111
XXVIII	Linear regression results for peak frequency (kHz) vs. click duration (μ s). 114
XXIX	Second order polynomial regression results for peak frequency (kHz) vs. click duration (μ s). 114
XXX	Linear regression results for dominant frequency (kHz) vs. click duration (μ s). 117
XXXI	Second order polynomial regression results for dominant frequency (kHz) vs. click duration (μ s). 117
XXXII	Linear regression results for -3 dB bandwidth (kHz) vs. click duration (μ s). 120

TABLE	Page
XXXIII Second order polynomial regression results for -3dB Bandwidth (kHz) vs. click duration (μ s).	120
XXXIV Linear regression results for peak-to-peak source level (dB re 1 μ Pa) vs. radiated acoustic power (dB re 1 watt).	123
XXXV Linear regression results for energy flux density (dB re 1 μ Pa ² s) vs. radiated acoustic power (dB re 1 watt).	126
XXXVI Linear regression results for peak frequency (kHz) vs. radiated acoustic power (dB re 1 watt).	129
XXXVII Linear regression results for dominant frequency (kHz) vs. radiated acoustic power (dB re 1 watt).	132
XXXVIII Linear regression results for -3 dB bandwidth (kHz) vs. radiated acoustic power (dB re 1 watt).	135
XXXIX Classifications of clicks based upon spectral shape.	140
XL Physical measurements of <i>Tursiops truncatus</i> skulls.	165

LIST OF FIGURES

FIGURE		Page
1	Lateral view of a skull of a bottlenose dolphin.	2
2	Dorsal view of a skull of a bottlenose dolphin.	3
3	Ventral view of a skull of a bottlenose dolphin.	3
4	Diagram derived from a cryosection of the anatomy of the upper bony nares to the blowhole.	4
5	Representative multi-channel data sample.	26
6	Average intranarial pressure in all complete pressurization events (pooled data).	33
7	Average intranarial pressure in complete pressurization events without whistle ensonds (pooled data).	33
8	Average intranarial pressure in complete pressurization events with whistle ensonds (pooled data).	34
9	Average intranarial pressure in all complete pressurization events (BRT).	34
10	Average intranarial pressure in complete pressurization events without whistle ensonds (BRT).	35
11	Average intranarial pressure in complete pressurization events with whistle ensonds (BRT).	35
12	Average intranarial pressure in all complete pressurization events (BUS).	36
13	Average intranarial pressure in complete pressurization events without whistle ensonds (BUS).	36

FIGURE	Page
14	Average intranarial pressure in complete pressurization events with whistle ensonds (BUS). 37
15	Average intranarial pressure in all complete pressurization events (SAY). 37
16	Average intranarial pressure in complete pressurization events without whistle ensonds (SAY). 38
17	Average intranarial pressure in complete pressurization events with whistle ensonds (SAY). 38
18	Representative bottlenose dolphin click time domain sample. 68
19	Representative bottlenose dolphin power spectral density plot. 69
20	Histogram of peak-to-peak source level (dB re 1 μ Pa) (pooled data). 70
21	Histogram of peak-to-peak source level (dB re 1 μ Pa) (BRT). 70
22	Histogram of peak-to-peak source level (dB re 1 μ Pa) (BUS). 71
23	Histogram of peak-to-peak source level (dB re 1 μ Pa) (SAY). 71
24	Histogram of click duration (μ s) (pooled). 73
25	Histogram of click duration (μ s) (BRT). 73
26	Histogram of click duration (μ s) (BUS). 74
27	Histogram of click duration (μ s) (SAY). 74
28	Histogram of energy flux density (dB re 1 μ Pa ² s) (pooled). 76
29	Histogram of energy flux density (dB re 1 μ Pa ² s) (BRT). 76
30	Histogram of energy flux density (dB re 1 μ Pa ² s) (BUS). 77
31	Histogram of energy flux density (dB re 1 μ Pa ² s) (SAY). 77
32	Histogram of radiated acoustic power (watts) (pooled). 79
33	Histogram of radiated acoustic power (watts) (BRT). 79

FIGURE	Page
34	Histogram of radiated acoustic power (watts) (BUS). 80
35	Histogram of radiated acoustic power (watts) (SAY). 80
36	Histogram of intranarial pressure difference (kPa) (pooled). 82
37	Histogram of intranarial pressure difference (kPa) (BRT). 82
38	Histogram of intranarial pressure difference (kPa) (BUS). 83
39	Histogram of intranarial pressure difference (kPa) (SAY). 83
40	Histogram of peak frequency (kHz) (pooled). 85
41	Histogram of peak frequency (kHz) (BRT). 85
42	Histogram of peak frequency (kHz) (BUS). 86
43	Histogram of peak frequency (kHz) (SAY). 86
44	Histogram of dominant frequency (kHz) (pooled). 88
45	Histogram of dominant frequency (kHz) (BRT). 88
46	Histogram of dominant frequency (kHz) (BUS). 89
47	Histogram of dominant frequency (kHz) (SAY). 89
48	Histogram of -3dB bandwidth (kHz) (pooled). 91
49	Histogram of -3dB bandwidth (kHz) (BRT). 91
50	Histogram of -3dB bandwidth (kHz) (BUS). 92
51	Histogram of -3dB bandwidth (kHz) (SAY). 92
52	Bivariate plot of radiated acoustic power (dB re 1 watt) vs. in- tranarial pressure difference (kPa) (pooled). 94
53	Bivariate plot of radiated acoustic power (dB re 1 watt) vs. in- tranarial pressure difference (kPa) (BRT). 94

FIGURE	Page
54	Bivariate plot of radiated acoustic power (dB re 1 watt) vs. intranarial pressure difference (kPa) (BUS). 95
55	Bivariate plot of radiated acoustic power (dB re 1 watt) vs. intranarial pressure difference (kPa) (SAY). 95
56	Bivariate plot of peak frequency (kHz) vs. intranarial pressure difference (kPa) (pooled). 97
57	Bivariate plot of peak frequency (kHz) vs. intranarial pressure difference (kPa) (BRT). 97
58	Bivariate plot of peak frequency (kHz) vs. intranarial pressure difference (kPa) (BUS). 98
59	Bivariate plot of peak frequency (kHz) vs. intranarial pressure difference (kPa) (SAY). 98
60	Bivariate plot of dominant frequency (kHz) vs. intranarial pressure difference (kPa) (pooled). 100
61	Bivariate plot of dominant frequency (kHz) vs. intranarial pressure difference (kPa) (BRT). 100
62	Bivariate plot of dominant frequency (kHz) vs. intranarial pressure difference (kPa) (BUS). 101
63	Bivariate plot of dominant frequency (kHz) vs. intranarial pressure difference (kPa) (SAY). 101
64	Bivariate plot of -3dB bandwidth (kHz) vs. intranarial pressure difference (kPa) (pooled). 103
65	Bivariate plot of -3dB bandwidth (kHz) vs. intranarial pressure difference (kPa) (BRT). 103
66	Bivariate plot of -3dB bandwidth (kHz) vs. intranarial pressure difference (kPa) (BUS). 104
67	Bivariate plot of -3dB bandwidth (kHz) vs. intranarial pressure difference (kPa) (SAY). 104

FIGURE	Page
68	Bivariate plot of peak-to-peak source level (dB re 1 μPa) vs. click duration (μs) (pooled). 106
69	Bivariate plot of peak-to-peak source level (dB re 1 μPa) vs. click duration (μs) (BRT). 106
70	Bivariate plot of peak-to-peak source level (dB re 1 μPa) vs. click duration (μs) (BUS). 107
71	Bivariate plot of peak-to-peak source level (dB re 1 μPa) vs. click duration (μs) (SAY). 107
72	Bivariate plot of energy flux density (dB re 1 $\mu\text{Pa}^2\text{s}$) vs. click duration (μs) (pooled). 109
73	Bivariate plot of energy flux density (dB re 1 $\mu\text{Pa}^2\text{s}$) vs. click duration (μs) (BRT). 109
74	Bivariate plot of energy flux density (dB re 1 $\mu\text{Pa}^2\text{s}$) vs. click duration (μs) (BUS). 110
75	Bivariate plot of energy flux density (dB re 1 $\mu\text{Pa}^2\text{s}$) vs. click duration (μs) (SAY). 110
76	Bivariate plot of radiated acoustic power (dB re 1 watt) vs. click duration (μs) (pooled). 112
77	Bivariate plot of radiated acoustic power (dB re 1 watt) vs. click duration (μs) (BRT). 112
78	Bivariate plot of radiated acoustic power (dB re 1 watt) vs. click duration (μs) (BUS). 113
79	Bivariate plot of radiated acoustic power (dB re 1 watt) vs. click duration (μs) (SAY). 113
80	Bivariate plot of peak frequency (kHz) vs. click duration (μs) (pooled). 115
81	Bivariate plot of peak frequency (kHz) vs. click duration (μs) (BRT). 115
82	Bivariate plot of peak frequency (kHz) vs. click duration (μs) (BUS). 116

FIGURE	Page
83	Bivariate plot of peak frequency (kHz) vs. click duration (μs) (SAY). 116
84	Bivariate plot of dominant frequency (kHz) vs. click duration (μs) (pooled). 118
85	Bivariate plot of dominant frequency (kHz) vs. click duration (μs) (BRT). 118
86	Bivariate plot of dominant frequency (kHz) vs. click duration (μs) (BUS). 119
87	Bivariate plot of dominant frequency (kHz) vs. click duration (μs) (SAY). 119
88	Bivariate plot of -3dB bandwidth (kHz) vs. click duration (μs) (pooled). 121
89	Bivariate plot of -3dB bandwidth (kHz) vs. click duration (μs) (BRT). 121
90	Bivariate plot of -3dB bandwidth (kHz) vs. click duration (μs) (BUS). 122
91	Bivariate plot of -3dB bandwidth (kHz) vs. click duration (μs) (SAY). 122
92	Bivariate plot of peak-to-peak source level (dB re 1 μPa) vs. radiated acoustic power (dB re 1 watt) (pooled). 124
93	Bivariate plot of peak-to-peak source level (dB re 1 μPa) vs. radiated acoustic power (dB re 1 watt) (BRT). 124
94	Bivariate plot of peak-to-peak source level (dB re 1 μPa) vs. radiated acoustic power (dB re 1 watt) (BUS). 125
95	Bivariate plot of peak-to-peak source level (dB re 1 μPa) vs. radiated acoustic power (dB re 1 watt) (SAY). 125
96	Bivariate plot of energy flux density (dB re 1 $\mu\text{Pa}^2\text{s}$) vs. radiated acoustic power (dB re 1 watt) (pooled). 127
97	Bivariate plot of energy flux density (dB re 1 $\mu\text{Pa}^2\text{s}$) vs. radiated acoustic power (dB re 1 watt) (BRT). 127
98	Bivariate plot of energy flux density (dB re 1 $\mu\text{Pa}^2\text{s}$) vs. radiated acoustic power (dB re 1 watt) (BUS). 128

FIGURE	Page
99	Bivariate plot of energy flux density (dB re 1 $\mu\text{Pa}^2\text{s}$) vs. radiated acoustic power (dB re 1 watt) (SAY). 128
100	Bivariate plot of peak frequency (kHz) vs. radiated acoustic power (dB re 1 watt) (pooled). 130
101	Bivariate plot of peak frequency (kHz) vs. radiated acoustic power (dB re 1 watt) (BRT). 130
102	Bivariate plot of peak frequency (kHz) vs. radiated acoustic power (dB re 1 watt) (BUS). 131
103	Bivariate plot of peak frequency (kHz) vs. radiated acoustic power (dB re 1 watt) (SAY). 131
104	Bivariate plot of dominant frequency (kHz) vs. radiated acoustic power (dB re 1 watt) (pooled). 133
105	Bivariate plot of dominant frequency (kHz) vs. radiated acoustic power (dB re 1 watt) (BRT). 133
106	Bivariate plot of dominant frequency (kHz) vs. radiated acoustic power (dB re 1 watt) (BUS). 134
107	Bivariate plot of dominant frequency (kHz) vs. radiated acoustic power (dB re 1 watt) (SAY). 134
108	Bivariate plot of -3dB bandwidth (kHz) vs. radiated acoustic power (dB re 1 watt) (pooled). 136
109	Bivariate plot of -3dB bandwidth (kHz) vs. radiated acoustic power (dB re 1 watt) (BRT). 136
110	Bivariate plot of -3dB bandwidth (kHz) vs. radiated acoustic power (dB re 1 watt) (BUS). 137
111	Bivariate plot of -3dB bandwidth (kHz) vs. radiated acoustic power (dB re 1 watt) (SAY). 137
112	Histogram of percentages of clicks in classes. 139

FIGURE	Page
113	Time series representation of a dolphin click. 146
114	PSD of click using 2048 points and a Hamming window as processed in this study. 147
115	PSD of click using 2048 points and a rectangular window. 147
116	PSD of click using 256 points and a rectangular window as processed in Houser <i>et al.</i> (1999). 148
117	Histogram of joules in complete pressurization events (pooled). . . . 166
118	Histogram of joules in complete pressurization events where no whistle ensonds occur (pooled). 167
119	Histogram of joules in complete pressurization events where whistle ensonds occur (pooled). 167
120	Histogram of watts in complete pressurization events (pooled). 168
121	Histogram of watts in complete pressurization events where no whistle ensonds occur (pooled). 169
122	Histogram of watts in complete pressurization events where whistle ensonds occur (pooled). 169
123	Effect of depth on work required to achieve the same intranarial pressure difference. 170

CHAPTER I

INTRODUCTION

The Atlantic bottlenose dolphin (*Tursiops truncatus*) utilizes actively emitted sound to interrogate its environment. Dolphins may use this *biosonar* for both navigation and prey detection tasks. The ability to use biosonar appears to be universal among odontocete species, based upon experimental or observational evidence for every odontocete species so far examined (Wood and Evans, 1980).

One terminological issue needs to be addressed here, which is what to call sounds emitted by bottlenose dolphins. Some researchers argue for use of *vocalization*, and others for *phonation*. Vocalization is deprecated on grounds that dolphins have no *vocal cords* and that this term implies a laryngeal mechanism of production. Phonation, though, offers no particular advantage as far as examination of etymology is concerned. Instead, a term with rare usage (and thus few implications by history of usage) will be used: *ensond*. An *ensond* is here used to refer to any emitted sound. This term shares its root with *ensonification*, and seems appropriate to discussion of biosonar.

The research described in this dissertation comes in a particular context of inquiry, that of dolphin biosonar. Debate over basic issues in the study of dolphin biosonar has lasted for decades, as in the instance of determining the source of *click* ensonds. There have been a variety of hypotheses generated and approaches taken toward empirical study of biosonar sound sources. The questions of interest here concern the mechanism of biosonar sound production, the relationships of parameters of the sound production mechanism with the emitted sound, and the energetic

This dissertation follows the style of the Journal of the Acoustical Society of America.



FIG. 1. Lateral view of a skull of a bottlenose dolphin. Scale bar is 5cm.

cost biosonar sound production imposes on the bottlenose dolphin. The approach taken here combines physiologic and acoustic data with digital signal processing and computational modelling techniques.

A. Relevant anatomy

In this chapter, a brief history of work on cetacean biosonar will be given to place the current study in its context. Form may follow function, as the saying goes, but in order to appreciate the function of biosonar in the bottlenose dolphin it is helpful to have some familiarity with the relevant anatomy before considering the historical debate over the roles which have been assigned by researchers to various parts. Figures 1-3 show photographs of a skull of a bottlenose dolphin in lateral, dorsal, and ventral views, respectively. The upper mandible extends toward the left in all these figures. In the dorsal and ventral views, the superior and inferior openings of the bony nares are prominent features. The bony septum separating



FIG. 2. Dorsal view of a skull of a bottlenose dolphin. Scale bar is 5cm.



FIG. 3. Ventral view of a skull of a bottlenose dolphin. Scale bar is 5cm.

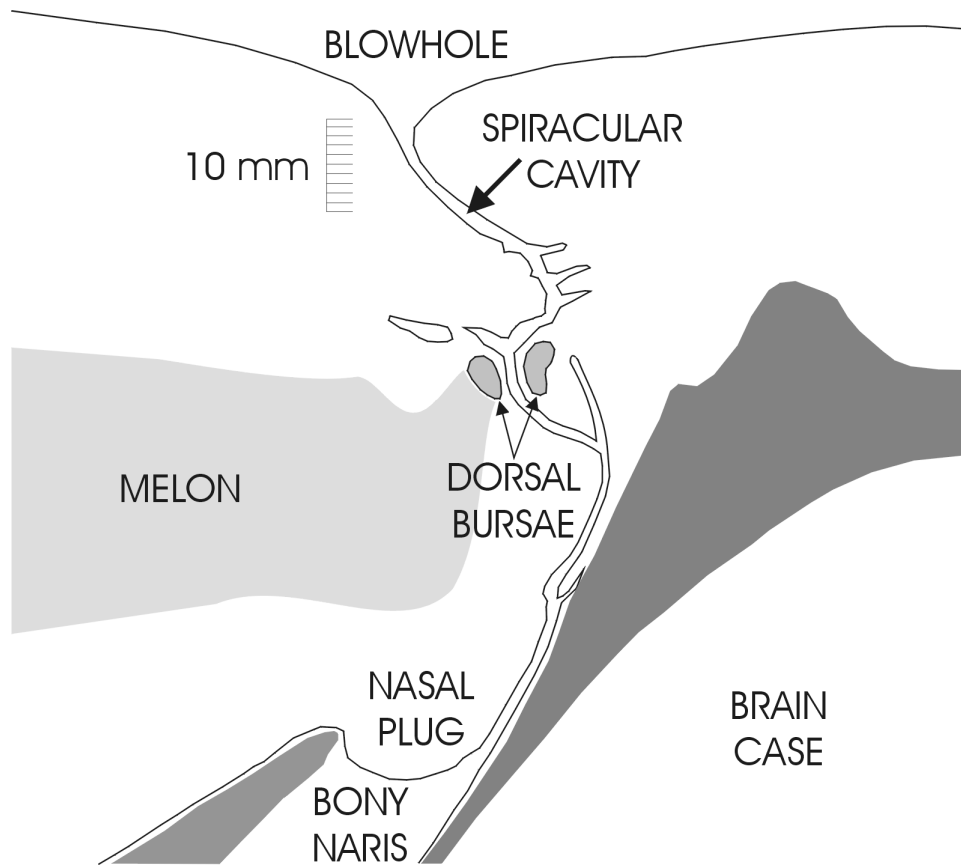


FIG. 4. Diagram derived from a cryosection of the anatomy of the upper bony nares to the blowhole. (From Figure 1b of Cranford *et al.* (1996).)

right and left sides of the bony nares is also visible. For most odontocetes, the external opening of the respiratory tract, the *blowhole*, is considerably posterior to the position of nasal openings seen in terrestrial mammals. If one drew a vertical line down from the position of the blowhole, it would come near the anterior edge of the brain case in the bottlenose dolphin. Figure 4 shows a new diagram made from a right sagittal cryosection originally published in Cranford *et al.* (1996). The tissue structures between the blowhole and the bony nares show considerable complexity, as described by Lawrence and Schevill (1956); Purves and Pilleri (1983); Cranford

(1992); Cranford *et al.* (1996). An air passage, the *spiracular cavity*, passes ventrally from the blowhole through the *vestibular sacs*. This air passage bifurcates to the left and the right to pass through paired lip-like structures, which have been called *monkey lips* due to resemblance to those simian features. The air passages then turn posteriorly and then ventrally to pass around the posterior edge of the *nasal plugs*. Each passage, left and right, enters its respective *bony naris*. Each bony naris is defined on the anterior edge by the premaxillary bones and on the posterior by the bones of the cranium. The lumen of this space is gas-filled and cannot collapse when the animal makes deep dives. This is in contrast to the lungs, which have been shown to collapse on deep dives (Ridgway and Howard, 1979). Ventrally, the *palatopharyngeal muscle complex* attaches to the walls of the bony nares and the anterodorsal portion of the larynx. When the larynx is closed, this seals the ventral portion of the bony nares.

B. An overview of dolphin biosonar research

The history of biosonar research in dolphins and other odontocetes has been summarized in a variety of sources (Kellogg, 1961; Norris, 1964, 1969; Evans and Maderson, 1973; Wood, 1973; Norris, 1975; Cranford, 2000; Cranford and Amundin, 2003). The purpose here is to briefly set the stage, showing the place of the current research in the historical context. The conceptual emphasis in research has itself taken a historical evolution, complete with contingency and some apparent ego-involvement with respect to some theories. The problem of sound production is of particular interest here.

The concepts of interest to researchers change over time, and for bottlenose dolphins this change reflects the change in perception of these animals among humans.

To start with, dolphins (though probably not bottlenose dolphins specifically) figured in superstition and myth in minor roles as harbingers of luck or as the repositories for the souls of departed sailors. Later, dolphins were largely just zoological oddities for the consideration of anatomists and taxonomists. The large size of many odontocetes restricted the flow of information, as most knowledge came for a long time primarily from stranded animals. Because large animals posed considerable difficulties in preserving tissues, often it was a case of the zoologist coming to the specimen rather than the specimen being shipped to the zoologist.

Scammon (1968) devoted a scant portion of a page to discussion of “the cow-fish” or Pacific bottlenose dolphin (*Tursiops gilli*). Scammon’s viewpoint was one of commercial value, and in this bottlenose dolphins lacked the high value accorded other species. The availability of bottlenose dolphins through commercial fisheries provided some opportunities for these animals to be displayed at aquaria early in the 20th century (Wood, 1973).

General interest in the biology of bottlenose dolphins had to await a general interest in bottlenose dolphins *per se*. This is commonly attributed to public perception changing through exposure to the animals at aquaria, oceanaria, or zoos and popular accounts in the mass media (Lilly, 1978).

One question posed by stocking Atlantic bottlenose dolphins at Marine Studios of St. Augustine, Florida, was how to efficiently catch them. Arthur McBride, the curator, found that the dolphins could detect the nets used to attempt to catch the animals, even in murky water or at night. The mesh of the net had to be changed from a small mesh size to a large mesh size in order to catch dolphins efficiently. McBride suspected that bottlenose dolphins had some form of echolocation, as had recently been discovered in bats. McBride’s notes were published posthumously in 1956 by William Schevill (Wood, 1973).

Winthrop Kellogg conducted several early studies on the hearing range of the Atlantic bottlenose dolphin. These established sensitivity to sounds in the ultrasonic range, and caused him to speculate that these animals might also emit sounds with ultrasonic frequency content (Kellogg, 1961; Wood, 1973). Further work demonstrated that this was the case. Kellogg reported frequency components as high as 170 kHz (Kellogg, 1961). Kellogg (1961) also identified the anatomy between the dorsal openings of the bony nares and the blowhole as the most likely source of dolphin clicks.

Lawrence and Schevill (1956) incorporated observations of live dolphins and dissections to present an extensive review of the anatomy of the nasal passages. Lawrence and Schevill espoused a hypothesis of laryngeal production of sounds in odontocetes, citing their own experimental work. They note the additional complexity of anatomy of the upper nasal passages in odontocetes as compared to mysticetes, but do not provide an explanation for this difference between groups. This paper also provides the earliest measurements of air pressure within the bony nares of odontocetes, though these measurements were obtained by pumping air into these passages in dead specimens.

Norris *et al.* (1961) used an experimental approach to exclude the visual modality in an Atlantic bottlenose dolphin to establish use of biosonar. They also attempted to interfere with the sound reception and sound transmission of the subject, but found that covering the external meatus of the subject failed to reduce its sensitivity to sound and the subject was transferred back to use in public shows before they were able to train it to accept apparatus which would block sound coming from the forehead.

Evans and Dreher (1962) serendipitously recorded a group of wild Pacific bottlenose dolphins (*Tursiops gilli*). The observations of animal movements and recorded

sounds were consistent with scouting by use of biosonar.

Evans and Prescott (1962) utilized observations of live animals and manipulation of dead specimens to examine sound production. They found three classes of sounds: clicks, whistles, and barks. In dead specimens, they passed air under pressure through the larynx and the nasal tract and found that sounds were produced in each case. They noted that click-like sounds were produced in the nasal passages of a *Tursiops truncatus* specimen when air at 1.5 psi (10.3 kPa) and a 10 liters per minute flow rate was passed through them. They also inferred that the mechanisms of click production and whistle production must be different since none of the acoustic properties of clicks could be detected in the whistles observed. They concluded that the nasal-sac system of dolphins was the most likely source of click sounds and offered the *tubular sacs* or *nasofrontal sacs* as the best candidate for a specific location for click production.

Purves (1966) advocated a laryngeal source of clicks and whistles in the dolphin. Purves provided evidence for the plausibility of laryngeal sound production in the form of studies with dead specimens in which a Galton whistle tuned to 20kHz was placed in the larynx. Purves measured the resulting sound levels at various points around the head. His hypothesis of sound production involved gas in the laryngeal air sacs being passed through the larynx to produce clicks and whistles. Purves criticized non-laryngeal hypotheses of click production. Certain criticisms showed merit, but many were based upon faulty chains of reasoning. For example, Purves urged exclusion of the involvement of the upper nasal passages for sound production because the vestibular sacs had a necessary function of capturing water that came in through the blowhole and expelling it again. Necessary functions, though, are not exclusive functions, as would be required to carry Purves's contention to its desired conclusion.

Diercks *et al.* (1971) utilized custom transducers and recording equipment to

examine biosonar use in *Tursiops truncatus*, *Inia geoffrensis*, and *Orcinus orca*. The transducers were attached to the foreheads of the subjects via suction cups. They found that the recorded signals differed in form depending on where each transducer was placed, but that for any given position the signal waveform was reliably acquired and stable in shape. In *Tursiops truncatus*, they used acoustic localization with an assumption of straight-line transmission and a uniform sound speed to determine that clicks originated “at the location of the nasal plugs.”

Norris *et al.* (1971) used a cineradiographic technique to examine movements of structures during sound production in *Stenella longirostris*. They observed characteristic movements of the nasal plugs during the production of “squeals.” They did not observe an open air path through the larynx during sound production. They concluded that these cineradiographic records supported hypotheses of sound production in the upper nasal passages.

Evans (1973) reported on various issues in echolocation by cetaceans. The mechanism of sound production was discussed at some length. Evans proposed criteria which any hypothesis of sound production in cetaceans would have to meet. These were based upon observational and experimental findings. They include the duration of clicks, the inter-click interval, the duration of a click train, the amplitude of clicks, the duration and frequency range of whistles, the simultaneous production of clicks and whistles, and conformance to established beam patterns. Evans (1973) critiqued the laryngeal production hypothesis of Purves (1966). Given Purves’s proposed source of aryepiglottic folds in the larynx for both whistles and clicks, similar radiation patterns should be observed for both classes of sounds. This was not the case.

Dormer (1979) utilized cineradiography to study sound production in living bottlenose dolphins. Characteristic patterns of motion of structures were observed.

Dormer concluded that the clicks and whistles were produced at the right and left nasal plugs, respectively. A slower rate of filling of the vestibular sac was observed in click production as opposed to whistle production, indicating that less gas must flow for click production than for whistle production.

Ridgway *et al.* (1980) studied sound production in a bottlenose dolphin, collecting simultaneous data in several modes: acoustic, intranarial and intratracheal pressure, and electromyography of muscle groups. Click sound production consistently involved the pressurization of the intranarial space, no increase in intratracheal pressure, and associated muscle activity in the upper nasal passages. These findings taken together strongly argue for sound production in the upper nasal passages.

Amundin and Andersen (1983) studied sound production in the harbor porpoise (*Phocoena phocoena*) and bottlenose dolphin (*Tursiops truncatus*). They also utilized acoustics, intranarial pressure measurements, and electromyography in their approach. They found that in both species, click production required pressurization of the intranarial space, and that muscle activity in the nasal plugs was always associated with click production. They found considerable maximum intranarial pressures of about 54 kPa in the harbor porpoise and about 81 kPa in the bottlenose dolphin. They concluded that sound production occurred at some location in the vicinity of the nasal plugs.

Purves and Pilleri (1983) used a popular book as a means of responding to various studies that gave evidence for non-laryngeal mechanisms of click sound production in dolphins. They forcefully continued to espouse a laryngeal mechanism as the primary source of click and whistle sound production. In doing so, they took up many criticisms and work supporting non-laryngeal findings. In some cases, they were able to make substantial criticisms concerning points of anatomy. However, many times they simply dismissed an experimental or observational finding for no

apparent reason.

Ridgway and Carder (1988) studied sound production in conjunction with biosonar in a white whale (*Delphinapterus leucas*). Both the acoustic output and intranarial pressure were recorded simultaneously. This was the first study to examine such physiological measurements with the animal actively engaged in a biosonar task. The same pattern of intranarial pressure increases associated with click production was found for the white whale as had been established for the bottlenose dolphin (Ridgway *et al.*, 1980). This closed off a criticism that *ad libitum* sounds might be produced in the upper nasal passages, but actual biosonar clicks were only produced in the larynx.

Recent work (Cranford *et al.*, 1997, 2000) provides multiple lines of evidence that clicks can be produced by bottlenose dolphins at either the left or the right *dorsal bursae*. These paired structures lie about 2.5 cm beneath the blowhole and are just above the *nasal plug*. In reference to an earlier study (Diercks *et al.*, 1971), Evans and Maderson (1973) noted that the position of the likely sound source was about 2 to 3 cm below the level of the blowhole. This specific figure was not in the published text of the earlier study, but is in good agreement with these recent findings.

The research reported in this dissertation is aimed at contributing some answers to very broad questions: How can the physiology and acoustics of biosonar sound production be measured? What techniques are used for analysis of biosonar clicks? How do parameters of click sound production affect the sounds which are produced? How much does biosonar sound production cost? These questions are addressed, in order, in the following four chapters. The approach taken integrates observations of anatomy, histology, physiology, and acoustics to reach conclusions which were not evident from considering each topic in isolation.

CHAPTER II

MEASURING INTRANARIAL PRESSURE DURING BIOSONAR

A. Introduction

Intranarial pressure has long been implicated as a primary factor in sound production in odontocete cetaceans (Norris *et al.*, 1961; Norris and Harvey, 1972; Ridgway *et al.*, 1980; Amundin and Andersen, 1983; Ridgway and Carder, 1988). There are several good reviews concerning odontocete sound production (Norris, 1964, 1969; Evans and Maderson, 1973; Norris, 1975; Cranford, 2000; Cranford and Amundin, 2003). Previous studies identified and measured intranarial pressure as a physiologic correlate of both click and whistle sound production in the bottlenose dolphin (Ridgway *et al.*, 1980; Amundin and Andersen, 1983; Ridgway and Carder, 1988; Cranford *et al.*, 2000). Ridgway and Carder (1988) is notable as the first study where both wide-bandwidth acoustics and intranarial pressure were measured during a cetacean biosonar task, where their subject was the white whale (*Delphinapterus leucas*).

The current study extends previous work on localization and characterization of sound sources in the bottlenose dolphin (Cranford *et al.*, 1997). It also provides the first report of simultaneous acoustic and intranarial pressure recordings from the bottlenose dolphin during biosonar.

Ridgway *et al.* (1980) first reported intranarial pressure recorded during ensounds in bottlenose dolphins (*Tursiops truncatus*). That study utilized pressure catheters introduced via the blowhole and passed into the intranarial space. The subjects were restrained in small pools with two-thirds of the body covered by water. There are some difficulties in interpreting the results from the Ridgway *et al.* (1980) study in that the experimental conditions are not the normal conditions for respiration and productions

of ensonds in bottlenose dolphins completely in the water. When out of the water, the lung tissue is compressed by the weight of the animal's body on the compressible thorax. This may present a problem in directly trying to compare pressures taken in the Ridgway *et al.* (1980) study with those taken when the subjects are in water. However, the patterns noted in Ridgway *et al.* (1980) have been supported by later work. Intranarial pressure was found to increase before the onset of any ensond. Higher pressures were found to be associated with whistle production than for click ensonds. Experiments showed that only abbreviated sounds could be produced with a small diameter open catheter connecting the intranarial passage to the outside air, and that sound production was completely ineffective when a large diameter catheter was deployed in the same fashion. This provided strong evidence that sound production was largely, if not exclusively, accomplished by mechanisms in the nasal passages rather than in the larynx. Because the subjects were not performing an echolocation task, this study did not link the physiological data with biosonar behavior.

Amundin and Andersen (1983) measured intranarial pressure, ensonds, and electromyographic data simultaneously in the harbor porpoise (*Phocoena phocoena*), and both intranarial pressure and ensonds in a bottlenose dolphin (*Tursiops truncatus*). They noted that in both species, click sound production was preceded by an increase in intranarial pressure. They also reported that manipulation of the *nasal plug*, such that the air pressure within the intranarial space could be vented, terminated any ensonds in progress. The electromyographic data collected in the harbor porpoise implicated the nasal plugs as part of an active neuromuscular control system for “metering out” pressurized gas used in click production. They also reported that no clicks were produced without a minimum intranarial pressure, and gave a range of 25 to 81 kPa for intranarial pressure during click production in bottlenose dolphins.

Amundin and Andersen (1983) noted that attaining a certain pressure level in

the intranarial space was a necessary precondition to click production, but not a sufficient condition. The simple fact of high intranarial pressure did not guarantee that clicks or any ensound would ensue.

Ridgway and Carder (1988) extended the previous work on bottlenose dolphins to white whales (*Delphinapterus leucas*). Again, a pressure catheter was passed through the blowhole and into the intranarial space in trained cooperating subjects. Ridgway and Carder observed the same pattern of pressurization as was found in the earlier study on bottlenose dolphins: intranarial pressure increased prior to click ensounds, and higher pressures were observed in association with whistles than with clicks. This study also was the first where both intranarial pressure and acoustic data were obtained during use of biosonar by an odontocete.

Cranford *et al.* (2000) modified and extended the earlier work on bottlenose dolphins (*Tursiops truncatus*). The subjects remained in the water and made both ad libitum ensounds and performed a biosonar task. Various scenarios of data collection occurred, ranging from simply recording during ensounds using hydrophones, one or two pressure-sensitive catheters, and one or two endoscopes. Measurements of intranarial pressure were taken with the catheters at a depth of 10 cm, which placed the sensor within the bony nasal passages. High-speed video recordings were made of the endoscopic views, and normal video recordings were made of a composite of the high-speed view, an overview of the study area, and a view of an oscilloscope and LCD panel. The oscilloscope displayed a trace of a signal from the low frequency acoustic hydrophone, while the LCD panel presented information about the current file and sequence number for where the data were being stored online. An LED indicator mounted next to the LCD panel turned on during analog-to-digital sampling. More than fifty days of data collection occurred over a seven month period. Each day's data collection yielded between 15 and 30 minutes of high-speed video, two to

three hours of normal video, and between 2 and 4 gigabytes of digital data on the computer.

The study by Cranford *et al.* (2000) confirmed certain aspects of the prior work. The pressurization of the two bony nasal passages occurred simultaneously and equally. Manipulation which compromised the ability to maintain pressure in the intranarial space prevented the production of ensonds.

The Cranford *et al.* (2000) study also yielded new information. A change in terminology was recommended, in that the structures formerly called the *monkey lips* should now be called the *phonic lips*, for their apparent critical role in sound production (Cranford, 1992; Cranford *et al.*, 1996, 2000; Cranford, 2000). Manipulation of the *monkey lips/dorsal bursae* (MLDB) complex on one side prevented ensonds from being produced on that side. Activity of MLDB complexes was synchronous with recorded ensonds.

The research presented in this dissertation is based upon the data collected in the Cranford *et al.* (2000) study.

B. Methods

Data were collected over a period of about nine months, during which time there were significant changes in equipment, configuration, and procedure. Each scenario for data collection will be described separately. The subjects of the study are the same throughout the scenarios, so they will be described first.

Three Atlantic bottlenose dolphins (*Tursiops truncatus*) were subjects in this study. Table I lists information about these individuals. Each dolphin has a different history of training, and each one had a different level of familiarity with the biosonar task in the study.

TABLE I. Physical characteristics of subjects.

Name	Gender	Date of birth	Weight (kg)*	Length (m)*
BRT	Female	1961/06 (est.)	197	2.52
SAY	Female	1979/06	263	2.78
BUS	Male	1980/06	192	2.50

* Weights and lengths are averages during the study period.

1. Biosonar task training

Biosonar task training consisted of teaching several behaviors to the dolphins. Dolphins were trained to station on an underwater bite plate. This put the dolphins in a known position and orientation. They were trained to emit clicks when an underwater target was presented and to accept the use of visual occlusion devices in the form of soft rubber eye cups or a visual barrier placed between the dolphin and the target. They learned to respond to specific targets with an acoustic response, and to remain quiet otherwise. All the dolphins were trained to respond with a whistle ensound to a 7 cm stainless steel water-filled sphere. SAY was taught to respond to a rock of similar size with a pulse ensound. The other subjects would remain quiet for presentations of anything other than the stainless steel sphere, except that BUS was being trained to emit a pulse ensound when presented with a water-filled 1 liter fuel bottle. This set up a target recognition biosonar task. The purpose behind the choice of targets was to establish a relatively easy biosonar task which could be accomplished in the context of research into the physiology of biosonar sound production.

The use of a bite plate permitted recording of clicks with hydrophones in the far field and put the subject and the recording hydrophones into a consistent and

repeatable orientation. This was an issue noted by Nichols *et al.* (1971), who utilized hydrophones placed directly on the melon of their subjects in order to obtain consistent recordings of clicks throughout a click train. Being able to record in the far field and in the beam pattern of clicks is important for making statements about the *radiated acoustic power* of those clicks. In the near field, small changes in position or orientation of the hydrophone can result in large changes in recorded amplitude, which makes reporting amplitudes of ensounds problematic if measurements are taken in the near field. The determination of the minimum distance to the acoustic far field for signals at a particular frequency is discussed in Au (1993).

Because the biosonar task differed between subjects, each subject’s performance on its task was analyzed separately. The differences in task relate to the number and type of “target” stimuli used, and in the possible responses and associations of responses to stimuli. For BRT, the set of target stimuli was “target absent”, “ball” (a 7.5 cm diameter water-filled stainless steel sphere), and “rock” (a rock of size similar to the “ball” target). BRT’s trained responses were to remain quiet for all non-ball target stimuli, and to emit a whistle response to the ball stimulus. For BUS, the set of target stimuli was “no target”, “ball” (a 7.5 cm diameter water-filled stainless steel sphere), and “bottle” (a 1 liter capacity water-filled aluminum fuel bottle, sold at camping supply stores for storing white gas). BUS’s set of responses was to remain quiet for no target present or rock, to give a whistle response to the ball, and to give a high repetition rate burst pulse response to the bottle. For SAY, the set of target stimuli was “no target”, “ball” (a 7.5 cm diameter water-filled stainless steel sphere), and “rock” (a rock of size similar to the “ball” target). SAY’s trained responses were to remain quiet for “no target”, to give a whistle response to the ball, and to give a high repetition rate burst pulse response to the “rock”. Table II lists the stimulus/response pairs for each subject.

TABLE II. Biosonar target recognition response matrix by subject and stimulus.

Subject	Stimulus				
	Sphere	Rock	Catch	Fuel Bottle	Other
BRT	Whistle	Quiet	Quiet	Quiet	Quiet
BUS	Whistle	Quiet	Quiet	Pulse	Quiet
SAY	Whistle	Pulse	Quiet	Quiet	Quiet

2. Data acquisition software

Custom data acquisition software recorded one acoustic channel with high bandwidth while permitting a variable number of other channels of data to also be digitized. Since the bandwidth of one digital data acquisition card had to be shared among all data input channels for our available hardware, the program had to take this into account. By programming the channel gain queue of the National Instruments PCI-MIO-16E-1 data acquisition card, the acoustic channel was sampled every other sampling cycle, thus yielding to the acoustic channel half the available bandwidth. Up to a total of seven other channels could be specified, and the remaining bandwidth would be split evenly between them. For example, if three pressure catheter channels and a low-frequency acoustic channel were recorded in addition to the high-frequency acoustic channel at a total data acquisition card bandwidth of one mega-samples per second, then the high-frequency acoustic channel would be recorded at an effective bandwidth of 500 kilo-samples per second, and the remaining 500 kilo-samples per second bandwidth would be shared among four channels, giving an effective 125 kilo-samples per second sampling rate for each of those channels.

3. Calibration of equipment

A Brüel & Kjær Model 8103 hydrophone and Brüel & Kjær Model 2635 charge amplifier was used to record high-frequency underwater sound emitted from each dolphin subject. The hydrophone was placed such that it was on the longitudinal axis of the dolphin and on line between the dolphin and the position in which the target was placed for presentation. The distance was selected to be in the far field for high-frequency sounds made by the dolphin. The acoustic signal was filtered by a Krohn-Hite high-pass filter module (8-pole Butterworth, cut-off frequency of 80 Hz). The filtered acoustic signal was passed into a National Instruments PCI-MIO-16E-1 multifunction input-output data acquisition card through a National Instruments BNC-2990 rack mount BNC connector breakout box.

For transducer signals passing through Brüel & Kjær model 2635 charge amplifiers, low-pass filtering was set for a cutoff frequency of 100 kHz. This low-pass filter has a gradual roll-off characteristic.

Sometimes an uncalibrated low-frequency hydrophone was deployed to obtain dolphin whistle sounds emitted as responses to targets. Two different types of hydrophone were employed in this fashion, both salvaged from used sonobuoys. The signals were amplified using a Radio Shack Mini-Amplifier (RS-277-1008C), passed through a Krohn-Hite high-pass filter module, and routed into a breakout box for the National Instruments data acquisition card. The hydrophones were placed off-axis and in close proximity to the dolphin's melon. This worked because whistle responses are both low-frequency and close to omnidirectional. The signals recorded via these transducers can be analyzed for low-frequency spectral content but cannot be used to obtain absolute amplitude information.

Calibration of hydrophones was accomplished through the use of a Brüel &

Kjær Pistonphone Hydrophone Calibrator Model 4223, serial number 1152539. The Pistonphone pressurizes a chamber of known size via movement of a piston with the hydrophone to be calibrated held in place. This produces a repeatable sinusoidal pressure of known amplitude. The Pistonphone pressure is known for each model hydrophone calibrated within it, but differs between hydrophone models because of different volumes needed for the various adapters. A small correction must be taken into account for atmospheric pressure. A custom program was written to help make calibration via pistonphone measurements easier. The program records the acoustic signal obtained with the hydrophone in the pistonphone, collects peak-to-peak amplitudes for the pistonphone's characteristic frequency, stores the original acoustic recording in digital format, and outputs a text file describing the conditions of the calibration. The conditions recorded include which model and serial number hydrophone is being calibrated, the charge amplifier used, the hydrophone sensitivity setting, the amplification setting, the uncorrected pistonphone calibration amplitude, the atmospheric pressure, the pistonphone calibration amplitude adjusted for atmospheric pressure, the frequency of the pistonphone, the number of cycles recorded, the average peak-to-peak amplitude measured in the data, and the standard deviation measured in the data. The average peak-to-peak amplitude can be used to find the absolute amplitude of signals recorded with the hydrophone. Hydrophone calibrations made via use of the pistonphone were taken daily, typically before data collection began.

The calibration method depends upon accurate calibration charts provided by the hydrophone manufacturer. Frequency-dependent variations in sensitivity are recorded there. Fortunately, both the Brüel & Kjær model 8103 and model 8105 hydrophones have a flat frequency response over a wide range of frequencies, including the pistonphone calibrator frequency of 251 Hz. This simplifies application of the single-point

calibration method in that no corrective adjustment is needed over much of the applicable frequency range of the hydrophone.

The data acquired from the hydrophone and charge amplifier is a signal of varying voltage. The data acquisition card converts the voltage value into a numeric value. The scale for the measured value depends upon settings in effect at the time of measurement. This leaves the problem of relating measured values taken under particular conditions to the calibration measurements, which may utilize different equipment settings. The relevant parameters from the calibration and data collection scenarios are the amplification set on the charge amplifier, the voltage range set on the data acquisition card, and the number of possible values which the data acquisition card fits into that voltage range. Additionally, the signal level for the calibration signal must be known. Given all these parameters, the procedure for obtaining an absolute sound pressure level can be stated as follows.

- Note calibration signal level in data acquisition card units (CAL_{units})
- Convert calibration signal level from RMS db re 1 μ pascal to a peak-to-peak value by adding 9 dB to the RMS value.
- Convert dB re 1 μ pascal to μ pascals by this equation:

$$\mu pascals = 10^{dB/20} \quad (2.1)$$

- Determine μ pascals per unit ($uppu$)

$$uppu = \frac{\mu pascals}{CAL_{units}} \quad (2.2)$$

- Determine the factor by which units of the calibration measurement differ from those in data collection. This is the change in voltage range set.

$$ppfactor = VoltRange_{CAL}/VoltRange_{DATA} \quad (2.3)$$

- Determine the difference in amplification between the calibration settings and those for data collection.

$$\Delta dB = 10^{CALGain} - 10^{DATAGain} \quad (2.4)$$

- With a peak-to-peak measurement x , apply the factors and adjustments.

$$PP \text{ dB re } 1 \mu\text{Pascal} = 20 \log(x * ppFactor * uppu) - \Delta dB \quad (2.5)$$

This yields the desired units of measurement for an absolute peak-to-peak acoustic amplitude.

Intranarial pressure was measured via use of Millar pressure catheters and line conditioners. Three different models of pressure catheter were employed at various points during the observation period. All were flexible, thin tubes. Two models (Mikro-Tip PC-350 Size 5 French and Mikro-Tip SPR-524 Size 2.5 French) have single strain-gage transducers for pressure measurement at the end of the catheter. The other (Mikro-Tip SPR-673 Size 6 French) has three strain-gage transducers. The trainer inserted the catheter into the blowhole to a specified depth (usually 10 cm), which put the transducer at the tip within the bony nasal passage of the dolphin. The trainer also monitored the catheter position over time as the dolphin stationed on the bite plate and performed biosonar tasks. Two types of Millar pressure catheter signal conditioner were used, models TCB-100 and TCB-500.

Calibration of the pressure catheters was accomplished via use of a mercury column manometer manufactured by the E.H. Sargent Company. A syringe and series of valves was used to establish a known pressure differential. The reading at

the known pressure was recorded by the data acquisition computer by taking 10,000 samples and computing the average and standard deviation. Any measurements with a high standard deviation were discarded as indicating changing conditions or noise. The location of the manometer in a floating equipment shelter led to occasional problems because of swells or other wave action. The subsidence of swells typically allowed making a stable calibration measurement.

Over time, the value reported by a pressure catheter for a particular pressure can drift. In order to account for this property, calibrations were usually taken every day both before data collection and after data collection. Values were then interpolated between readings taken before the data collection session and readings taken after the data collection session. This assumes linear drift. The basis of this assumption was tested by taking calibration readings every thirty minutes with the catheters on a day when no subject testing was undertaken. The catheters showed linear drift over time.

The data collection process included a large amount of equipment and the cooperation of at least four people. Acoustic and physiological data were collected via use of a computer-based analog-to-digital (A/D) conversion card, and stored on computer. For many of the sessions, simultaneous high-speed video was recorded through an endoscope placed in the subject's nasal cavity. Video of the work area during sessions was also recorded separately on a standard video-cassette recorder (VCR). Operation of the high-speed video required one person, another was needed for operation of the computer, a trainer was needed for handling the dolphin, and a veterinarian was needed to operate the endoscopy equipment.

The first scenario for data collection involved the use of one or two pressure catheters, but no endoscopes. The second scenario was where one or two pressure catheters were deployed, and also one endoscope. The third scenario was where one or

two pressure catheters were deployed, and also two endoscopes. Endoscopy primarily focused upon the region of the phonic lips, about 2.5 to 3 cm below the blowhole of the dolphin. Other areas examined endoscopically included the nasal plugs and the nasopharynx.

A high-speed video recorder (Hi-Val 400) permitted capture of endoscope views at 200 or 400 frames per second. It included a built-in screen splitter to allow two high-speed video cameras to be attached. Since it was simply a screen splitter, and not picture-in-picture with compression, one could only adjust which parts of the field of view were recorded. In order to capture a second endoscope view, a special adapter was machined to allow the secondary camera's lens to be mounted off-axis. An NTSC video signal from the high-speed video recorder was routed through a Videonics MX-1 video mixer. A camcorder video output provided a second video source. The camcorder was used to obtain a view of the trainer interacting with the dolphin. An audio microphone in the work area was also recorded with the output of the MX-1 on standard VHS videotape. These two video tape systems provide much information about the events which occurred during data collection.

At the end of the data collection session, the digital data on the computer required some post-processing. The data from a sample period was contained in a single file, and a second text file indicated the offsets in that file where the data from each channel could be found. A custom application then split the sampled data so that a data file was created for each sample period and channel. Another custom application then produced (640x480 pixel) bitmap representations of the multi-channel digital data. These were printed, twenty to a page, to produce a notebook with a visual representation of the digital data collected.

By viewing the VHS video with the audio from the session, annotations were recorded on the printed notebook pages to indicate which samples contained biosonar

trials, the type of target stimulus, and the subject's response. Other relevant notes on conditions of recording were also noted in the notebook pages. These annotations helped link the vagaries of data collection to the final form of the recorded data.

Intranarial pressure changes in characteristic ways in relation to sound production. In sequence, the following actions occur: The dolphin inhales air and seals off the blowhole. The gas inside the dolphin's bony nasal passages has a certain pressure, usually not equal to the ambient atmospheric pressure, termed here the basal pressure. In sound production, the dolphin increases intranarial pressure over the basal pressure, yielding an intranarial pressure difference (see 5). After sound production ends, intranarial pressure returns to the basal pressure. The sequence which begins with a change in pressure over basal pressure and ends with a return to basal pressure is called a pressurization event (see Results section for a figure).

Pressurization events were split into different classes based upon the placement and duration of the event in relation to the digitally recorded sample period. These classes are complete, indicating that the entire duration of the pressurization event falls within the sampled period; open at beginning, where the sampled period begins some time after the start of the pressurization event; open at end, where the sampled period ends before the end of the pressurization event; and open at both, where the sampled period captures a portion of the middle of the pressurization event. Statistics are presented here only for those pressurization events classed as complete.

C. Results

While there are too many samples and clicks to all be reproduced here in figures, a representative multi-channel data sample of 2 seconds duration is shown in Figure 5. Figure 5 also shows pressure and sound levels over the time period of 2 seconds.

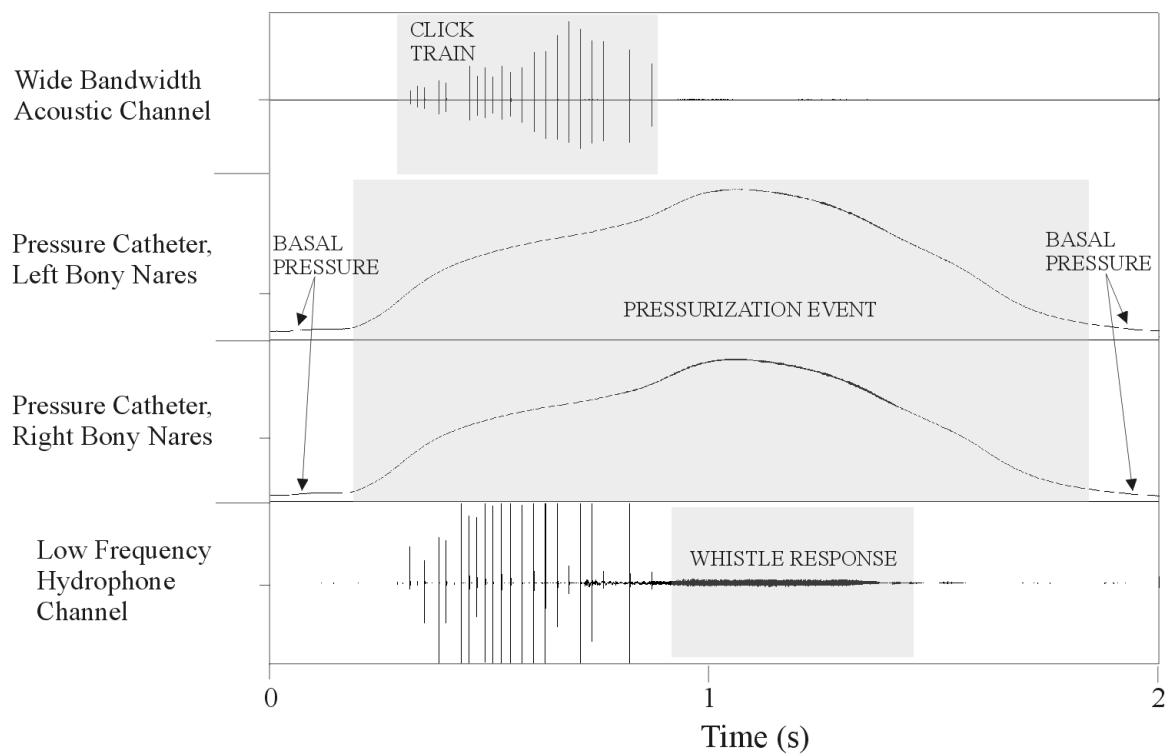


FIG. 5. Representative multi-channel data sample.

In Figure 5, there are several features to be noted. The sample period shown comprises 2 seconds of time and there are 4 channels of data. In both intranarial pressure channels, a non-zero basal pressure can be seen at the start of the sample period. In the intranarial pressure channels, pressure increases above basal pressure simultaneously and equally in both bony nasal passages. It is only after this pressure increase occurs that the dolphin begins to emit clicks. A series of clicks (click train) is emitted to interrogate the target field. In this case, the stainless steel sphere target was present and recognized by the dolphin, who then increased intranarial pressure well above the level seen during the click train. A whistle response follows this further increase in intranarial pressure. After the whistle occurs, intranarial pressure drops back to the basal pressure, completing the pressurization event associated with the biosonar click train.

Examination of the video recordings of sessions and the data show several important characteristics of pressurization events. First, both the right and left nasal passages show simultaneous and equal changes in pressure. The second is that clicks are only emitted during pressurization events. In the data examined thus far, there is no indication that the dolphin is able to produce clicks without first achieving a minimum intranarial pressure difference above the basal pressure. Observations show that there is a one-to-one correspondence between clicks and lip movements (Cranford *et al.*, 1997, 2000).

The performance on the biosonar task is evaluated by analysis of contingency tables. A comparison of observed and expected frequencies of associations between stimuli and responses yields a chi-square statistic. There were some differences in biosonar tasks between the three subjects. These differences correspond to the state and type of training which each subject had in biosonar target recognition tasks at the time of data collection. Table II lists the stimulus/response pairs for each subject.

TABLE III. Observed and expected frequencies of target and response for BRT.

Target	Response			Total
	Pulses	Quiet	Whistle	
None	0 (2.3)	179 (124.0)	1 (53.7)	180
Sm. Ball	7 (2.4)	21 (127.4)	157 (55.2)	185
Sm. Rock	0 (2.3)	172 (120.5)	3 (52.2)	175
Total	7	372	161	540

Expected values are in parentheses.

For BRT, the analysis of biosonar performance is given in Tables III-IV.

BRT's overall correct performance on the biosonar task was 508 correct responses out of a total of 540 trials, or 94%. An overall chi square analysis has 4 degrees of freedom, a chi square value of 434.761, and $p < 0.0001$. The chi square cell statistics show that the null hypothesis, that BRT's responses are due to chance, should be rejected for all "quiet" and "whistle" response cells. It is safe to say that BRT was demonstrably performing a biosonar task in the experiments.

For BUS, the analysis of biosonar performance is given in Tables V-VI.

BUS's overall correct performance on the biosonar task was 130 correct responses out of a total of 215 trials, or 60%. Overall chi square statistics at 4 degrees of freedom yield a chi square value of 51.972 and $p < 0.0001$. The chi square statistics show that the null hypothesis, that BUS's responses are due to chance, should be rejected only for "quiet" and "pulse" responses to the "bottle" stimulus. BUS's overall performance does not give confidence that he was performing a biosonar task reliably during these experiments. The non-chance performance on one of the target stimuli is suggestive

TABLE IV. Cell chi squares for target and response for BRT.

Target	Response		
	Pulses	Quiet	Whistle
None	2.333	24.395(*)	51.685(*)
Sm. Ball	8.831	88.905(*)	188.042(*)
Sm. Rock	2.269	21.953(*)	46.348(*)

(*)Chi square critical value for 4 df and $p=0.05$ is 9.48773.

TABLE V. Observed and expected frequencies of target and response for BUS.

Target	Response			Total
	Pulses	Quiet	Whistle	
Fuel Bottle	56 (33.2)	19 (42.2)	9 (8.6)	84
None	26 (39.9)	68 (50.7)	7 (10.3)	101
Sm. Ball	3 (11.9)	21 (15.1)	6 (3.1)	30
Total	85	108	22	215

TABLE VI. Cell chi squares for target and response for BUS.

Target	Response		
	Pulses	Quiet	Whistle
Fuel Bottle	15.64(*)	12.75(*)	0.019
None	4.860	5.875	1.076
Sm. Ball	6.619	2.334	2.797

(*)Chi square critical value for 4 df and $p=0.05$ is 9.48773.

that BUS is capable of performing a biosonar task.

For SAY, the analysis of biosonar performance is given in Tables VII-VIII.

SAY's overall correct performance on the biosonar task was 186 correct responses out of a total of 265 trials, or 70%. Overall chi square statistics at 4 degrees of freedom yield a chi square value of 200.247 and $p < 0.0001$. The chi square cell statistics show that the null hypothesis, that SAY's responses are due to chance, should be rejected for all correct response cells. The null hypothesis should also be rejected for three of the remaining six cells. It is safe to say that SAY was performing a biosonar task in the experiments. It should also be noted that SAY's detection task was the most complex of those given to the three subjects.

Statistics are presented only for those pressurization events classed as complete, i.e., beginning and ending during the observation period. Table IX summarizes the statistics on average intranarial pressure by individual subjects and pooled over all subjects.

The average intranarial pressure within a pressurization event is calculated by summing intranarial pressure values over the course of the pressurization event and

TABLE VII. Observed and expected frequencies of target and response for SAY.

Target	Response			Totals
	Pulses	Quiet	Whistle	
None	17 (31.5)	67 (32.8)	2 (21.7)	86
Sm. Ball	25 (33.7)	3 (35.0)	64 (23.3)	92
Sm. Rock	55 (31.8)	31 (33.2)	1 (22.0)	87
Totals	97	101	67	265

TABLE VIII. Cell chi squares for target and response for SAY.

Target	Response		
	Pulses	Quiet	Whistle
None	6.660	35.73(*)	17.93(*)
Sm. Ball	2.235	29.32(*)	71.35(*)
Sm. Rock	16.84(*)	0.141	20.04(*)

(*)Chi square critical value for 4 df and $p=0.05$ is 9.48773.

TABLE IX. Descriptive statistics for complete pressurization events.

Subject	N	Average Absolute Pressure(kPa)		
		Min	Max	Ave
BRT	96	120.3	165.4	142.3
BUS	23	117.5	154.8	141.6
SAY	29	122.0	146.1	132.2
Pooled	148	117.5	165.4	140.2

dividing by the number of samples. Figures 6-17 show histograms of average intranarial pressure within complete pressurization events. Figures 6-8 show the pooled data from all three subjects. Figures 9-11 show the data for subject BRT. Figures 12-14 show the data for subject BUS. Figures 15-17 show the data for subject SAY.

The effect of the presence of a whistle ensond on average intranarial pressure of a pressurization event was tested using analysis of variance (ANOVA). Given two categories, whistle and non-whistle, yields one degree of freedom. The value of F was 54.806, which gives $p < 0.0001$. The average intranarial pressure of pressurization events with whistle ensonds was different than in pressurization events without whistles. By reference to the data, pressurization events with associated whistle ensonds had higher average intranarial pressure values.

The differences in average intranarial pressure during pressurization events (PEs) between subjects was tested by ANOVA. Given three subjects, this had two degrees of freedom, $F=15.911$, and $p < 0.0001$. Average intranarial pressure during PEs differed significantly among the test subjects.

Further analysis using Fisher's PLSD gave pairwise-comparison results between

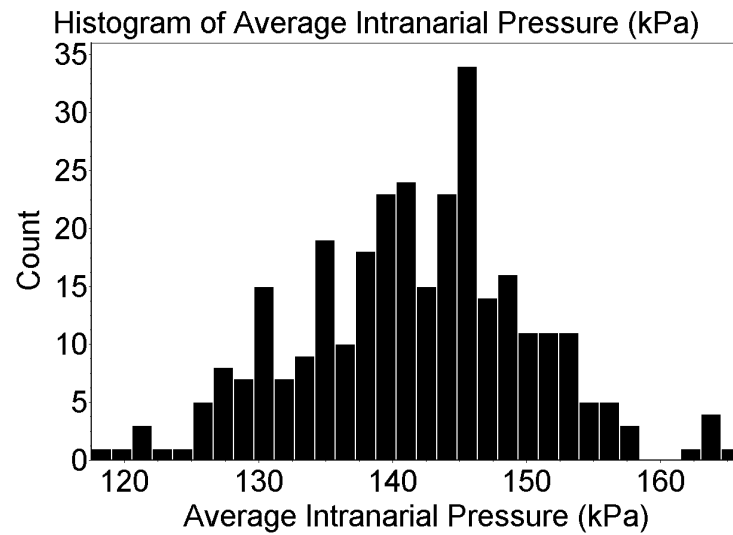


FIG. 6. Average intranarial pressure in all complete pressurization events (pooled data).

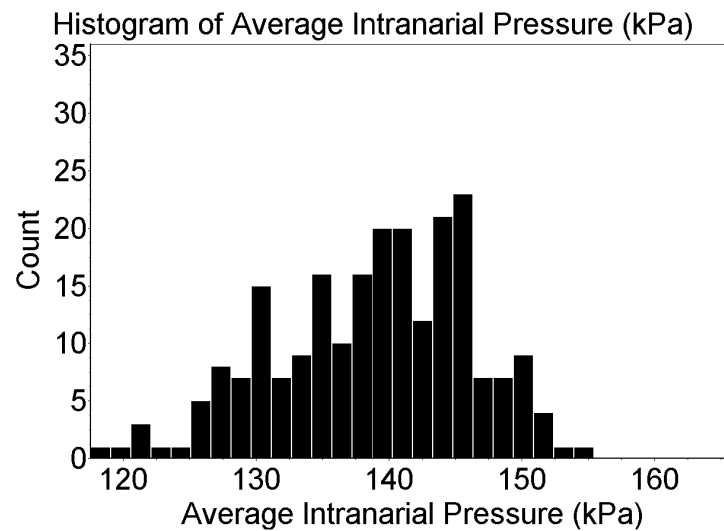


FIG. 7. Average intranarial pressure in complete pressurization events without whistle ensonds (pooled data).

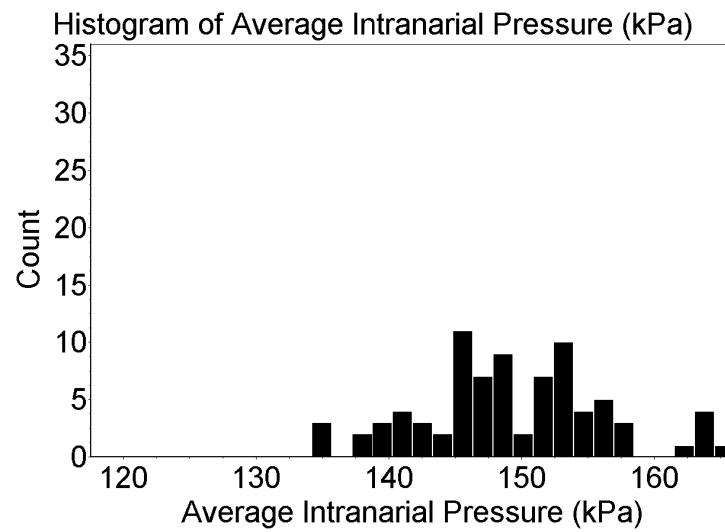


FIG. 8. Average intranarial pressure in complete pressurization events with whistle ensonds (pooled data).

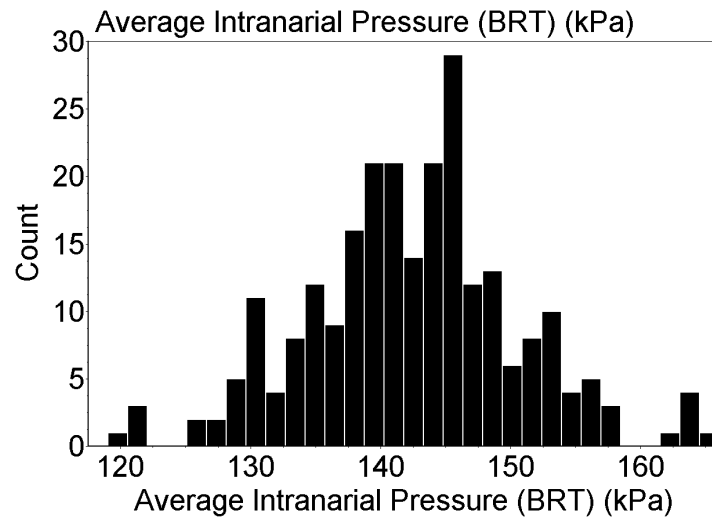


FIG. 9. Average intranarial pressure in all complete pressurization events (BRT).

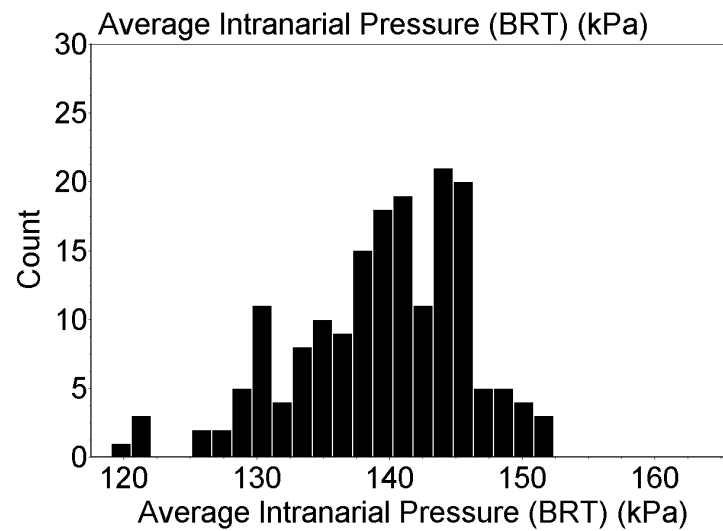


FIG. 10. Average intranarial pressure in complete pressurization events without whistle ensonds (BRT).

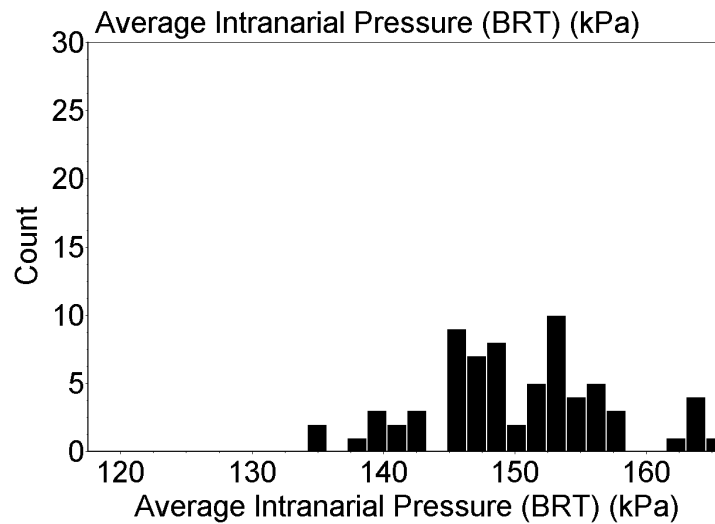


FIG. 11. Average intranarial pressure in complete pressurization events with whistle ensonds (BRT).

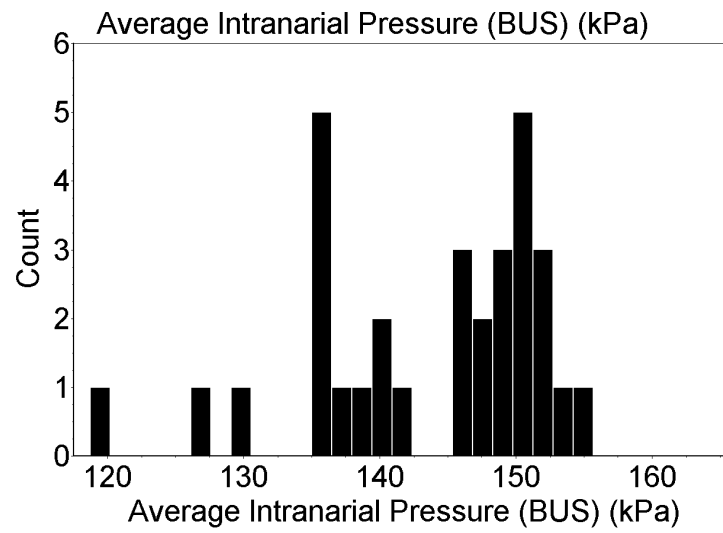


FIG. 12. Average intranarial pressure in all complete pressurization events (BUS).

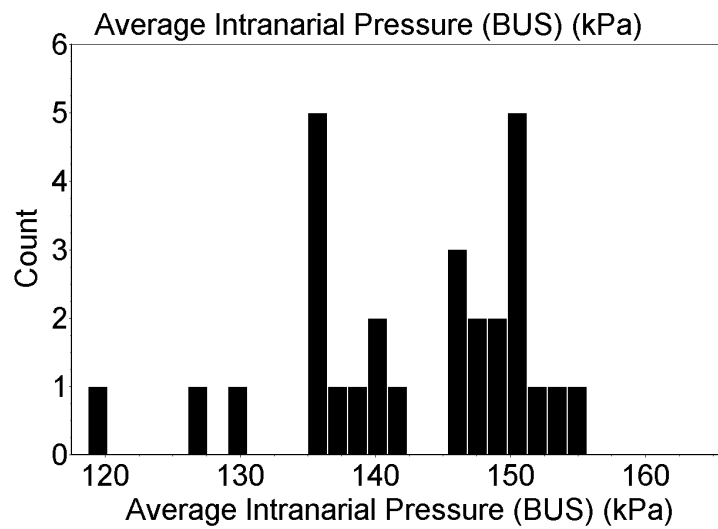


FIG. 13. Average intranarial pressure in complete pressurization events without whistle ensonds (BUS).

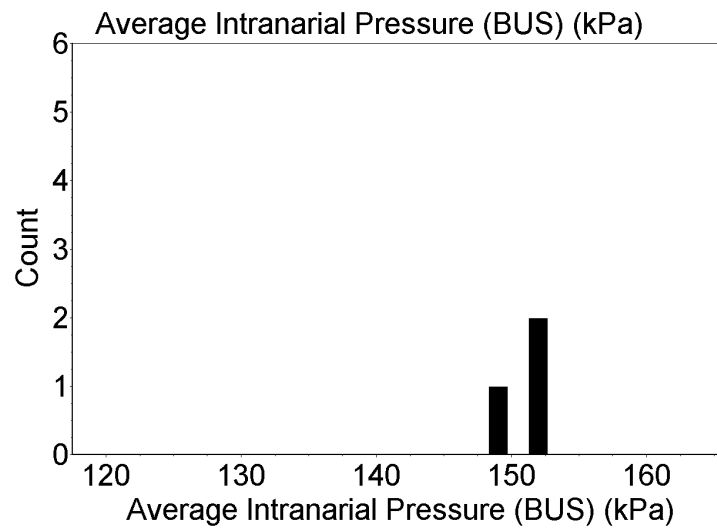


FIG. 14. Average intranarial pressure in complete pressurization events with whistle ensonds (BUS).

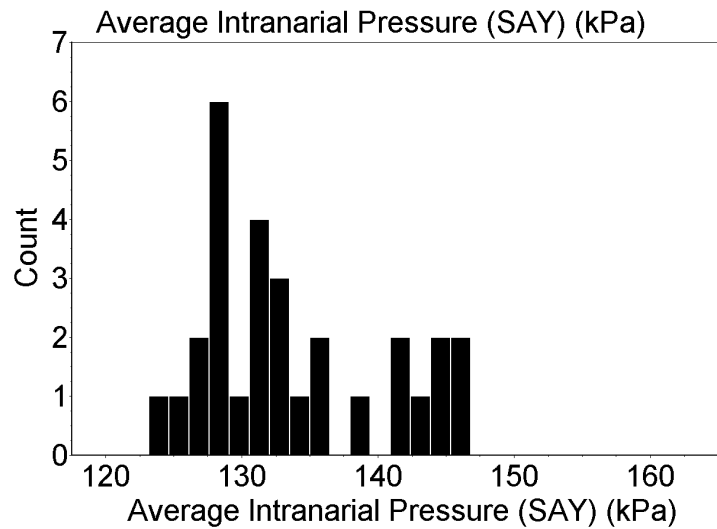


FIG. 15. Average intranarial pressure in all complete pressurization events (SAY).

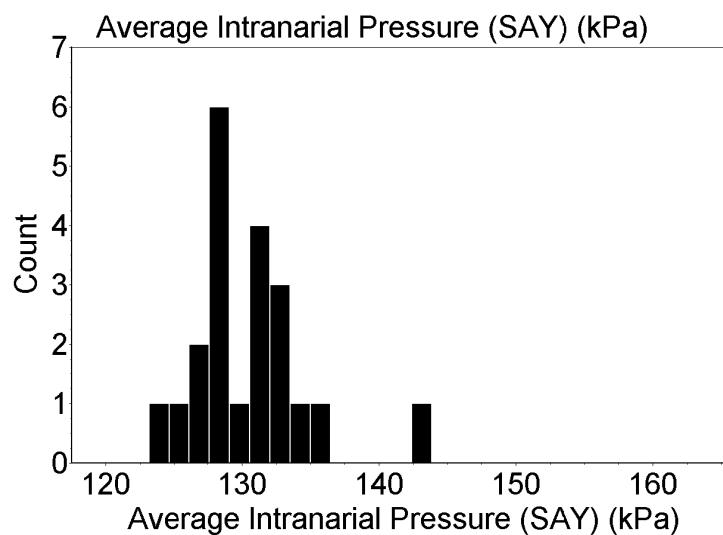


FIG. 16. Average intranarial pressure in complete pressurization events without whistle ensonds (SAY).

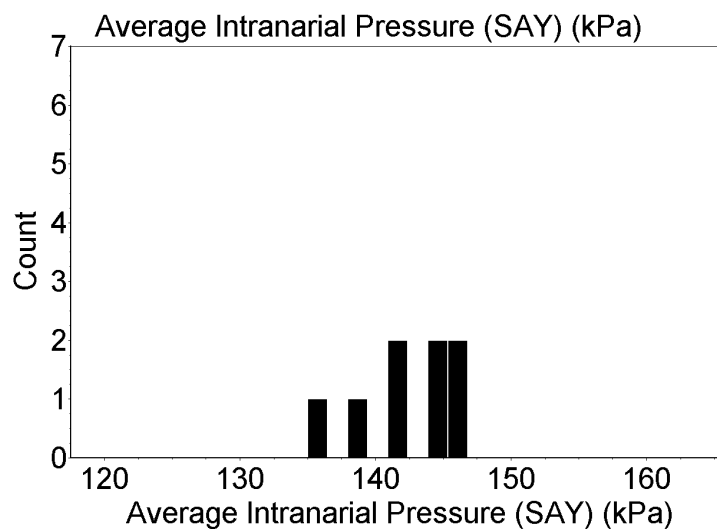


FIG. 17. Average intranarial pressure in complete pressurization events with whistle ensonds (SAY).

the subjects. This gives an approach to determining the significant differences between subjects. For comparison of BRT and BUS, $p=0.6975$, revealing no significant difference in average intranarial pressure in pressurization events for these two subjects. But comparison of BRT and SAY yielded $p<0.0001$, and comparison of BUS and SAY gave $p=0.0001$, which indicates that average intranarial pressure in pressurization events for SAY was significantly different from both BRT and BUS. Possible reasons for the difference between SAY and the other subjects is given in the discussion section.

Only the presence or absence of a whistle response was included in the dataset analyzed here; a quantification of the delay time between the end of a biosonar click train and an associated whistle response will be part of a future analysis of biosonar click train characteristics. Qualitatively, whistle responses, when observed, occurred during the same pressurization event as the biosonar click train which elicited that response.

D. Discussion

This study confirms several findings of Ridgway *et al.* (1980). The exclusive association of clicks with periods of increased intranarial pressure was also observed in the current study. This has been a consistent feature across all previous studies. Ridgway *et al.* (1980) also utilized several recording modalities which were not part of the current study. The focus of their paper was to falsify certain claims concerning the theory of laryngeal production of clicks. To this end, they also measured electromyographic data from several muscle bundles or complexes and intratracheal pressure. The key finding of Ridgway *et al.* was that intratracheal pressure remained unchanged during sound production, but intranarial pressure was elevated during all

sound production events. This is a finding that is fundamentally incompatible with theories of laryngeal sound production, and serves as a falsifying test of theories of laryngeal sound production in bottlenose dolphins. This finding arguably extends to all other odontocetes because of morphological similarity. Purves and Pilleri (1983) asserts that no increase in intratracheal pressure is necessary for laryngeal production of clicks, since they propose the laryngeal air sacs as the reservoir of pressurized gas for sound production. However, the combination of observations of no intratracheal pressure increase and intranarial pressure increase argues against that stance. The mechanism of laryngeal sound production proposed by Purves and Pilleri (1983) requires that gas passes through the larynx and empties into the intranarial space. Raising the intranarial pressure prior to sound production, as observed by Ridgway *et al.* (1980); Amundin and Andersen (1983); Ridgway and Carder (1988); Cranford *et al.* (2000), would decrease the amplitude and duration of any sounds produced in the larynx, but would be a necessary prerequisite to producing sound in the nasal passages via a pneumatic mechanism.

Electromyography of the intercostal and hyoepiglottal muscles revealed activity only during the production of “raspberry” noises, involving large amounts of air being forced out of the blowhole. Ridgway *et al.*, however, did not have a means for checking the placement of the electrodes, which leaves the possibility that some of the recordings may not have been made from the muscle groups to which they were attributed. The anatomic complexity and its potential impact on electrode placement is apparent by reference to Green *et al.* (1980).

While the current study utilized pressure catheters deployed to a depth of 10 cm and maintained there by either the attending veterinarian or the trainer, the depth of the pressure catheters in the Ridgway *et al.* (1980) study was not reported, they simply stated that the catheter was placed “through the blowhole into the nares.”

(They also placed a pressure catheter into the trachea.) One interesting difference is that in four of the published intranarial traces from Ridgway et alia, one can see intranarial pressure decrease during inhalation, which is very rare within the data from the current study. It is possible that this may be an effect of the different deployment methods utilized in each study. Ridgway and Carder (1988) used a catheter tube connected to a pressure sensor outside the nasal cavity, such an arrangement may have been more affected by Bernoulli forces as the animal breathed in.

The results reported here are in substantial agreement with the study of Amundin and Andersen (1983), who measured intranarial pressure during sound production in both the harbor porpoise (*Phocoena phocoena*) and the Atlantic bottlenose dolphin (*Tursiops truncatus*). Both studies found that there was simultaneous and equal pressurization of the left and right bony nasal passages, a minimum intranarial pressure difference that was a necessary but not sufficient condition for the production of clicks, and indications of two click sound sources in the bottlenose dolphin. The differences in results are interesting as well. The range of pressure during click production in this study is 11 to 86 kPa, while Amundin and Anderson's study reported a range of 25 to 81 kPa.

There are some reasons that would indicate that these results are comparable and commensurate. First, the dataset of this study is almost two orders of magnitude larger (>300 click trains analyzed versus 4 click trains), so it should be expected that some values beyond the extremes seen in the Amundin and Anderson study would be observed. This follows from the usual expectations of statistical sampling, that a larger number of samples drawn from a population will include more samples at the extremes of the distribution. While this may account for the difference seen at the upper end of the range (81 versus 86 kPa), it seems less likely to account for the difference seen at the low end of the range (25 versus 11 kPa). This leads to

consideration of the second reason to expect differences, which concerns differences in methodology. In this study, the actual acoustic signal from a hydrophone in the far field was recorded (with an effective bandwidth of 80 Hz to 150 kHz). In the Amundin and Anderson study, acoustic data were indirectly recorded and the hydrophone was manually held in contact with the dolphin's melon. This yields two concerns. One is that the signals were recorded in the complex acoustic environment of the near field, and the other is that placement of the hydrophone may not have been repeatable or consistent. The bandwidth of the recording device used by Amundin and Andersen was well below that needed to sample the entire bandwidth of the acoustic signal from the dolphin and porpoise. Instead, supra-threshold energy in a 1/3 octave band centered at 125 kHz triggered a waveform generator to produce a 2 kHz pulse, which was recorded. This indirect method of marking click production is biased towards the clicks with high peak frequencies and would tend to ignore lower-energy clicks with lower peak frequencies. Other reasons to expect some minor differences in results include individual differences in subjects and differences in training procedures.

Ridgway and Carder (1988) were the first to show a link between intranarial pressure and acoustics during biosonar. They utilized a white whale (*Delphinapterus leucas*) for their study. This link between physiologic and functional behavior is critical for a study of subjects in a laboratory setting. The functional behavior aspect of the study argues for comparable behavior in the wild. The difference has to do with context, where the clicks produced in a properly conducted test of biosonar actually mean something to the subject. If only *ad libitum* responses are examined, a cogent criticism is that the parameters seen could simply be the result of superstitious behavior trained into the subject in preparation for the study. Ridgway and Carder found that a substantial increase in intranarial pressure always occurred before emission of biosonar clicks. The production of whistle ensounds was preceded by an additional

increase in intranarial pressure. The data of the current study replicates these same findings for the bottlenose dolphin.

Even though intranarial pressure was always equal and simultaneous in both nasal passages, these observations do not preclude the possibility that the animals might be capable of pressurizing the nasal passages independently. In fact, anatomic observations cannot eliminate this possibility. Norris *et al.* (1971) reported cineradiographic evidence of the occlusion of one naris but not the other by the tissue of the nasopharynx. The fact that unequal pressurization of the passages has not been observed in the current study might indicate only that the task did not require such behavior.

The analysis of differences in average intranarial pressure in pressurization events between the three subjects gives statistical confirmation to a previously noted qualitative observation, that SAY seemed to be approaching the biosonar recognition task with a different strategy than the other two subjects. As reference to figure 15 shows, SAY tended to have pressurization events weighted towards the lower end of the observed range of average intranarial pressure. SAY also seemed to put less effort and resources into performing the biosonar task than either BRT or BUS. It should be noted that SAY was born and raised in a research setting and has considerable experience as a subject of biosonar research. While BRT also has extensive experience in biosonar research, she was born and raised in the wild. BRT's experience in using biosonar during foraging is likely to be more extensive than for SAY. This may well provide a partial explanation for the observed difference in approach to biosonar use between these two subjects.

E. Conclusion

This study presents the first quantification of the average intranarial pressure of pressurization events in an odontocete, the Atlantic bottlenose dolphin (*Tursiops truncatus*), and the first report of results concerning intranarial pressure during a biosonar task in the bottlenose dolphin. Previous studies have treated intranarial pressure as an associated property of click or whistle ensonds and presented sample measurements of intranarial pressure in graphical form. The single previous study of intranarial pressure during a biosonar task in an odontocete was done with the white whale (*Delphinapterus leucas*). The results of this study support and confirm several significant findings of those previous studies, including the necessity for a substantial increase in intranarial pressure before emission of biosonar clicks occur, the further increase in intranarial pressure before emission of whistle ensonds, and the pneumatic production of biosonar clicks in the nasal region. Quantitative analysis of the average intranarial pressure in pressurization events confirms previous qualitative findings that intranarial pressure is higher for those pressurization events in which whistles occur.

The results reported here and prospects for further findings have significant consequences. First, this approach and the data collected gives a window on biosonar behavior at the level of individual pressurization events. Second, the approach gives a means of examining the process of sound production. Exploration of the interrelationships of intranarial pressure, the “driving force” of the sound generation system, with the sounds emitted offers a different approach to teasing apart the sound generation process. Third, this work is a preparatory step for examination of the bioenergetics of sonar in the bottlenose dolphin. This will yield a better understanding of the relative costs of biosonar use for bottlenose dolphins.

CHAPTER III

DIGITAL SIGNAL PROCESSING FOR ODONTOCETE BIOSONAR

A. Introduction

Digital Signal Processing (DSP) is a broad field. The following summary covers some of the basic concepts needed for practical processing of odontocete biosonar signals. The overview is that we sample our signal of interest in such a way that the relevant features of the data are preserved, and process the data with respect to potential problem areas. Some issues impose countervailing constraints, and thus choices must be made to find parameter values that yield a good compromise.

B. Sampling

Real-world signals, such as those found in odontocete biosonar, are continuous in time. Handling and dealing with continuous signals is possible, but usually requires specialized hardware for analysis of spectral content. An alternative method based upon sampled data provides the means to utilize general computational equipment for spectral analysis. This alternative method is digital signal processing (DSP).

At the beginning of any DSP operation, there is the problem of sampling the data. Just as in statistical analysis, sampling should be done with care. The first point is that when we sample data, we should take our samples at a fixed sample interval. The second point is that we should sample periodic data at a sample rate that is at least double the maximum frequency of interest in our data.

There is a theorem in signal processing, known as the Nyquist theorem, that states that for a bandwidth-limited periodic signal, sampling at twice the maximum frequency captures all the information of the signal (Lyons, 1997). This is a finding

with far-reaching implications. It establishes that sampling need not be considered a necessary evil, since one can, for certain signals, be assured that one has obtained the information of the original signal. However, it is important to note that the Nyquist theorem comes with certain assumptions, and that these assumptions do not hold for some of our signals of interest in odontocete biosonar. In particular, the clicks produced by bottlenose dolphins (*Tursiops Truncatus*) are not periodic signals; they are transient signals (Diercks *et al.*, 1973). One can obtain more information about a transient signal by sampling at a higher sample rate than Nyquist suggests for a periodic signal of the same peak frequency.

The bandwidth-limit referred to in the Nyquist theorem also has important ramifications. If we do not limit the bandwidth, once we sample a signal at a particular rate, we have lost information about any part of our signal above the Nyquist frequency. This means that our samples may be ambiguous. They could represent a signal composed only of frequencies below the Nyquist frequency, or they might also represent a signal with higher frequency components. When we perform spectral analysis, any energy due to higher frequency components will be present within our results. This situation is called *aliasing*, and the energy of the high frequency components is said to be aliased into our lower frequency bins. Once a sample has been taken that has aliased frequencies in it, there is little that can be done to recover our signal of interest. The solution is to make sure that a low-pass, or anti-aliasing, filter is in place to reduce the energy of high frequency components to negligible levels. Because filters do not truncate signals abruptly, it is best to sample at a rate somewhat higher than twice the stated "cut-off" frequency of our anti-aliasing filter. In practice, this means that sampling at 1.25x the Nyquist rate or higher is reasonable in order to accommodate real-world filter designs. A more precise factor can be calculated using the characteristic roll-off of the anti-aliasing filter employed and the desired minimum

reduction in signal strength of a particular high frequency component.

The "digital" part of digital signal processing also is a factor in sampling. A digital sample is an integer value within a particular range. The range is determined by the hardware design and configuration. Analog-to-digital (A/D) conversion of a sample is characterized by the number of bits in the result. Typical bit numbers for modern equipment are 8, 10, 12, 14, 16, and 24. The number of bits determines the *dynamic range*, and is roughly equal to 6 times the number of bits for underwater acoustics, yielding an approximate figure in dB re 1 μ Pa. Signals of lower amplitude than can be accommodated in the dynamic range do not show up in the recording, while signals exceeding the high end of the dynamic range result in *clipping*. A clipped recording has two or more consecutive values at an extreme of the range. Clipping reduces the usefulness of a recording by inducing spurious frequency components when the signal is converted to the frequency domain. The number of bits also affects the *quantization error*. Because the input sample can vary continuously, but the digital representation must take one of a finite set of values, there is likely to be some difference between the actual sample value and the digital value after conversion. This difference is the quantization error.

A tradeoff is necessary in selecting sampling hardware. A larger number of bits per sample is desirable to increase dynamic range and reduce quantization error. Typically, though, a larger number of bits decreases the maximum sampling rate possible (and increases the cost). In order to obtain the necessary sampling rate for the application, one may be forced to use a smaller number of bits per sample.

Another sampling issue concerns the aperture problem. The aperture in A/D sampling can be thought of as the window in time over which a sample value is evaluated. Because a sample varies over time, one would like to effectively limit this period to a brief enough time such that even when the signal of interest is changing

at its maximal rate, the largest amount of expected change covers no more than the range of the least significant bit in the result. In general, this amount of time is very much smaller than the actual time that it takes to convert a sample. In order to accomplish this, most modern A/D equipment utilizes "sample and hold" circuitry that briefly samples the original signal and then holds that value throughout the time needed for the A/D conversion to take place.

C. Analysis

It is now appropriate to lay out how various characteristics of these signals are quantified. Broadly, these can be split into those characteristics determined from the time domain data, and those which are determined from the frequency domain. The time domain features of interest for biosonar clicks in the present study are the click duration, the peak-to-peak source-level amplitude, the Energy Flux Density (EFD), and the radiated acoustic power. The frequency domain features of interest are the peak frequency, the dominant frequency, the -3dB bandwidth, the relative frequency, and the classification of the click under the scheme proposed by Houser *et al.* (1999).

A concept whose application will recur often in analysis is that of a *centroid*. A centroid of a sequence of values is a weighted mean, where for each item in the sequence, the index number is multiplied by the value of the item at that point. A sum of these products is taken, and then this is divided by the sum of the values. The result is a number within the range of index numbers examined. The main property of interest in calculating a centroid is that the sum of values below the centroid is equal to the sum of values above it.

$$Centroid_x = \frac{\sum_{i=k}^{n+k} i * x_i}{\sum_{i=k}^{n+k} x_i} \quad (3.1)$$

1. Time-domain characteristics of clicks

An important characteristic of a click vocalization is the amplitude. Because clicks are transients, the peak-to-peak source level amplitude is taken as the relevant metric (Au, 1993). This is a measurement in the time domain of the absolute value of the amplitude difference between the maximum and minimum sample values within the click adjusted to account for sound spreading loss such that the level given is that as if the original signal was measured at one meter distance from the source.

Energy Flux Density (EFD) gives a concise way of representing the intensity of a vocalization. EFD measurement is accomplished by reference to the samples in the time domain. Urick (1983) gives the equation for EFD as

$$E = \int_0^{\infty} I dt = \frac{1}{\rho c} \int_0^{\infty} p^2 dt \quad (3.2)$$

(p.14)

where I is intensity, ρc is the *specific acoustic resistance* of the medium, and p is the instantaneous pressure. For sea water, Urick gives a ρc value of $1.5 * 10^5$ g/(cm²)(s).

Au (1993, eqs. 7-18 and 19) gives a formulation in terms of the click waveform in the time domain.

$$p(t) = As(t)E = A^2 \int_0^T s(t)^2 dt = A^2 E_N \quad (3.3)$$

where $p(t)$ is the time domain waveform of the click, A is the peak amplitude of the click, $s(t)$ is the normalized waveform, E is the EFD value, and E_N is the energy of the normalized waveform. Au's figure for EFD is expressed in dB re $1 \mu\text{Pa}^2\text{s}$.

The directivity index (DI) of a signal indicates the degree to which the signal is directional. An omnidirectional source has a DI of zero, while directional signals have

a positive DI expressed in dB re 1 μ Pa. The determination of radiated acoustic power incorporates the directivity index as a factor. Directivity index was not determined for the subjects in this study. The average figure for directivity index found by Au *et al.* (1978); Au (1980); Au *et al.* (1986) of 25.8 dB is used in making the calculation of radiated acoustic power.

Au (1993, pp. 129-130) outlines a method of estimating the radiated acoustic power within a click. Radiated acoustic power is the total energy per unit time actually transferred to the conducting medium. A direct measurement of radiated acoustic power would require characterizing the sound field around the subject at some distance, requiring multiple transducers in practice. Au's method of estimation relies upon obtaining the root-mean-square (RMS) source level of a click on the major axis and applying a directivity index. Because no measurements of directivity have been made for the individual subjects used in this study, the averaged value obtained by Au *et al.* (1978); Au (1980); Au *et al.* (1986) in studies of three bottlenose dolphins, 25.8 dB re 1 μ Pascal, is used here as the best available estimate. The RMS source level is obtained from the peak-to-peak level by the following equation:

$$SL_{rms} = SL_{pp} - 6 + 20 \log \left(\sqrt{\frac{1}{T} \int_0^T s^2(t) dt} \right) \quad (3.4)$$

Au (1993, eq. 7-15, p.130)

where $s(t)$ is the normalized click waveform. For one particular averaged set of clicks in a click train, Au reports a 15.5 dB reduction from peak-to-peak source level to obtain the RMS source level. This figure will vary depending upon the specific click analyzed.

To find the radiated acoustic power of a click, one can use Au's Eq. 7-12 (Au, 1993, p.130).

$$10 \log P_D = SL_{rms} - DI - 171 \quad (3.5)$$

The constant of 171 holds for a distance of 1 meter, the density of sea water, the sound velocity of sea water, and a factor of 10^{-12} used as a conversion from μ Pascals. DI is the directivity index. Because directivity was not determined for the subjects of this study, the directivity index value of 25.8 dB re 1 μ Pascal reported by Au *et al.* (1978); Au (1980); Au *et al.* (1986); Au (1993) is used instead. The RMS source level and the peak-to-peak source level will be found to differ by some number of dB, as determined by application of Au's Eq. 7-15 shown above. Refer to this factor as and modify Au's Eq. 7-12 as follows:

$$10 \log P_D = SL_{pp} - DI - 171 - (PP \rightarrow RMS) \quad (3.6)$$

Because the directivity index for bottlenose dolphin clicks is taken here as a constant, this can be further simplified as

$$10 \log P_D = SL_{pp} - 196.8 - (PP \rightarrow RMS) \quad (3.7)$$

The resulting figure is in dB re 1 Watt. The determination of acoustic power is done by reference to the time domain samples.

2. Frequency domain characteristics of clicks

The use of spectral methods in analysis of bioacoustics is ubiquitous, and with good reason. However, there are a variety of issues that arise in using standard Fourier analysis of the click vocalizations of bottlenose dolphins. These are commonly encountered in engineering whenever transient signals are the focus of interest. The Discrete Fourier Transform (DFT) takes time domain data and converts it into a

frequency domain representation. The time domain data is a series of samples taken at regular intervals (the sampling period), where each value represents an amplitude at the sensor at that time. The frequency domain, though, is a complex plane. When just the magnitude is considered, each index in the frequency domain represents a summation of energy within an analytical bandwidth of frequencies.

The Discrete Fourier Transform (DFT) is founded upon a set of assumptions about the signal under analysis. First, the signal is assumed to be bandwidth-limited. Second, the signal is assumed to be periodic. The click vocalizations of bottlenose dolphins are transients, and thus violate the second assumption.

The DFT conceptually allows the conversion of time domain information into the frequency domain, but as a practical matter the DFT is impractical to compute for larger window sizes. A more efficient means of computing the DFT for a restricted class of window sizes was developed by Cooley and Tukey (1965), and is known as the Fast Fourier Transform (FFT). It should be emphasized that the FFT is a DFT, and does not represent a different type of transform (such as z or wavelet transforms). It is arguable that the appropriate term for the Fast Fourier Transform would be the Faster Discrete Fourier Transform, or FDFT. However, it is likely far too late to change this convention. The principal restriction on window size is that it must be an integer power of two. The FFT algorithms avoid the redundant calculations of the general DFT algorithm. This gives a speed-up of several orders of magnitude for window sizes of 1024 points or larger. The restriction to integer powers of two for the window size in the FFT introduces some issues pertaining to analysis frequencies and leakage.

Window size in the DFT, coupled with the original sampling rate, defines the base analytical frequency of the transform. This is the frequency which, multiplied by some integer factor, is at the center of each bin of the output. Given a fixed-amplitude

sinusoidal signal, increasing window sizes yield larger values in the frequency bins. Thus, results from the DFT must be scaled to account for the window size.

A property of the DFT is that energy in the signal that is not an integer multiple of the base analytical frequency “leaks” into other frequency bins, and is not fully represented within the frequency bin closest to the actual frequency of the signal. This leakage is a well-recognized problem in discrete Fourier signal analysis (Lyons, 1997). When dealing with narrowband signals, three approaches help reduce leakage. The first is to select a window size/sampling rate combination that places the peak frequency of the signal of interest at an integer multiple of the base analytical frequency. This is most easily accomplished when using the general DFT algorithm, where even if a fixed sampling rate is used, the window size is free to vary. The second approach is to apply a windowing function to the signal before performing the DFT. Windowing functions (other than the rectangular window) typically reduce the size of samples at the beginning and end of the sample window, while not much affecting the sample values in the middle of the sample window. This reduces the amount of apparent leakage, but does not eliminate leakage entirely.

A variety of windowing functions have been applied to signals for the DFT. The rectangular window simply passes the original sample values unchanged (or one may consider it multiplication by a constant value of one). The Bartlett window goes linearly from a factor of zero at the beginning to a factor of one at the middle, then linearly down from a factor of one to a factor of zero at the end of the sample window. Hamming and Hann windows are similar to each other, and use a trigonometric function to reduce the amplitude of early and late samples more than that of samples in the middle of the window (Lyons, 1997).

Selection of a windowing function involves a tradeoff between reduction of side-lobes (spurious energy in other bins due to leakage) and frequency resolution (the

ability to distinguish distinct frequency components). For much work reported on bottlenose dolphin vocalizations, the Hamming window has been the window of choice. For the purpose of allowing comparison to existing work, the Hamming window is adopted in this study as well. It provides good frequency resolution and a moderate reduction in sidelobe size.

When applying the DFT to a transient signal or to a signal which is not periodic in the window size, it is typical to “pad out” the remaining samples in the sample window with zeroes. This zero-padding helps reduce scalloping loss and allows the use of larger window sizes to increase the frequency resolution.

While bottlenose dolphin clicks have been well-characterized as being broadband signals, there will be some frequency which represents the peak frequency of the click. The peak frequency is found by converting the time domain signal into the frequency domain and finding the frequency with the greatest magnitude. This conversion of time domain to frequency domain is done here via use of the Discrete Fourier Transform (DFT) as implemented in a Fast Fourier Transform (FFT).

A slightly different measure than peak frequency is dominant frequency as defined by Wiersma (1982). This measurement is, like Wiersma’s definition of time duration, based upon the variance of the data, in this case of the power spectral density. Given $S(f)$ as the Fourier transform of the signal of interest, Wiersma defines dominant frequency as

$$f_d = \int_{\Omega} f |S(f)|^2 df \quad (3.8)$$

where Ω is the index of the last positive frequency in the Fourier transform. This measure is essentially the centroid of the power spectral density. Because frequency components may have a skewed distribution, dominant frequency gives information

about the center of the energy in the frequency domain that may not be reflected in the peak frequency property. The terminology established by Wiersma (1982) has not been followed exactly in later work. For example, Kamminga *et al.* (1993) utilize dominant frequency to refer to the frequency component with the greatest spectral energy density (what others have called the peak frequency), and use the phrase central frequency to refer to what Wiersma calls dominant frequency. When attempting to compare information between papers, this ambiguity of reference makes it especially important to verify which concept is referred to, and not simply assume that the same phrase always refers to the same concept.

In the frequency domain, a click vocalization can be characterized by its power spectral density (PSD) plot. The PSD for a signal graphically shows the relative magnitude of the various frequency components on a \log_{10} scale, and can be numerically analyzed to provide information on the bandwidth of the click. Bandwidth is commonly expressed in Hertz or kilohertz, and represents how broad the signal of interest is at some specified magnitude level down from the magnitude of the peak frequency. Commonly reported values are for -3dB, -6dB, -10dB, and -20dB bandwidths. Sometimes the minus signs are omitted, so a “3dB bandwidth” means the same thing as a “-3dB bandwidth”.

Wiersma (1982) provides a different method for finding a frequency bandwidth. This is a statistical measure, like his determination of click duration, and is based upon the variance of the signal in the frequency domain. Given the discrete Fourier transform of the signal of interest, $S(f)$, and the dominant frequency, f_d , (as defined above), the frequency bandwidth is found as

$$\sigma_f = \left[\int_T (f - f_d)^2 |S(f)|^2 df \right]^{1/2} \quad (3.9)$$

$$\Delta f = C_2 \sigma_f = C_2 \left[\int_T (f - f_d)^2 |S(f)|^2 df \right]^{1/2} \quad (3.10)$$

where C_2 is a positive proportionality constant selected to put this bandwidth measure into general accord with the usual -3dB bandwidth. Wiersma selected a value of 2 for C_2 , corresponding to 2 standard deviations.

D. Conclusion

Digital signal processing (DSP) for odontocete biosonar signals is a powerful technique for exploration of these signals. There are certain advantages which DSP has over techniques which require specialized analysis hardware. A properly sampled signal can be communicated and shared among researchers, allowing direct examination of the same signal and replication of analysis between many different researchers.

Data acquisition requires appropriate selection of a sampling rate. The suitability of the acquired data for particular analyses will be determined by the system bandwidth used and sampling rate. In reporting on acoustic signals, researchers should be careful to communicate the parameters of low-pass frequency, high-pass frequency, and sampling rate.

Analysis of signals requires the selection of a variety of parameters and even algorithms. One critical choice concerns how to determine the *click duration*, which will be discussed in detail in the next chapter. Other time-domain and frequency domain features of interest can then be extracted from the original signal. Results in frequency-domain analysis via Fourier methods are sensitive to the selection of window size, window function, and whether zero-padding is utilized. It is important for purposes of comparing results between researchers that the choices made in DSP analysis also be reported when analyses are published.

CHAPTER IV

BIOSONAR CLICK CHARACTERISTICS

A. Introduction

Atlantic bottlenose dolphins (*Tursiops truncatus*) produce a variety of sounds. Early descriptions utilized many different descriptors: clicks, blats, yelps, barks, mews, squeaks, buzzes, rasps, moans, groans, pops, and whistles (Slijper, 1979; Kellogg, 1961; Wood, 1973). These usefully reduce to three broad categories: clicks, whistles, and pops (Wood, 1973). (Whether pops are actually classifiable as clicks is a matter of argument.) Most of the sounds described with other terms are actually composed of a series of clicks. Clicks are thought to be employed by bottlenose dolphins in two broad functional categories, communication and biosonar (Wood, 1973).

Representing clicks is a perilous enterprise. The difficulties of measuring and analyzing clicks as transient signals have long been recognized (Diercks *et al.*, 1973). While the time domain representations all have certain features in common, the frequency domain representations show considerable variation. Attempts to find a “typical” click are problematic: out of a range of examples having variation in each of several dimensions or characters, how does one select a purportedly typical exemplar? What is needed is a presentation of the variation present in the entire range of clicks rather than concentrating on measures of central tendency.

1. Ensonds in bottlenose dolphins

This brings up the question of how to define the broad categories. A whistle can be considered as a tonal ensond of extended duration, while a click can be considered as a transient impulsive ensond of limited duration. As with any other attempt to

classify messy biological reality, there is often a certain fuzziness at the boundaries. One source of fuzziness comes from species other than *Tursiops*. Various porpoises and some delphinids emit clicks which are very narrow in bandwidth (and thus tonal like whistles), but relatively short in duration.

Many authors use “pulse” as a synonym for “click.” The term “click” is utilized here by preference. When a series of clicks is specified, the phrase “click train” will be used. A special case will also be made for those click trains with a very high repetition rate (>600 clicks per second), where the traditional and common phrase, “burst pulse,” will be used. Ridgway (1983) used three categories of sounds, as whistles, click trains, and burst pulse sounds. The distinction between click trains and burst pulses appears there to follow from work showing that there is brain response to individual clicks when the repetition rate is 600 clicks per second or less (Ridgway, 1983).

2. Determination of the duration of a click

Finding the duration of a click is a necessary prerequisite to finding other relevant information about a click, such as the energy flux density or radiated acoustic power of the click. This property of a click has long been noted as a difficult property to quantify (Diercks *et al.*, 1973). Because of the presence of noise in recording, there is necessarily uncertainty in determining the duration. There is some controversy over how this property should be measured, which traces back to how various researchers define a click. Click duration was determined according to three different procedures, as discussed by Wiersma (1982), Kamminga with a number of colleagues (Kamminga and Beitsma, 1990; Kamminga and Cohen Stuart, 1995; Kamminga *et al.*, 1993, 1996, 1998, 1999), and Au (1993). The differences between these approaches reflect differing concerns over defining the content of the transient biosonar signal of odontocetes.

Wiersma's approach is statistical in nature and is based upon a characterization of the variance in the time-domain signal of the click. Kamminga's procedure is based upon a theoretical assumption about what portion of a recording containing a click actually may be useful to the dolphin in performance of a biosonar task, and derives from Wiersma's approach. Kamminga takes the envelope of the click signal as a sufficient approximation to Wiersma's variance-based calculation. Kamminga instead prefers to consider only the very high-energy components of the recorded waveform as being the portions likely to be useful in biosonar tasks. Au's procedure is based upon attempting to include the majority of energy seen in a click recording. Given a click waveform recorded from a dolphin, Au utilizes a relationship between total energy in a click and energy at the tail of a click. All three provide useful information about click duration. Other approaches taken from signal processing might also be utilized, such as rectangular width, autocorrelation width, or mean-square width. These latter measures were not evaluated in this study.

To some extent, any approach will be arbitrary, and the choice of approach should be made with respect to the particular question under study. The primary goal is to delimit the choices that are arbitrary, and obtain the benefits of placing click duration determination on an objective and repeatable footing.

Au (1993, p. 130) says the following:

"[...] T was determined as the time at which $\int p^2(t) dt$ increased no more than 1% as t increased."

Au's reported method for finding the duration of a click gives the groundwork for an objective method of click duration determination, but does not account for all the problems that may be encountered. We wish to find a duration T for a click. Given an initial point i , we integrate numerically over a certain number n sampled points as $\int_i^{i+n-1} p^2(t_i) dt$. We also integrate for $n - 1$ points, and divide the two integrals, with

the $n - 1$ point integral as the denominator. If the quotient is greater than 1.01, we increment n and continue. If the quotient is less than 1.01, we take our click duration T to be the time necessary to make $n - 1$ samples.

The first problem to face is that attempting to pick an initial point is an endeavor likely to result in an arbitrary and subjective measurement of click duration. Choosing different initial points for the same click will produce different durations for the click. An algorithm that produces a single measurement of duration is desired. As discussed by Blackwood (1991), one solution to this sort of problem is not to select an initial value or even an end value, but rather to start in the middle and work outward in both directions. Fortunately, the typical shape of a dolphin click makes this easy to do. By taking the *centroid* of the rectified click as a landmark, the algorithm works in both directions to find the extreme values for the duration of the click. Fristrup and Watkins (1992) utilized a centroid determination to find the acoustic feature they termed the *signal center*. The following is a modified description of finding a click duration. By definition, the centroid is within the click. Start with the index of the centroid of a click and find the duration via a “greedy” algorithm. Greedy algorithms evaluate local data points and propagate outward based upon decision rules in the algorithm. Given some interval that is accepted as being within the click (initially the samples at either side of the index of the centroid of the click) and compare the two adjacent samples at each end of the interval to each other. The larger of the two adjacent samples is evaluated to see whether it meets the criterion of having more than 1% of the energy in the accepted click interval. The initial click interval is the energy within the single sample of the centroid of the click. As additional sample points are accepted by the algorithm, their energy is added to the sum for the click. If so, the interval is adjusted to incorporate that adjacent click, and another round of comparison of adjacent samples is performed. If not, the algorithm terminates.

The second problem is that a literal reading of Au’s method indicates that if a sample happens to lie close to zero, the click duration algorithm may be cut off at that point, even though significant energy could lie beyond that point. An approach to solving this problem is to find the click duration by reference to a smoothed waveform, rather than simply the squared sample values. Thus, the relevant equation to use becomes

$$\int g(t) dt \tag{4.1}$$

where

$$g(t) = 0.25 * p^2(t - 1) + 0.5 * p^2(t) + 0.25 * p^2(t + 1) \tag{4.2}$$

This smoothing function is selected simply as an efficient function to apply in computation, but other smoothing functions could be substituted. Such a smoothing function has the effect of spreading energy, reducing the occurrence of “premature” termination of the algorithm based simply upon a small absolute amplitude for a particular sample.

The third problem is that when looking at click signals individually, rather than averaged together as Au uses them, the relative amplitude of the click influences the computed duration. All real-world measurements have a certain amount of noise, and this background noise level will cause a lower-amplitude click signal to be measured as having a longer duration than a higher-amplitude click. While background noise also influences the computed duration of the highest-amplitude click, its effect is smaller when the signal-to-noise ratio is higher. When higher noise levels are present, click durations will be computed as being longer, even if the click otherwise is identical in amplitude and shape to another taken under less noisy conditions. This increase in

computed duration can be thought of as an effect of our uncertainty concerning where to fix the endpoints of a click. The more noise is present, the greater our uncertainty on this point, and thus the greater the computed duration. This concern affects all means of computing a click duration.

The procedure given by Wiersma (1982) for finding the time duration of the click signal is interesting. Wiersma begins with a click waveform, $s(t)$, and proceeds to convert it into a form analogous to a probability density function.

$$\int_T k|s(t)|^2 dt = 1 \quad (4.3)$$

The form of the equation as given here differs slightly from Wiersma, in that the factor k as a normalizing factor is omitted from Wiersma's equation. The next step is to find the mean or midpoint of the time domain waveform. Wiersma's equation for this task is

$$\bar{t} = \int_T kt|s(t)|^2 dt \quad (4.4)$$

Again, the normalization factor k is inserted into the relevant equation. The equation above is equivalent to finding the centroid of the time domain waveform. Now, Wiersma finds a property analogous to the standard deviation of the waveform.

$$\sigma_s = \left[\int_T k(t - \bar{t})^2 |s(t)|^2 dt \right]^{1/2} \quad (4.5)$$

This leads to an equation for the time duration of the signal.

$$\Delta t = C_1 \sigma_s = C_1 \left[\int_T k(t - \bar{t})^2 |s(t)|^2 dt \right]^{1/2} \quad (4.6)$$

where C_1 is a positive proportionality constant chosen to include the relevant energy of the click. Wiersma selected $2 * \pi$ as the value for C_1 . This gives us a click

duration based upon more than 6 standard deviations, which seems to be a generous estimate.

Kamminga's methodology differs substantially from that described above for Au. There are two somewhat different procedures that Kamminga discusses for finding the time duration of the click signal. In one, Kamminga follows the method used by Wiersma (1982), which is premised upon characterizing the variance of the waveform. In the other, in order to determine click duration, one must construct an *analytic signal* representation of the click. This is done by treating the time domain samples as the real component of a complex vector, and the Hilbert transform of the time domain as the imaginary component of that complex vector. By taking the magnitude of the complex vector, an envelope of the signal is produced. The indices of the local minima on either side of the highest magnitude lobe of the envelope then define the click duration.

B. Methods

The digital data records of intranarial pressure and sound were processed using a custom software application. The "bsp" (*biosonar program*) application permitted browsing of the digital data with multi-channel visual display. A sample record selected by the user could then be processed. This was a multi-step procedure.

In the first step, clicks were automatically selected by an algorithm, then checked for accuracy by the user. The automatic routine made occasional false positive and false negative picks, though false positives were relatively more common than false negatives. Through clicking the mouse on a visual display of the acoustic waveform, the user could select points and delete selections, add selections, and adjust selections of clicks. A button press would allow the clicks within the view on screen to be

displayed one at a time in sequence, with about 1/2 second interval between clicks. This produced an effect like a motion picture and an easy check on correct selection of clicks in a click train. Once clicks were selected and checked for accuracy, the user entered relevant information from the annotated data notebook, such as the treatment type and target stimulus for a particular biosonar recognition trial. Another button press would result in the 256 data points around each click being extracted and saved to the hard disk. Information about intranarial pressure at the time of each click was similarly saved to hard disk. The important feature here is that the selected information takes up much less space than the original data from which it is taken.

The second step is to save information concerning any whistle responses present in the current biosonar trial. A visual display of the acoustic waveform allows the user to select the start and end point of the whistle response. The data in the selected region is saved on the hard disk.

The third step is to save information concerning pressurization events. A reduced representation of the entire intranarial pressure sample is created. This procedure averages all the samples within each millisecond interval in the sample and writes out the average value for that millisecond interval. The resulting file is approximately 1/250th the size of the original sample data file. Then, the user selects a section of the time domain representation on-screen which characterizes the basal pressure, the intranarial pressure when the dolphin has closed off the blowhole but is not attempting to make sounds.

An automated procedure then examines the sample data to find potential pressurization events, elevations in intranarial pressure commonly associated with sound production (Ridgway *et al.*, 1980; Amundin and Andersen, 1983; Ridgway and Carder, 1988). Automating this selection of the starting and ending points of pressurization events was intended to reduce possible observer bias and inconsistency which would

have resulted from relying upon a user to select these points manually. This routine looks for an elevation in pressure over 10 measured units above the calculated basal pressure in the reduced data representation. The number 10 derives from the observation during calibration that the standard deviation of 10,000 samples at a constant pressure was usually a little over 3 measured units, which puts 10 well beyond two standard deviations out. Finding such a value marks the beginning of a candidate pressurization event. The routine then compares values until a value which drops below this threshold is found, marking the end of a potential pressurization event. A special case is checked, which is where a discontinuity in the data occurs, defined as a drop below 90% of basal pressure. During data collection, sometimes the subject would dislodge the pressure catheter from the bony nares, and this circumstance is marked by a sharp drop to local ambient pressure, usually well below the measured basal pressure. A potential pressurization event was highlighted visually on screen and the user was prompted to accept or reject a record based upon the selection. This was needed because the routine would produce false negatives – it would sometimes highlight a region of the intranarial pressure record which did not correspond to an actual pressurization event. The statistical nature of the recognition algorithm made this inescapable although the distinction was usually trivial for the user.

A pressurization event recognized by the program and accepted by the user would then be classified and a record stored on the hard disk. The classification was to a set of four alternative conditions based on the end points of the pressurization event: complete, open at beginning, open at end, and open at both. If both the beginning and end of the pressurization event met the threshold value above basal pressure, the pressurization event was classed as complete. The practical import is that all of the pressurization event occurred within the bounds of the trial period without any discontinuities. If the beginning of the pressurization event had a value higher

than the threshold above basal pressure, but the end of the pressurization event met the threshold value, the pressurization event was classed as open at beginning. This usually indicated that the pressurization event was already in progress at the start of the trial period. If the end of the pressurization event had a value higher than the threshold above basal pressure, but the beginning of the pressurization event met the threshold value, the pressurization event was classed as open at end. This indicated that the trial period ended while the pressurization event was in progress, or that a discontinuity in recording meant that the end of the pressurization event was not recorded. When both the beginning and end of the pressurization event were higher than the threshold above basal pressure, the pressurization event was classed as open at both. This usually indicated that the pressurization event began before the start of the trial period and continued past the end of the trial period, or until a discontinuity in recording. The recording period was normally 5 seconds in duration.

Another custom software application, “an” (*analysis*), was used to process the reduced data and quantify many aspects of clicks, click trains, and pressurization events. This application allowed the user to interactively examine all of the different types of data records saved by the data reduction program. A routine found and processed all click records to determine the following properties: click duration, peak-to-peak source-level amplitude, energy flux density (EFD), radiated acoustic power, peak frequency, dominant frequency, -3dB bandwidth, Wiersma bandwidth, relative frequency, and instantaneous intranarial pressure above basal pressure. The program also has a facility for the production of histogram and bivariate plots of the data, and also waterfall displays of spectra from click trains.

After implementing approaches for finding click duration based upon the descriptions from Au, Wiersma, and Kamminga, the variance-based approach from Wiersma appeared to yield the most stable and reliable results on the data. All click durations

reported here utilize the variance-based measurement from Wiersma (1982).

1. Automated classification of clicks

The custom analysis application “an” implemented the click classification scheme of Houser *et al.* (1999) as follows. The algorithm was given a *power spectral density* (PSD) plot to be classified. The parameters for production of the PSD were as follows. An FFT of 2048 points was used. Only the sample points within the click duration were used. A Hamming window function was applied to those points. The remainder of the FFT window was zero-padded. Within the classification algorithm, the peak frequency, -3 dB bandwidth, and -10 dB bandwidths were found. A subroutine counts the number of peaks in the band within -3 dB of the peak frequency. If the number of peaks is greater than 2, the click is classed as “M: Multiple”. If there are exactly two peaks in the -3 dB band, the click is classed as “C: Bimodal”. If the -3 dB bandwidth is greater than 85 kHz, the click is classed as “W: Wideband”. A click with a single peak in the -10 dB band with a peak frequency of 70 kHz or less is classed as “A: Unimodal Low”. A click with a single peak in the -10 dB band with a peak frequency of greater than 70 kHz is classed as “E: Unimodal High”. A click with a secondary peak within the -3 to -10 dB range and a peak frequency of 70 kHz or less is classed as “B: Dual Low Dominant”. A click with a secondary peak within the -3 to -10 dB range and a peak frequency of greater than 70 kHz is classed as “B: Dual High Dominant”.

C. Results

A representative high-amplitude click is shown in figure 18. The PSD plot of the FFT of the click of figure 18 is shown in figure 19. The FFT parameters were 2048 points

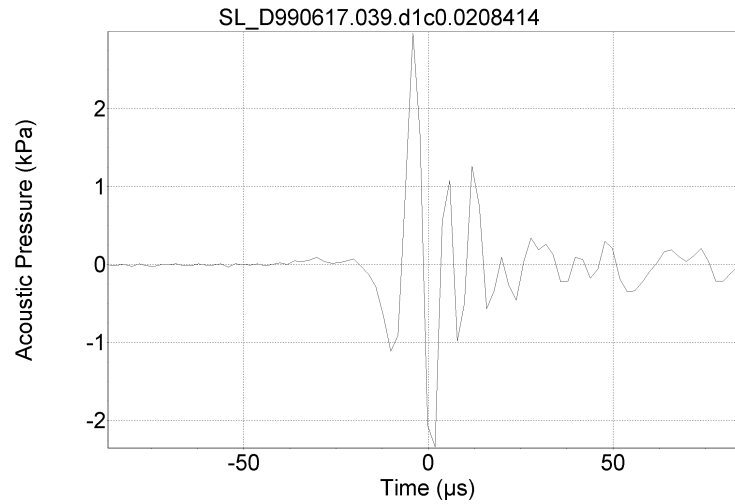


FIG. 18. Representative bottlenose dolphin click time domain sample.

in the window, with a Hamming window function applied over the sample points, and zero-padding applied to fill out the remainder of the points.

1. Time-domain characteristics

Peak-to-peak source level amplitude results are summarized in Table X and histograms are given in Figures 20-23.

Analysis of peak-to-peak source-level amplitude via ANOVA split by subjects shows significant differences at $p < 0.0001$ (2 DF, $F = 1669.445$). Using Fisher's PLSD, between subject comparisons were all significant at $p < 0.0001$.

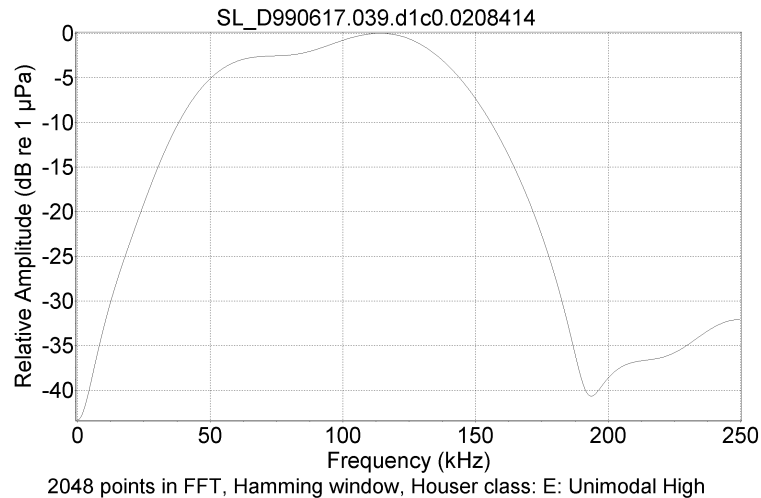


FIG. 19. Representative bottlenose dolphin power spectral density plot.

TABLE X. Descriptive statistics of peak-to-peak source amplitudes (in dB re 1 μ Pascal).

Subject	Count	Minimum	Maximum	Mean	S.D.
BRT	10,852	151.8	217.4	179.3	12.32
BUS	2,573	156.9	207.4	189.5	10.3
SAY	1,602	161.9	211.0	194.1	8.9
Pooled	15,027	151.8	217.4	182.6	12.9

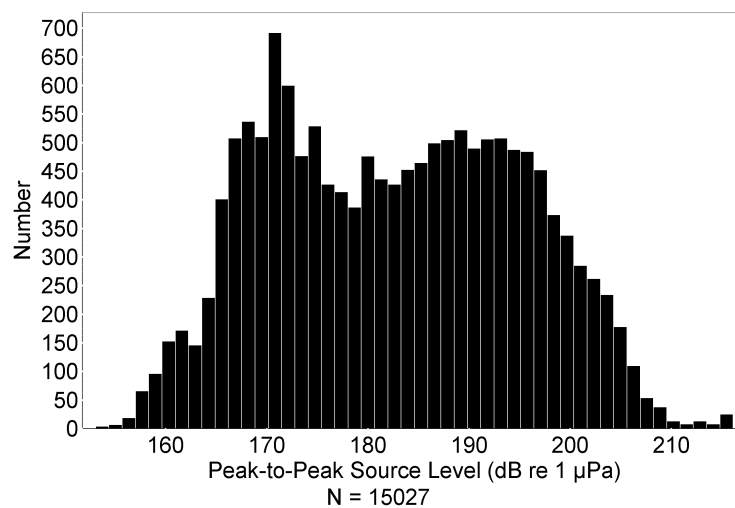


FIG. 20. Histogram of peak-to-peak source level (dB re 1 μ Pa) (pooled data).

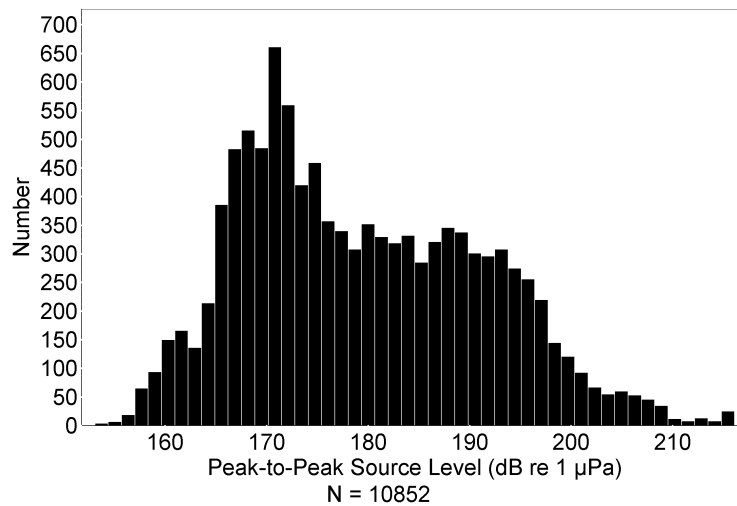


FIG. 21. Histogram of peak-to-peak source level (dB re 1 μ Pa) (BRT).

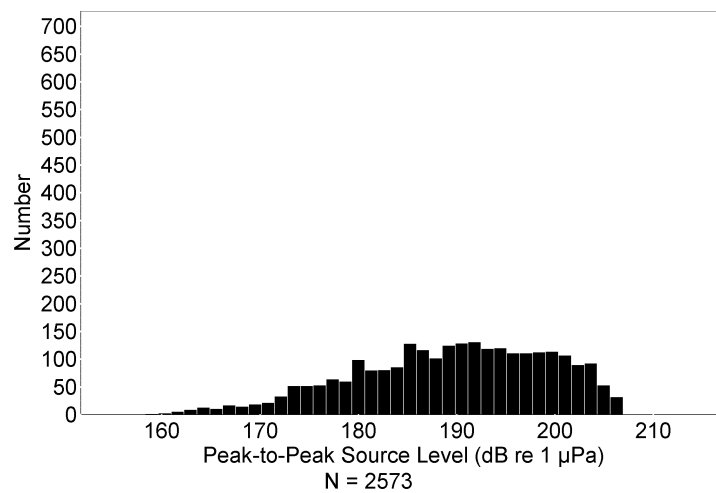


FIG. 22. Histogram of peak-to-peak source level (dB re 1 μ Pa) (BUS).

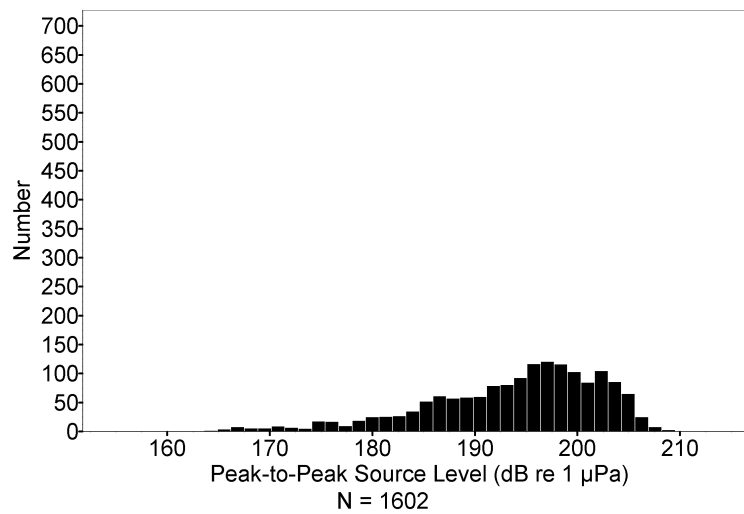


FIG. 23. Histogram of peak-to-peak source level (dB re 1 μ Pa) (SAY).

TABLE XI. Descriptive statistics for click duration (in μs).

Subject	Count	Minimum	Maximum	Mean	S.D.
BRT	10,852	23.8	217.6	69.7	36.0
BUS	2,573	25.9	182.4	48.8	22.3
SAY	1,602	24.5	151.2	44.5	12.0
Pooled	15,027	23.8	217.6	63.5	33.8

Descriptive statistics for the property of click duration are given in Table XI and histograms of click duration are shown in Figures 24-27.

Analysis of click duration split by subjects via ANOVA shows significant differences at $p < 0.0001$ (2 DF, $F = 747.8$). Using Fisher's PLSD, between subject comparisons were all significant at $p < 0.0001$.

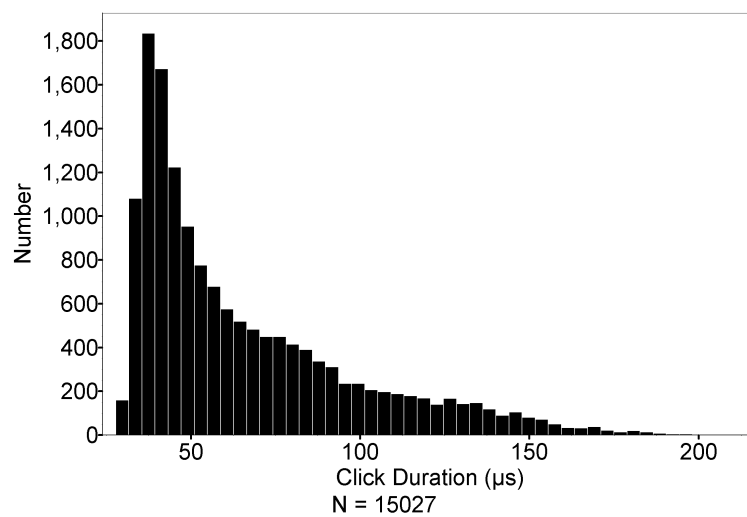


FIG. 24. Histogram of click duration (μs) (pooled).

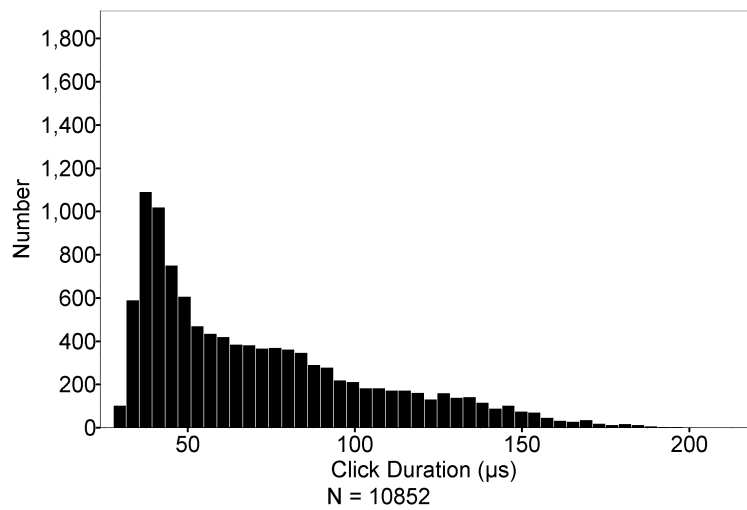


FIG. 25. Histogram of click duration (μs) (BRT).

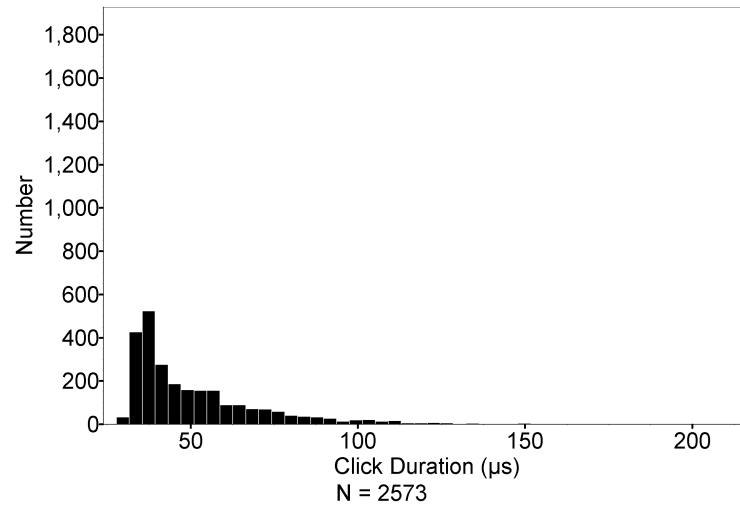


FIG. 26. Histogram of click duration (μs) (BUS).

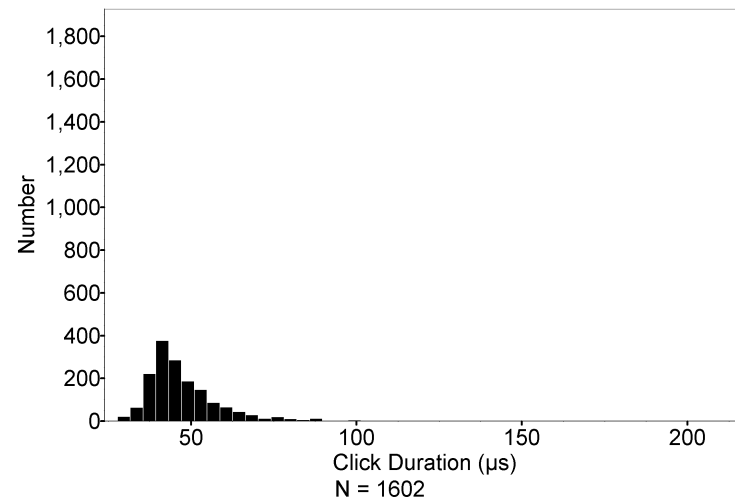


FIG. 27. Histogram of click duration (μs) (SAY).

TABLE XII. Descriptive statistics for energy flux density (dB re 1 $\mu\text{Pa}^2\text{s}$).

Subject	Count	Minimum	Maximum	Mean	S.D.
BRT	10,852	102.5	157.4	120.8	10.6
BUS	2,573	106.2	147.6	130.1	9.0
SAY	1,602	106.6	151.2	135.1	8.6
Pooled	15,027	102.5	157.4	123.9	11.4

Descriptive statistics for energy flux density (EFD) are given in Table XII and histograms are shown in Figures 28-31.

Analysis of energy flux density via ANOVA split by subjects shows significant differences at $p < 0.0001$ (2 DF, $F = 1953.079$). Using Fisher's PLSD, between subject comparisons were all significant at $p < 0.0001$.

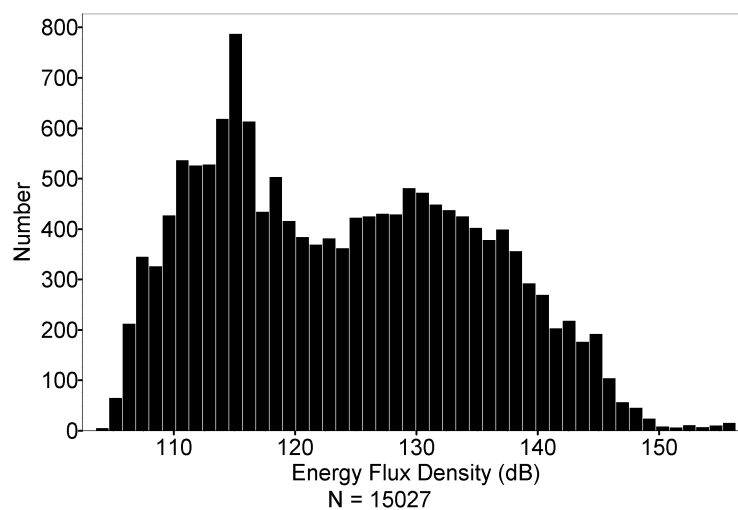


FIG. 28. Histogram of energy flux density (dB re 1 $\mu\text{Pa}^2\text{s}$) (pooled).

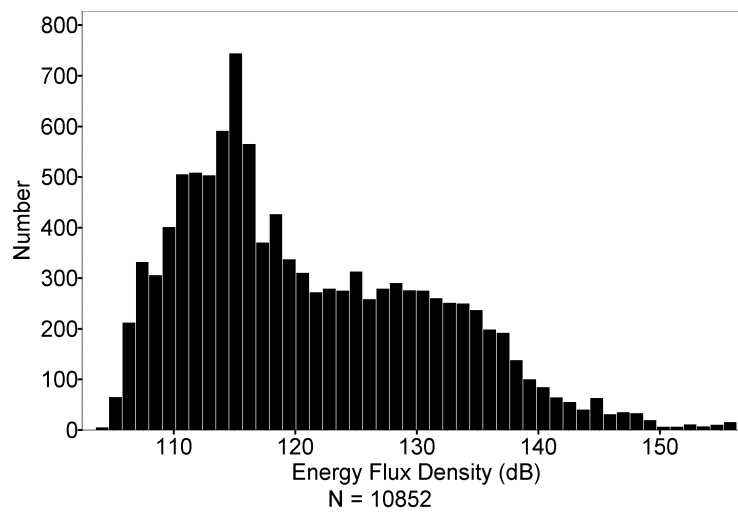


FIG. 29. Histogram of energy flux density (dB re 1 $\mu\text{Pa}^2\text{s}$) (BRT).

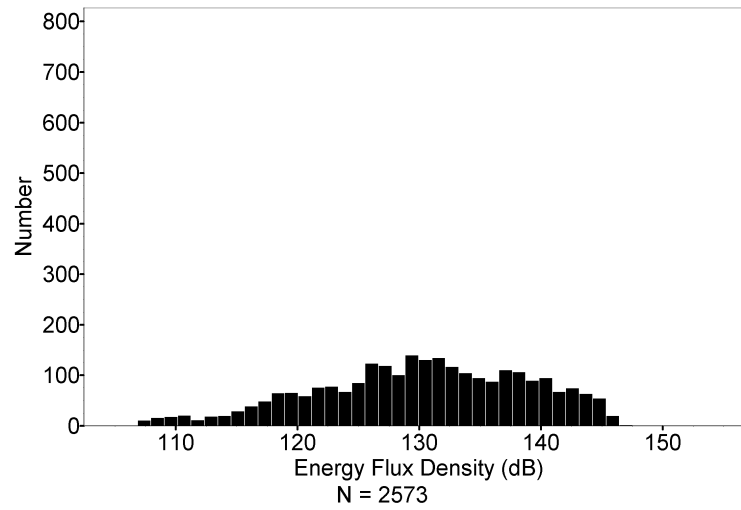


FIG. 30. Histogram of energy flux density (dB re 1 $\mu\text{Pa}^2\text{s}$) (BUS).

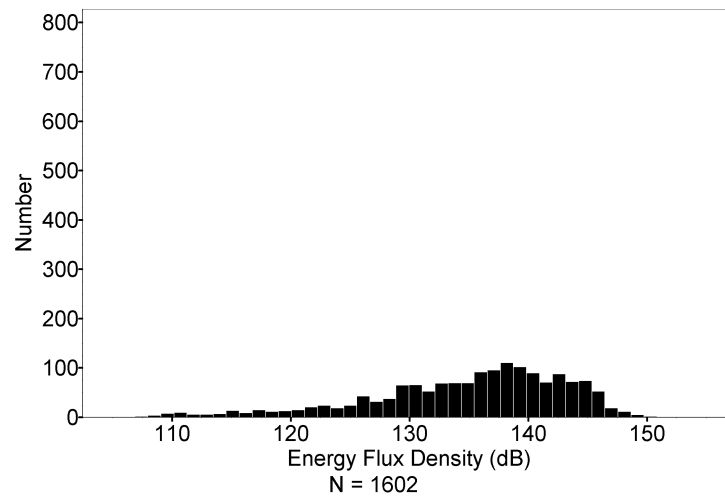


FIG. 31. Histogram of energy flux density (dB re 1 $\mu\text{Pa}^2\text{s}$) (SAY).

TABLE XIII. Descriptive statistics for radiated acoustic power (dB re 1 watt).

Subject	Count	Minimum	Maximum	Mean	S.D.
BRT	10,852	-46.9	30.6	-8.0	12.3
BUS	2,573	-34.5	20.4	1.7	10.3
SAY	1,602	-23.0	25.0	8.4	8.6
Pooled	15,027	-46.9	30.6	-4.6	13.0

Descriptive statistics for radiated acoustic power (RAP) are given in Table XIII and histograms are shown in Figures 32-35. The directivity index used in calculating these was 25.8 dB, as reported by Au (1993) for the bottlenose dolphin.

Analysis of radiated acoustic power via ANOVA split by subjects shows significant differences at $p < 0.0001$ (2 DF, $F = 1836.214$). Using Fisher's PLSD, between subject comparisons were all significant at $p < 0.0001$.

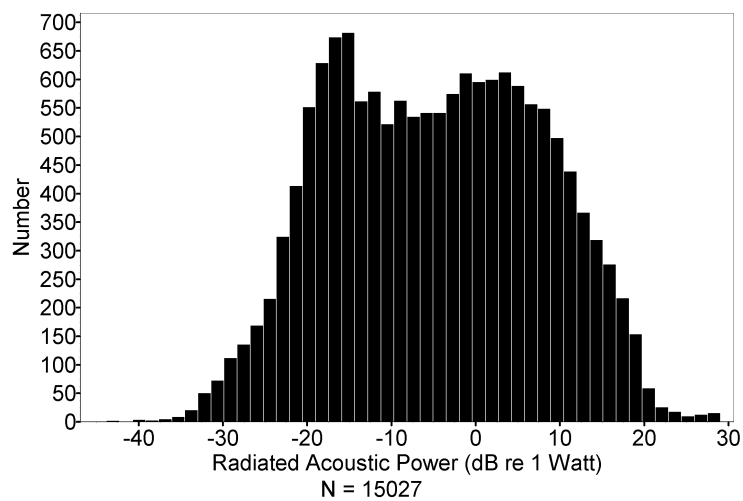


FIG. 32. Histogram of radiated acoustic power (watts) (pooled).

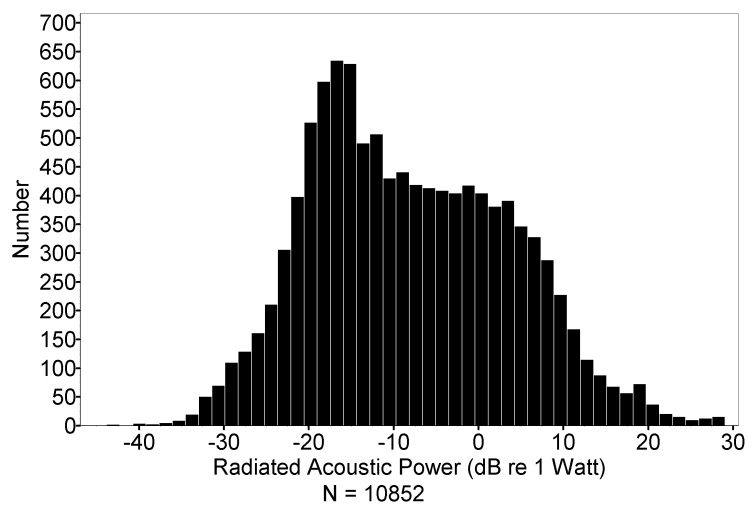


FIG. 33. Histogram of radiated acoustic power (watts) (BRT).

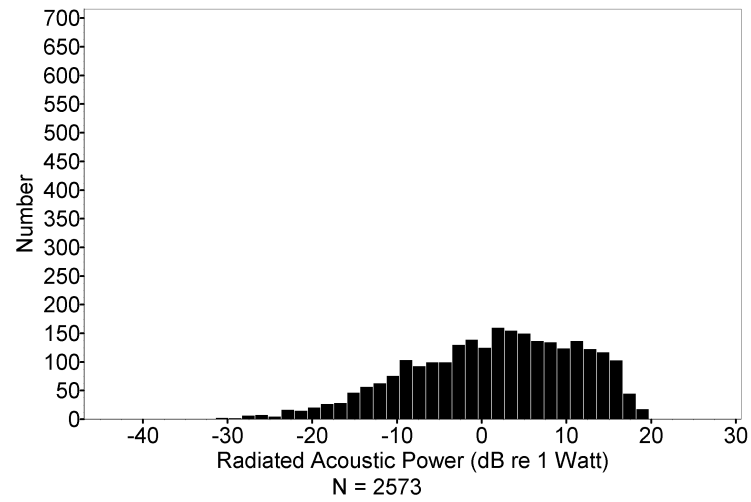


FIG. 34. Histogram of radiated acoustic power (watts) (BUS).

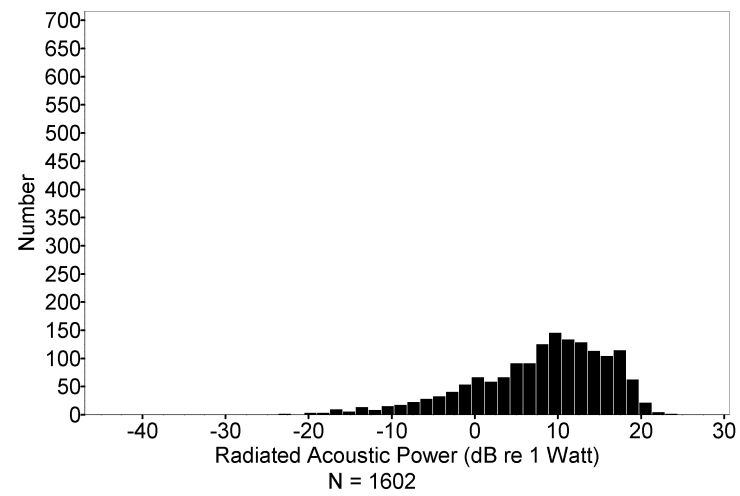


FIG. 35. Histogram of radiated acoustic power (watts) (SAY).

TABLE XIV. Descriptive statistics for intranarial pressure difference (kPa).

Subject	Count	Minimum	Maximum	Mean	S.D.
BRT	10,852	11.26	86.20	36.20	8.145
BUS	2,573	12.24	71.89	42.71	14.15
SAY	1,602	11.43	44.41	25.91	5.595
Pooled	15,027	11.26	86.20	36.22	10.20

Descriptive statistics for intranarial pressure difference (IPD) are given in Table XIV. Histograms of intranarial pressure difference are shown in Figures 36-39. Analysis of intranarial pressure difference split by subjects via ANOVA shows significant differences at $p < 0.0001$ (2 DF, $F = 1628.4$). Using Fisher's PLSD, between subject comparisons were all significant at $p < 0.0001$. Notice that all subjects have minimum intranarial pressures differences within 1 kPa of each other.

Analysis of intranarial pressure difference via ANOVA split by subjects shows significant differences at $p < 0.0001$ (2 DF, $F = 1628.451$). Using Fisher's PLSD, between subject comparisons were all significant at $p < 0.0001$.

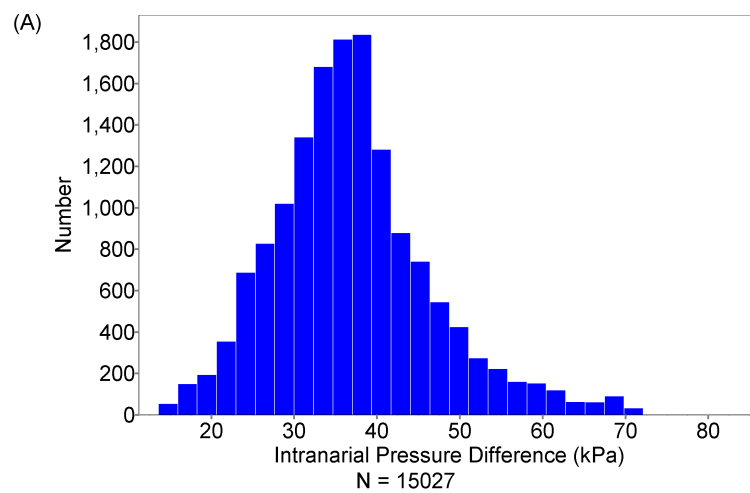


FIG. 36. Histogram of intranarial pressure difference (kPa) (pooled).

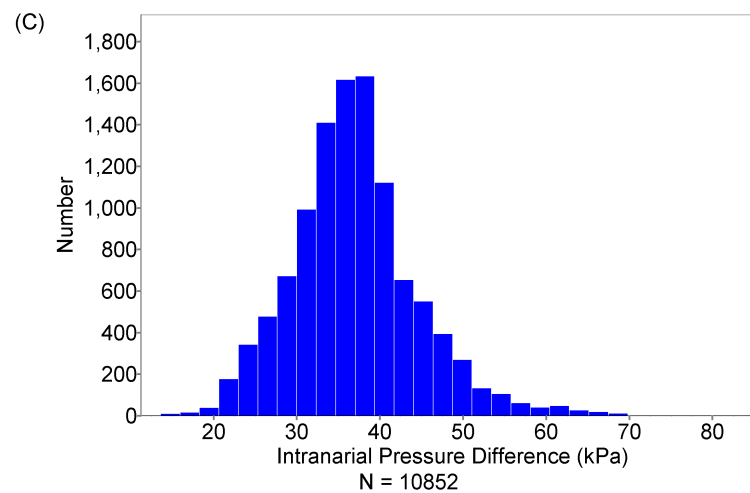


FIG. 37. Histogram of intranarial pressure difference (kPa) (BRT).

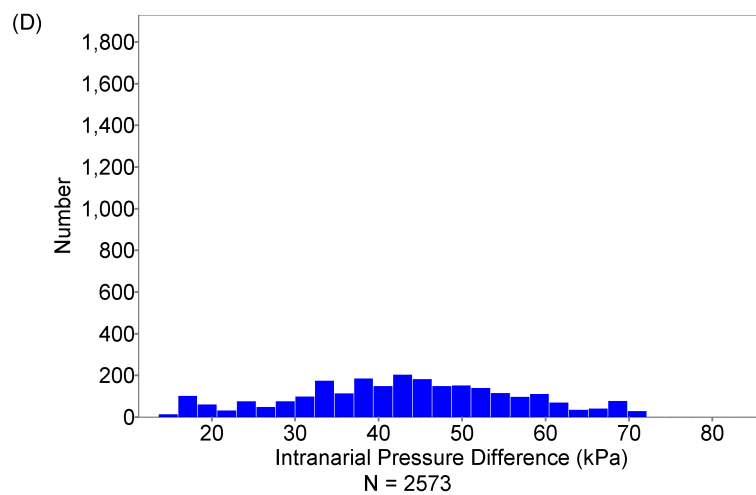


FIG. 38. Histogram of intranarial pressure difference (kPa) (BUS).

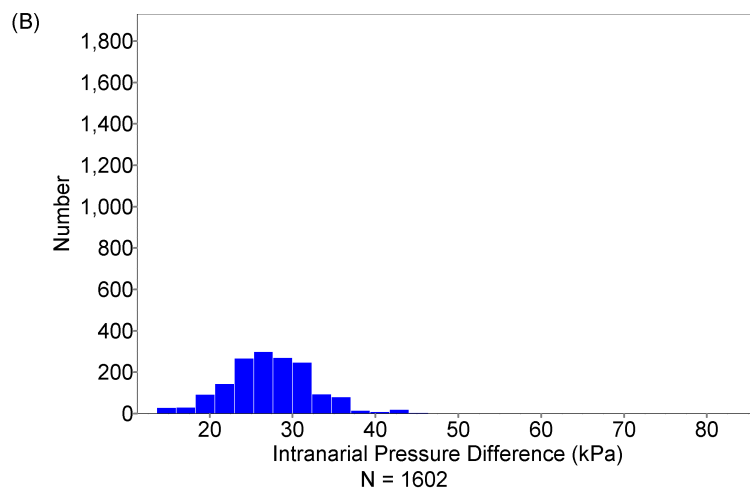


FIG. 39. Histogram of intranarial pressure difference (kPa) (SAY).

TABLE XV. Descriptive statistics for peak frequency (kHz).

Subject	Count	Minimum	Maximum	Mean	S.D.
BRT	10,582	0.203	129.4	55.6	35.3
BUS	2,573	0.203	123.7	59.0	30.5
SAY	1,602	0.244	145.0	100.9	19.5
Pooled	15,027	0.203	145.0	61.0	35.9

2. Frequency-domain characteristics

Descriptive statistics for peak frequency are given in Table XV and histograms are shown in Figures 40-43. Measures of central tendency are potentially misleading if the distribution of values is not unimodal, as we can see in the figures for peak frequency. For all frequency domain characteristics, low amplitude clicks may have less energy than the recorded noise, and thus values typical of ambient noise may be reported.

Analysis of peak frequency via ANOVA split by subjects shows significant differences at $p < 0.0001$ (2 DF, $F = 1306.754$). Using Fisher's PLSD, between subject comparisons were all significant at $p < 0.0001$.

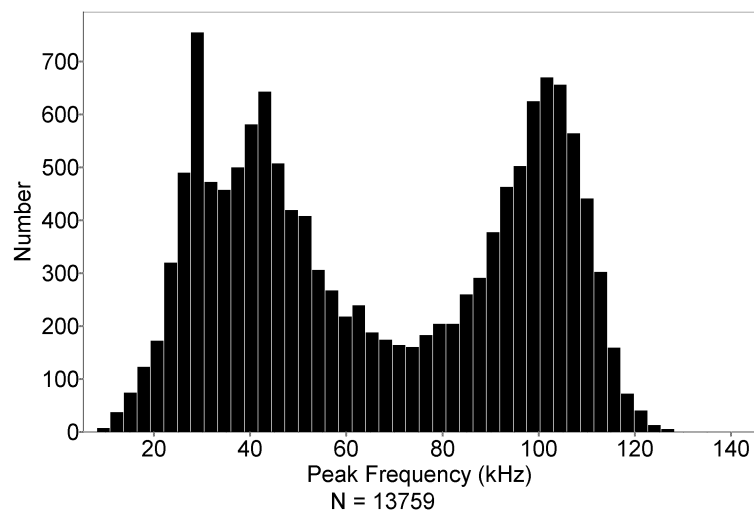


FIG. 40. Histogram of peak frequency (kHz) (pooled).

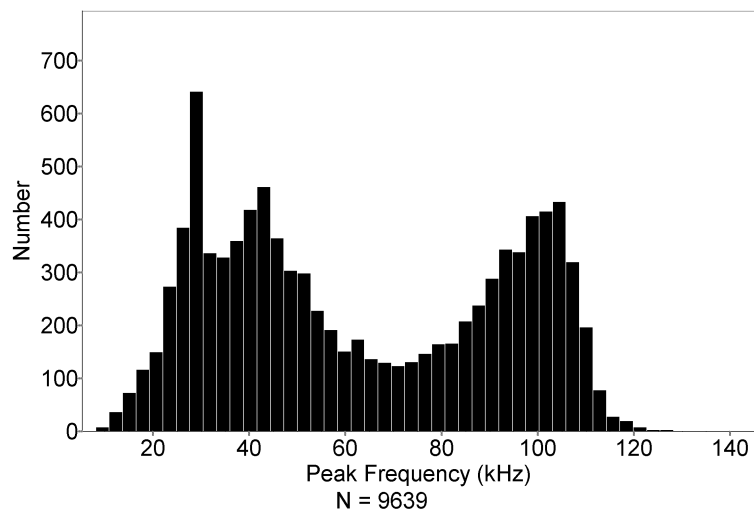


FIG. 41. Histogram of peak frequency (kHz) (BRT).

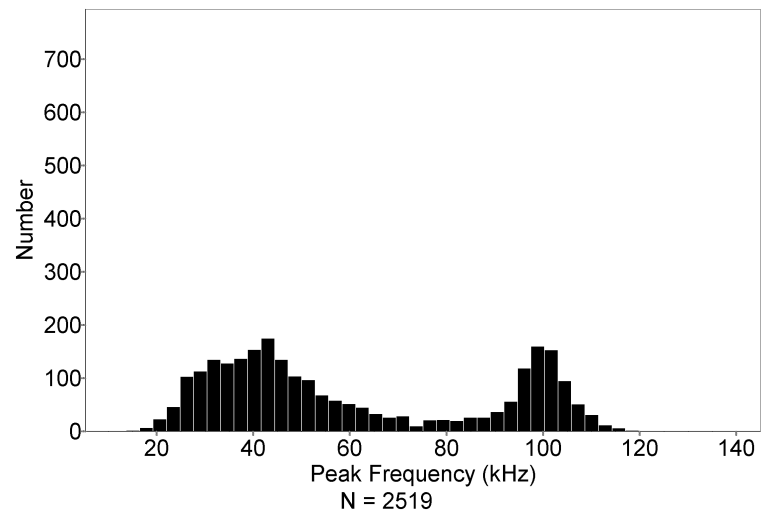


FIG. 42. Histogram of peak frequency (kHz) (BUS).

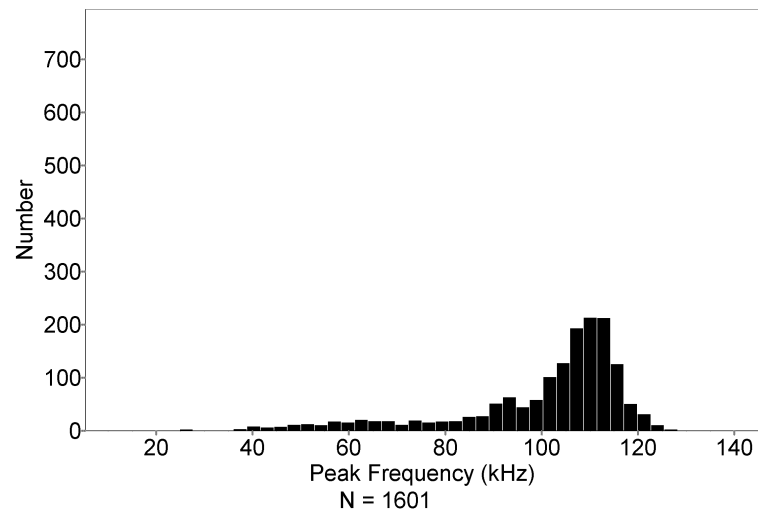


FIG. 43. Histogram of peak frequency (kHz) (SAY).

TABLE XVI. Descriptive statistics for dominant frequency (kHz).

Subject	Count	Minimum	Maximum	Mean	S.D.
BRT	10,852	11.5	113.7	60.6	25.1
BUS	2,573	14.3	107.1	60.2	21.5
SAY	1,602	38.3	125.0	96.2	13.9
Pooled	15,027	11.5	125.0	64.3	26.0

Dominant frequency is a statistical measure which finds the center of the energy distribution of a frequency spectrum. Descriptive statistics for dominant frequency are given in Table XVI and histograms are shown in Figures 44-47.

Analysis of dominant frequency via ANOVA split by subjects shows significant differences at $p < 0.0001$ (2 DF, $F = 1644.653$). Using Fisher's PLSD, between subject comparisons were significant at $p < 0.0001$ between BRT and SAY and also between BUS and SAY. BRT and BUS did not have significantly different values ($p = 0.4743$).

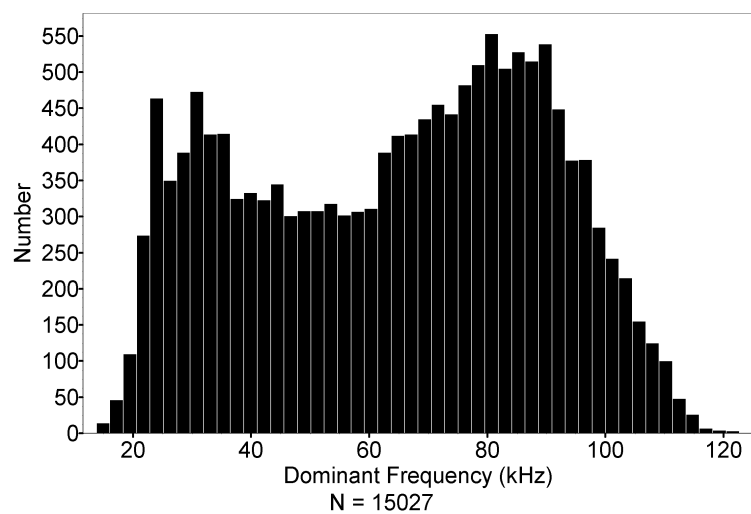


FIG. 44. Histogram of dominant frequency (kHz) (pooled).

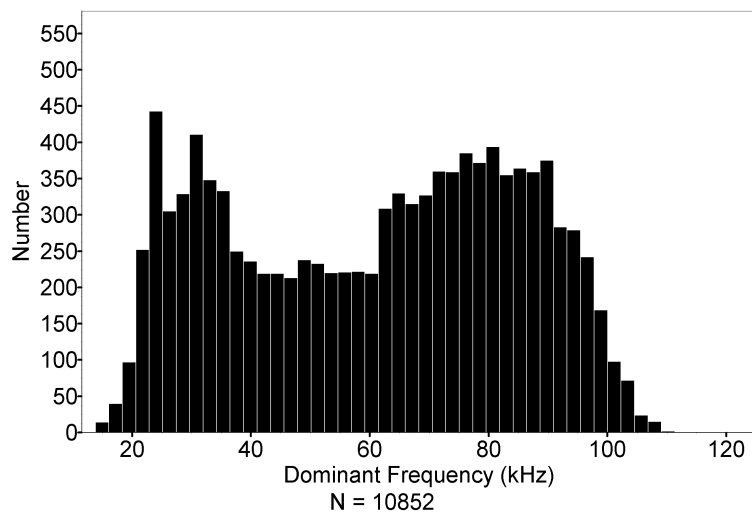


FIG. 45. Histogram of dominant frequency (kHz) (BRT).

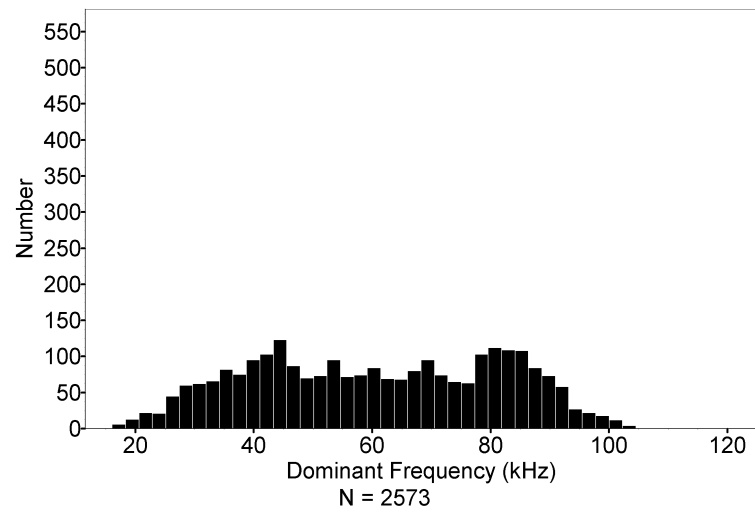


FIG. 46. Histogram of dominant frequency (kHz) (BUS).

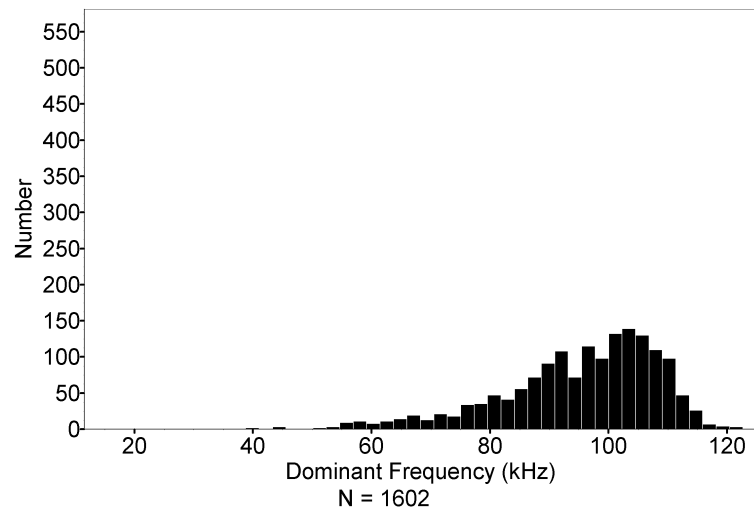


FIG. 47. Histogram of dominant frequency (kHz) (SAY).

TABLE XVII. Descriptive statistics for -3 dB bandwidth.

Subject	Count	Minimum	Maximum	Mean	S.D.
BRT	10,852	2.03	131.8	53.9	25.0
BUS	2,573	2.64	121.2	57.4	20.5
SAY	1,602	7.57	114.0	57.0	15.6
Pooled	15,027	2.03	131.8	54.8	23.5

Descriptive statistics for -3 dB bandwidths are given in Table XVII and histograms are shown in Figures 48-51.

Analysis of -3dB bandwidth via ANOVA split by subjects shows significant differences at $p < 0.0001$ (2 DF, $F = 30.464$). Using Fisher's PLSD, between subject comparisons were significant at $p < 0.0001$ between BRT and BUS and also between BRT and SAY. BUS and SAY did not have significantly different values ($p = 0.5562$).

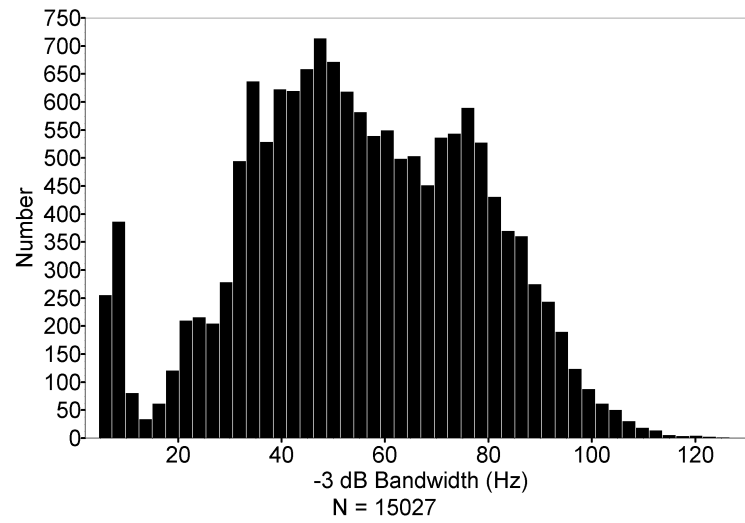


FIG. 48. Histogram of -3dB bandwidth (kHz) (pooled).

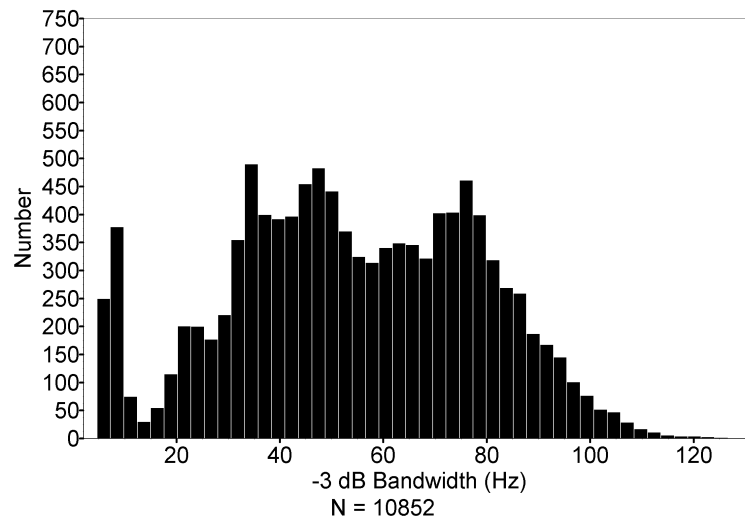


FIG. 49. Histogram of -3dB bandwidth (kHz) (BRT).

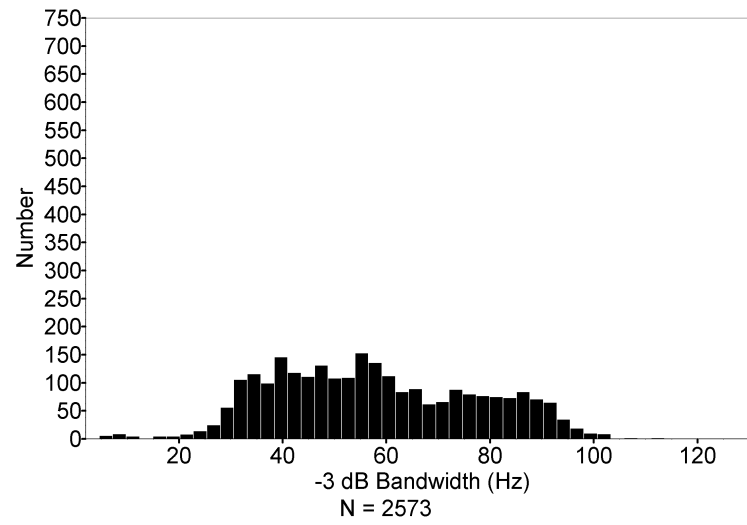


FIG. 50. Histogram of -3dB bandwidth (kHz) (BUS).

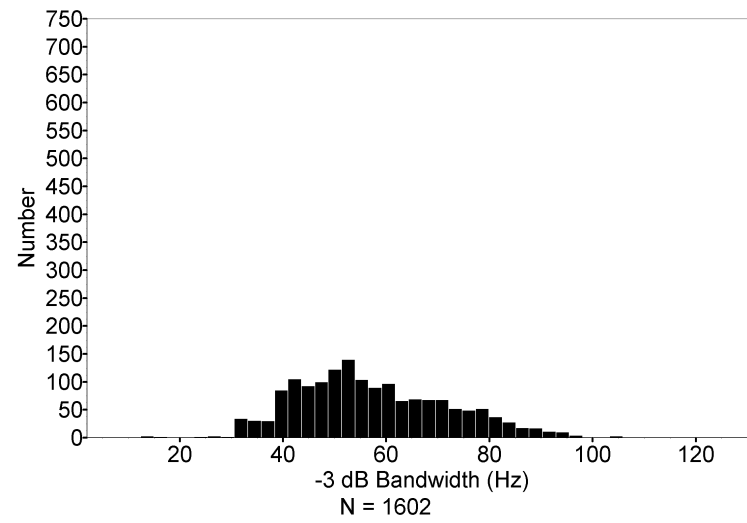


FIG. 51. Histogram of -3dB bandwidth (kHz) (SAY).

TABLE XVIII. Linear regression results for radiated acoustic power (dB re 1 watt) vs. intranarial pressure difference (kPa).

Subject	Count	X term	Intercept	R ²	t	p
BRT	10852	-0.2756	11.20	0.6492	-141.7	<0.0001
BUS	2573	-0.3776	20.14	0.6611	-70.81	<0.0001
SAY	1602	-0.3834	25.46	0.2846	-25.23	<0.0001
Pooled	15027	-0.3101	15.07	0.6484	-166.5	<0.0001

3. Intranarial pressure treated as an independent variable

Radiated acoustic power values plotted against intranarial pressure difference from basal pressure are shown in Figures 52-55. Linear regression statistics are given in Table XVIII.

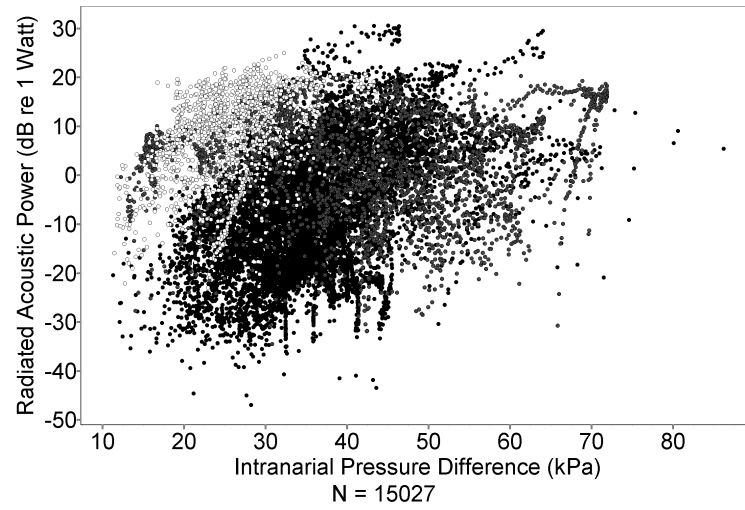


FIG. 52. Bivariate plot of radiated acoustic power (dB re 1 watt) vs. intranarial pressure difference (kPa) (pooled).

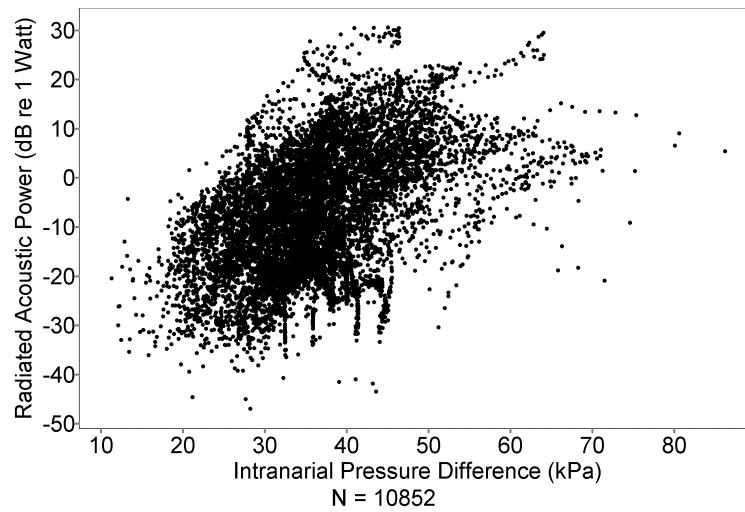


FIG. 53. Bivariate plot of radiated acoustic power (dB re 1 watt) vs. intranarial pressure difference (kPa) (BRT).

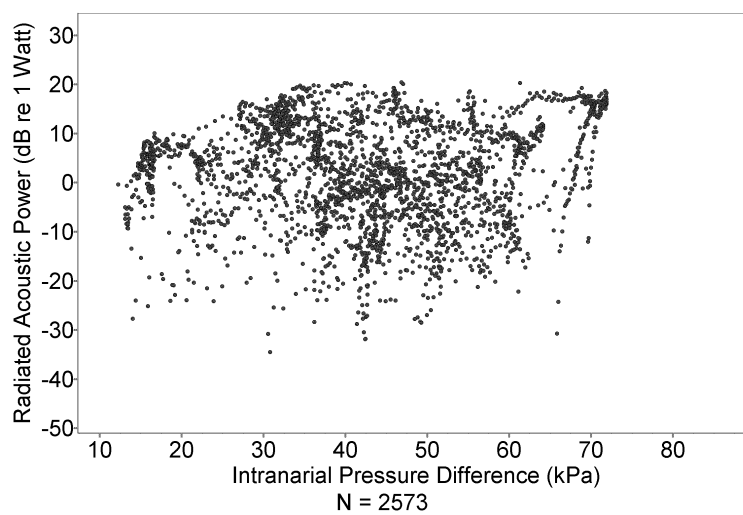


FIG. 54. Bivariate plot of radiated acoustic power (dB re 1 watt) vs. intranarial pressure difference (kPa) (BUS).

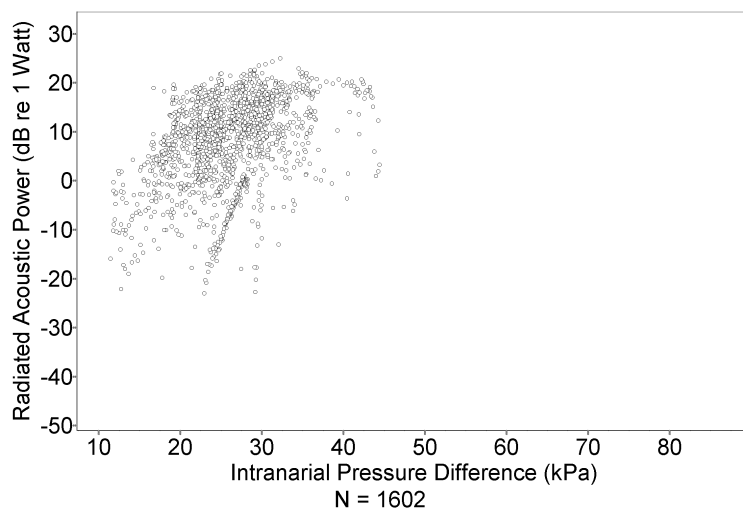


FIG. 55. Bivariate plot of radiated acoustic power (dB re 1 watt) vs. intranarial pressure difference (kPa) (SAY).

TABLE XIX. Linear regression results for peak frequency (kHz) vs. intranarial pressure difference (kPa).

Subject	Count	X term	Intercept	R ²	t	p
BRT	10852	0.9336	21.81	0.04647	22.99	<0.0001
BUS	2573	-0.3208	72.69	0.02221	-7.642	<0.0001
SAY	1602	0.7847	80.53	0.05044	9.219	<0.0001
Pooled	15027	-0.09275	64.37	0.0006944	-3.231	0.0006176

The distribution of peak frequency values with respect to intranarial pressure difference from basal pressure is shown in Figures 56-59. Linear regression statistics are given in Table XIX.

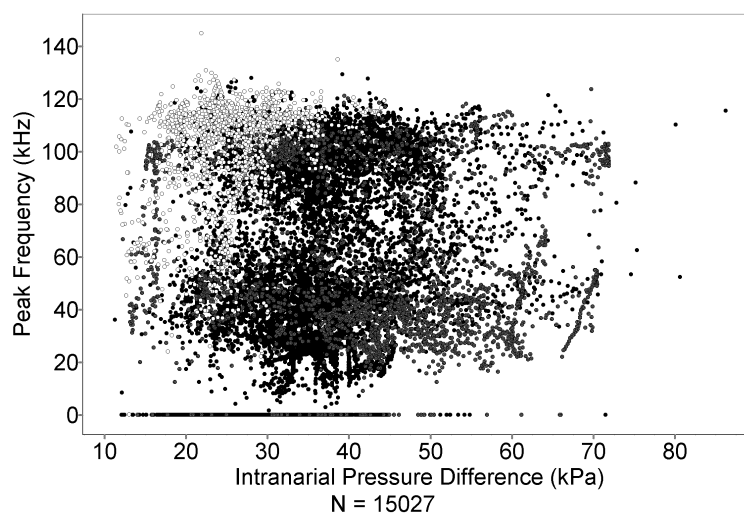


FIG. 56. Bivariate plot of peak frequency (kHz) vs. intranarial pressure difference (kPa) (pooled).

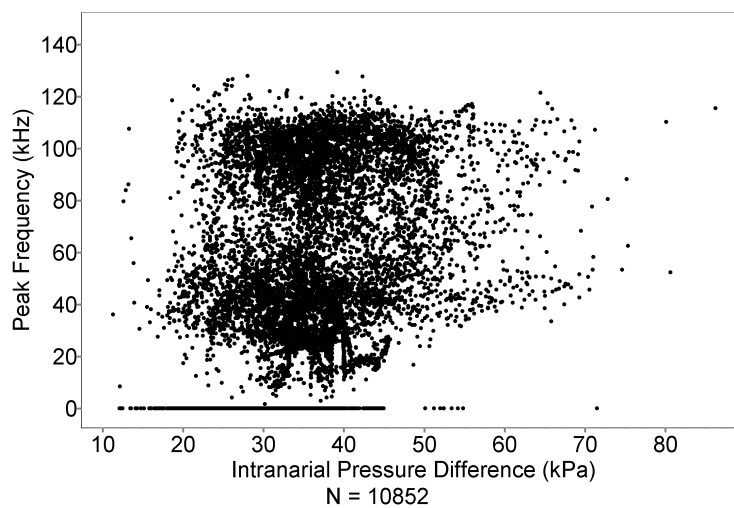


FIG. 57. Bivariate plot of peak frequency (kHz) vs. intranarial pressure difference (kPa) (BRT).

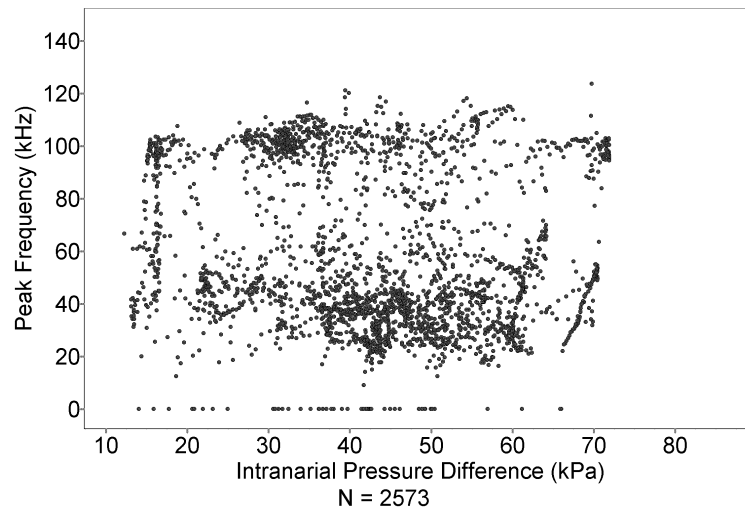


FIG. 58. Bivariate plot of peak frequency (kHz) vs. intranarial pressure difference (kPa) (BUS).

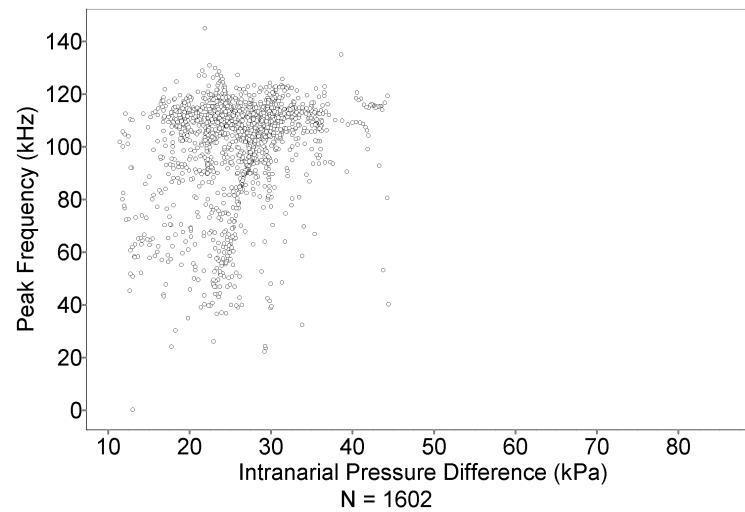


FIG. 59. Bivariate plot of peak frequency (kHz) vs. intranarial pressure difference (kPa) (SAY).

TABLE XX. Linear regression results for dominant frequency (kHz) vs. intranarial pressure difference (kPa).

Subject	Count	X term	Intercept	R ²	t	p
BRT	10852	0.5834	39.48	0.03589	20.10	<0.0001
BUS	2573	-0.2501	70.91	0.02714	-8.469	<0.0001
SAY	1602	0.6504	79.36	0.06819	10.82	<0.0001
Pooled	15027	-0.1732	70.61	0.004622	-8.353	<0.0001

Dominant frequency values plotted against intranarial pressure difference from basal pressure are shown in Figures 60-63. Linear regression statistics are given in Table XX.

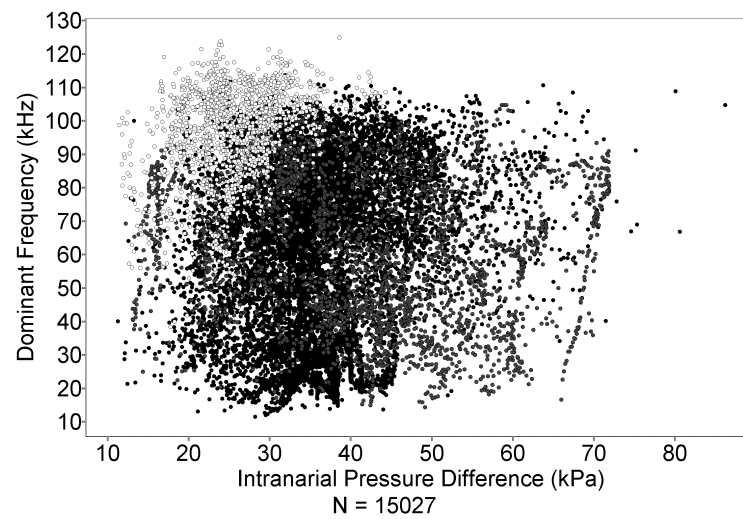


FIG. 60. Bivariate plot of dominant frequency (kHz) vs. intranarial pressure difference (kPa) (pooled).

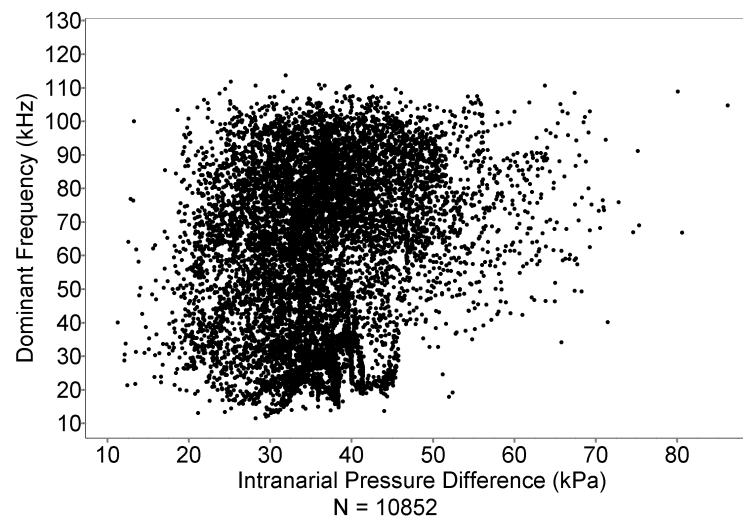


FIG. 61. Bivariate plot of dominant frequency (kHz) vs. intranarial pressure difference (kPa) (BRT).

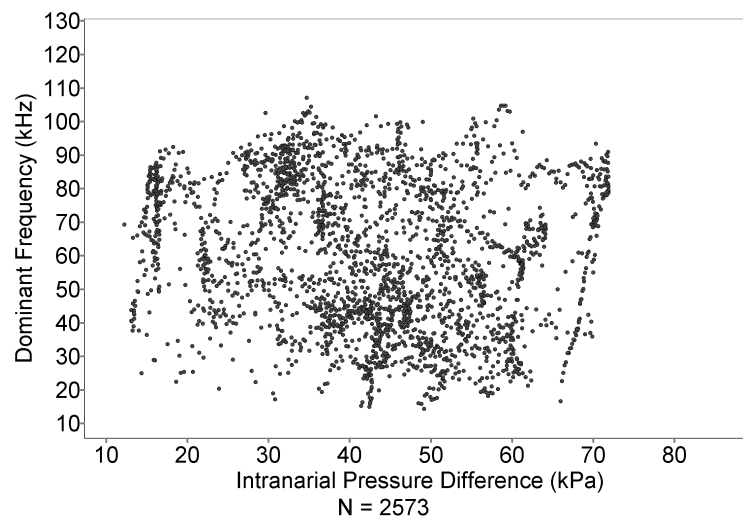


FIG. 62. Bivariate plot of dominant frequency (kHz) vs. intranarial pressure difference (kPa) (BUS).

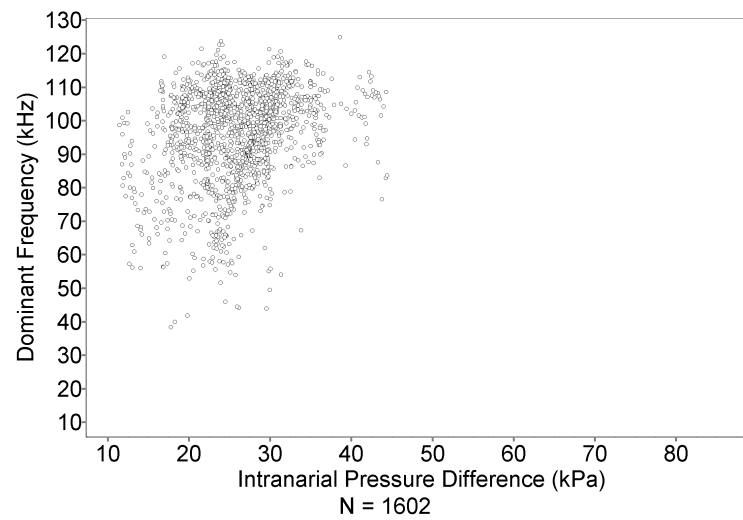


FIG. 63. Bivariate plot of dominant frequency (kHz) vs. intranarial pressure difference (kPa) (SAY).

TABLE XXI. Linear regression results for -3 dB bandwidth (kHz) vs. intranarial pressure difference (kPa).

Subject	Count	X term	Intercept	R ²	t	p
BRT	10852	0.6154	31.62	0.04012	21.29	<0.0001
BUS	2573	-0.1478	63.70	0.01042	-5.203	<0.0001
SAY	1602	-0.04930	58.23	0.0003142	-0.7092	0.2392
Pooled	15027	0.2380	46.20	0.01068	12.73	<0.0001

The distribution of -3 dB bandwidth values with respect to intranarial pressure difference from basal pressure is shown in Figures 64-67. Linear regression statistics are given in Table XXI.

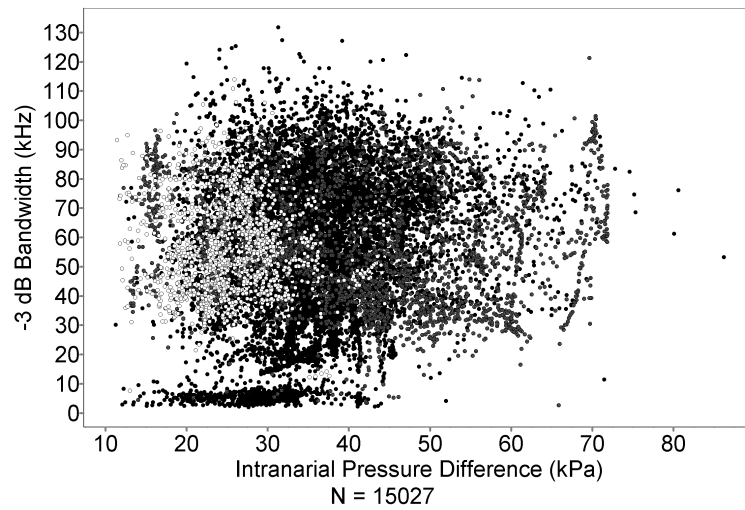


FIG. 64. Bivariate plot of -3dB bandwidth (kHz) vs. intranarial pressure difference (kPa) (pooled).

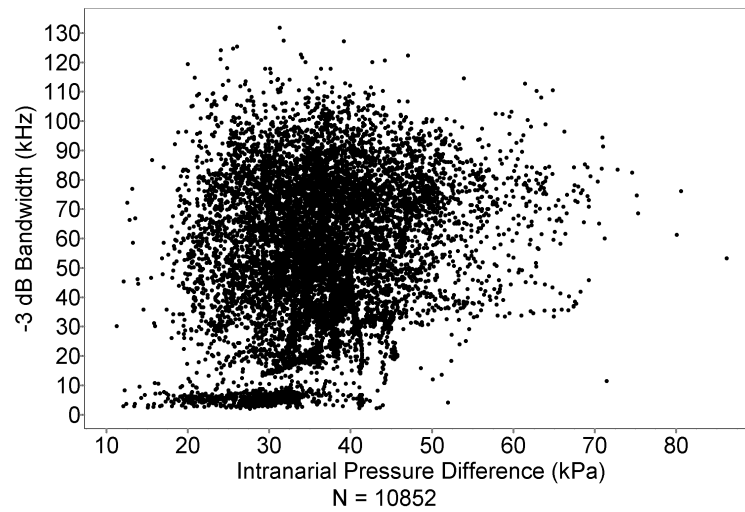


FIG. 65. Bivariate plot of -3dB bandwidth (kHz) vs. intranarial pressure difference (kPa) (BRT).

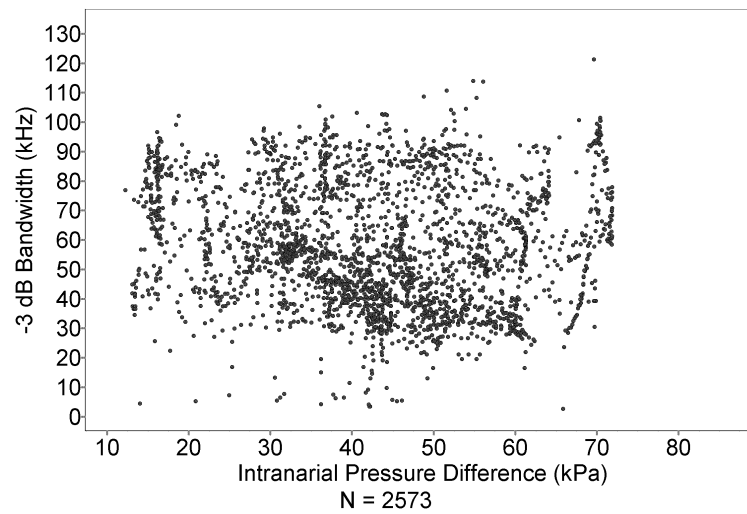


FIG. 66. Bivariate plot of -3dB bandwidth (kHz) vs. intranarial pressure difference (kPa) (BUS).

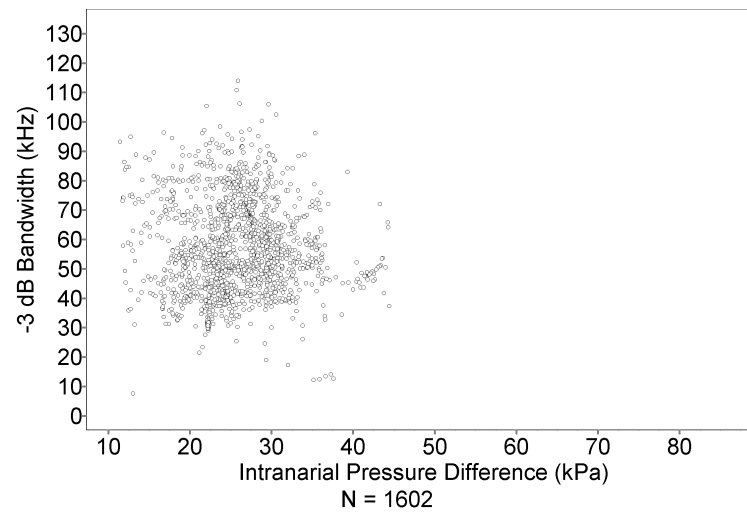


FIG. 67. Bivariate plot of -3dB bandwidth (kHz) vs. intranarial pressure difference (kPa) (SAY).

TABLE XXII. Linear regression results for peak-to-peak source level (dB re 1 μ Pa) vs. click duration (μ s).

Subject	Count	X term	Intercept	R ²	t	p
BRT	10852	-0.2727	198.3	0.6352	-137.4	<0.0001
BUS	2573	-0.3779	207.9	0.6670	-71.75	<0.0001
SAY	1602	-0.4122	212.5	0.3101	-26.82	<0.0001
Pooled	15027	-0.3065	202.0	0.6429	-164.5	<0.0001

TABLE XXIII. Second order polynomial regression results for peak-to-peak source level (dB re 1 μ Pa) vs. click duration (μ s).

Subject	Count	X ²	X term	Intercept	R ²	s ²	F	p
BRT	10852	0.003	-0.732	214.2	0.731	40.84	14741	<0.0001
BUS	2573	0.003	-0.826	220.7	0.740	27.66	3657	<0.0001
SAY	1602	0.002	-0.616	217.8	0.315	54.51	368.0	<0.0001
Pooled	15027	0.003	-0.786	217.9	0.730	45.03	20281	<0.0001

4. Click duration treated as an independent variable

Peak-to-peak source level amplitude is shown plotted against click duration in Figures 68-71. Linear regression statistics are given in Table XXII. Second order polynomial regression statistics are given in Table XXIII.

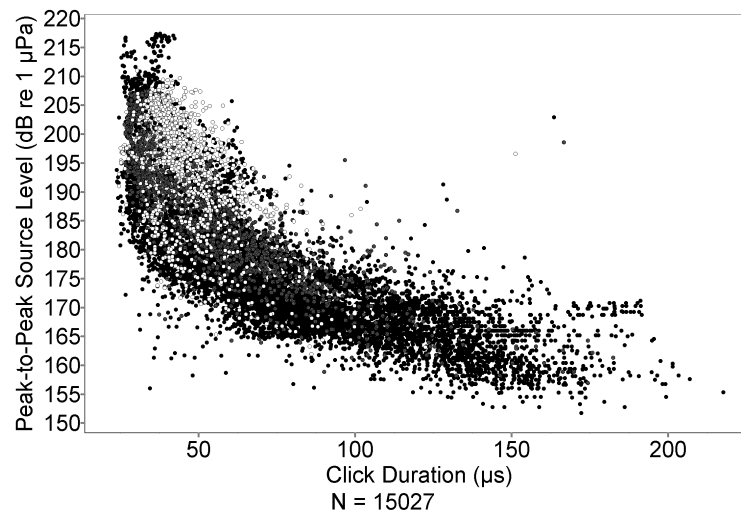


FIG. 68. Bivariate plot of peak-to-peak source level (dB re 1 μ Pa) vs. click duration (μ s) (pooled).

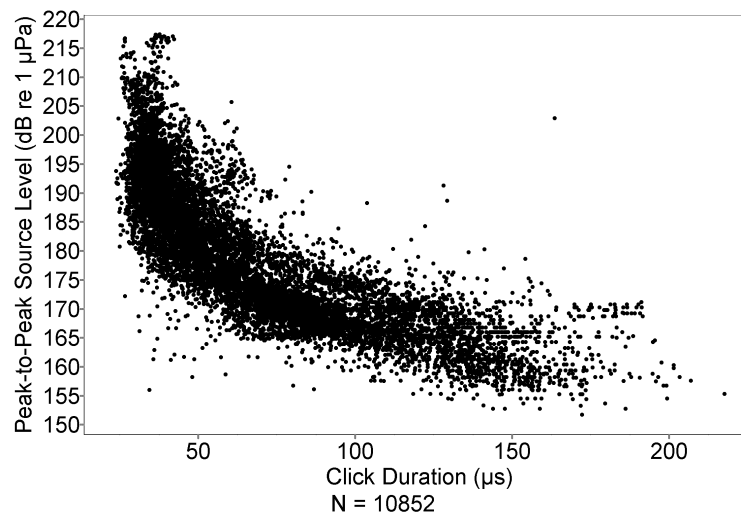


FIG. 69. Bivariate plot of peak-to-peak source level (dB re 1 μ Pa) vs. click duration (μ s) (BRT).

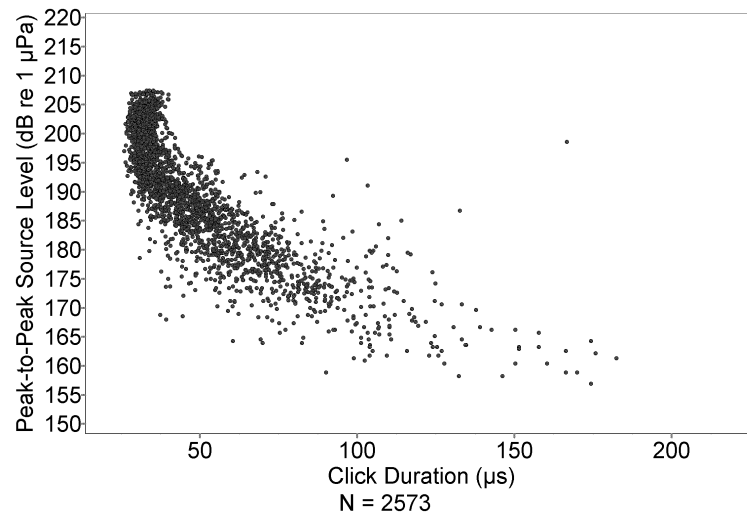


FIG. 70. Bivariate plot of peak-to-peak source level (dB re 1 μ Pa) vs. click duration (μ s) (BUS).

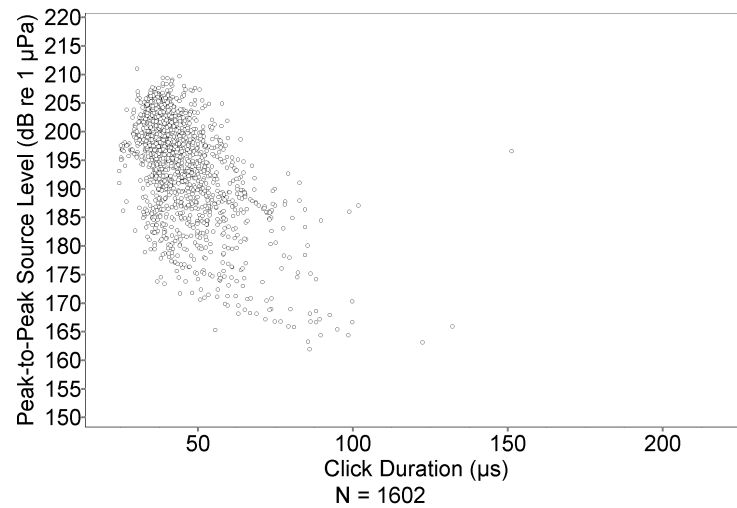


FIG. 71. Bivariate plot of peak-to-peak source level (dB re 1 μ Pa) vs. click duration (μ s) (SAY).

TABLE XXIV. Linear regression results for energy flux density (dB re 1 $\mu\text{Pa}^2\text{s}$) vs. click duration (μs).

Subject	Count	X term	Intercept	R ²	t	p
BRT	10852	-0.2165	135.9	0.5385	-112.5	<0.0001
BUS	2573	-0.3204	145.8	0.6301	-66.18	<0.0001
SAY	1602	-0.3699	151.5	0.2658	-24.07	<0.0001
Pooled	15027	-0.2525	139.9	0.5582	-137.8	<0.0001

TABLE XXV. Second order polynomial regression results for energy flux density (dB re 1 $\mu\text{Pa}^2\text{s}$) vs. click duration (μs).

Subject	Count	X ²	X term	Intercept	R ²	s ²	F	p
BRT	10852	0.003	-0.682	152.0	0.671	37.20	11044	<0.0001
BUS	2573	0.003	-0.710	156.9	0.703	24.08	3036	<0.0001
SAY	1602	0.001	-0.537	155.9	0.269	54.64	294.9	<0.0001
Pooled	15027	0.003	-0.735	155.9	0.670	42.91	15285	<0.0001

Energy flux density is shown plotted against click duration in Figures 72-75. Linear regression statistics are given in Table XXIV. Second order polynomial regression statistics are given in Table XXV.

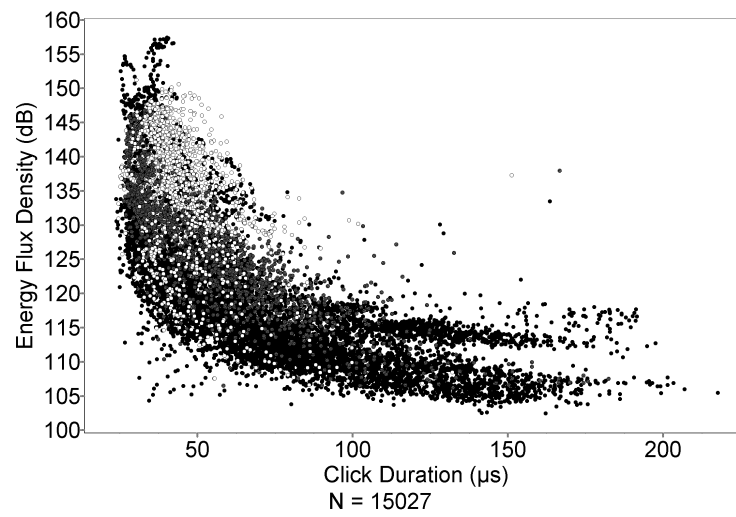


FIG. 72. Bivariate plot of energy flux density (dB re $1 \mu\text{Pa}^2\text{s}$) vs. click duration (μs) (pooled).

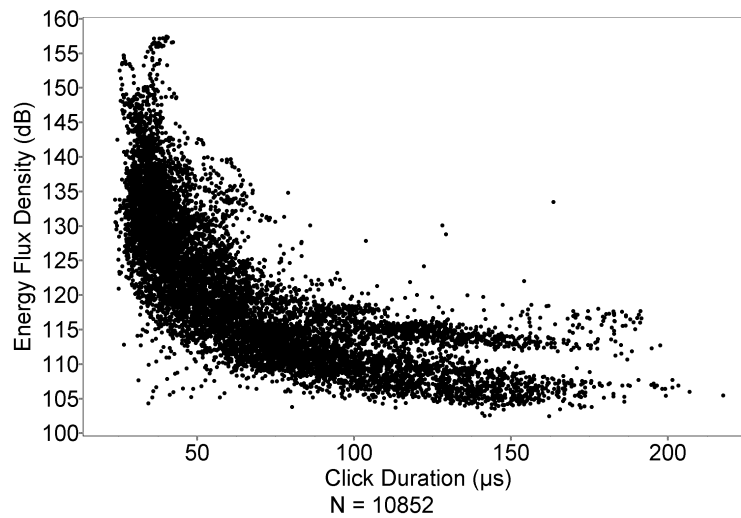


FIG. 73. Bivariate plot of energy flux density (dB re $1 \mu\text{Pa}^2\text{s}$) vs. click duration (μs) (BRT).

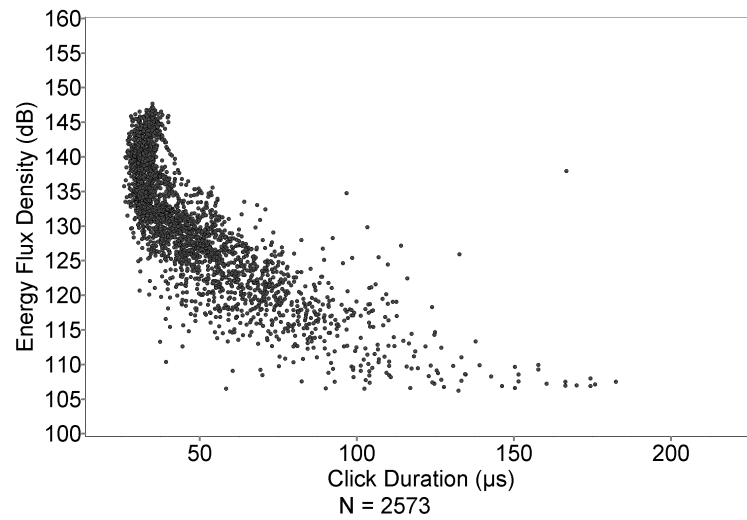


FIG. 74. Bivariate plot of energy flux density (dB re $1 \mu\text{Pa}^2\text{s}$) vs. click duration (μs) (BUS).

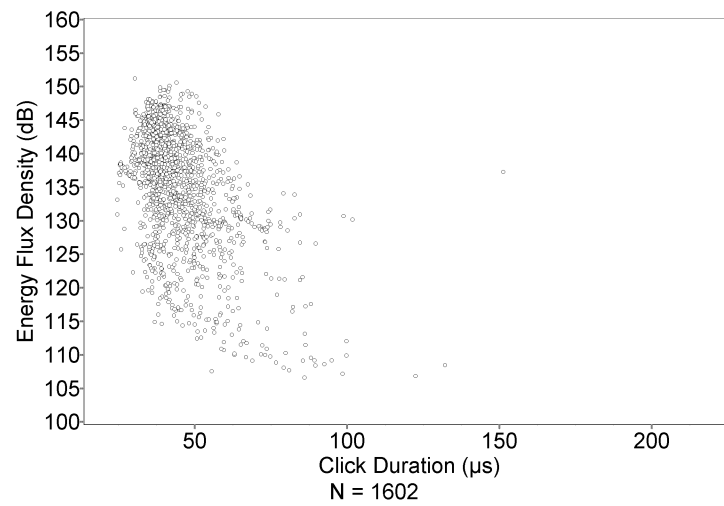


FIG. 75. Bivariate plot of energy flux density (dB re $1 \mu\text{Pa}^2\text{s}$) vs. click duration (μs) (SAY).

TABLE XXVI. Linear regression results for radiated acoustic power (dB re 1 watt) vs. click duration (μs).

Subject	Count	X term	Intercept	R^2	t	p
BRT	10852	-0.2756	11.20	0.6492	-141.7	<0.0001
BUS	2573	-0.3776	20.14	0.6611	-70.81	<0.0001
SAY	1602	-0.3834	25.46	0.2846	-25.23	<0.0001
Pooled	15027	-0.3101	15.07	0.6484	-166.5	<0.0001

TABLE XXVII. Second order polynomial regression results for radiated acoustic power (dB re 1 watt) vs. click duration (μs).

Subject	Count	X^2	X term	Intercept	R^2	s^2	F	p
BRT	10852	0.002	-0.665	24.64	0.718	42.78	13811	<0.0001
BUS	2573	0.003	-0.820	32.78	0.732	28.76	3504	<0.0001
SAY	1602	0.001	-0.544	29.63	0.288	53.45	323.2	<0.0001
Pooled	15027	0.002	-0.729	28.95	0.714	48.40	18730	<0.0001

Radiated acoustic power values plotted against click duration are shown in Figures 76-79. Linear regression statistics are given in Table XXVI. Second order polynomial regression statistics are given in Table XXVII.

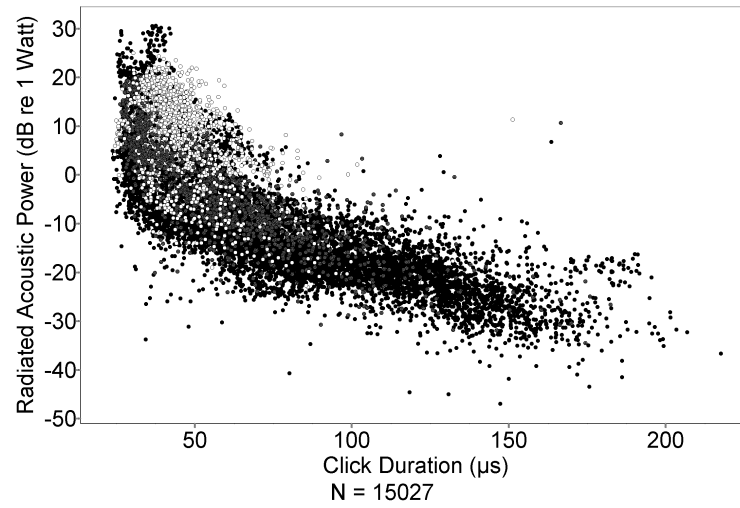


FIG. 76. Bivariate plot of radiated acoustic power (dB re 1 watt) vs. click duration (μs) (pooled).

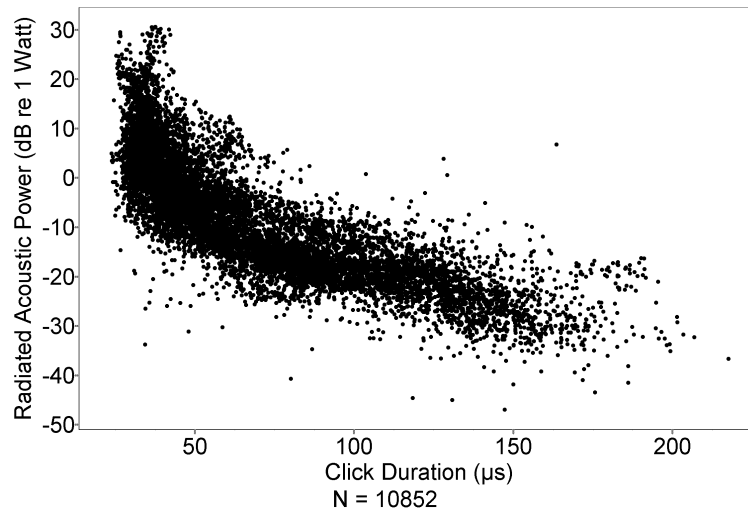


FIG. 77. Bivariate plot of radiated acoustic power (dB re 1 watt) vs. click duration (μs) (BRT).

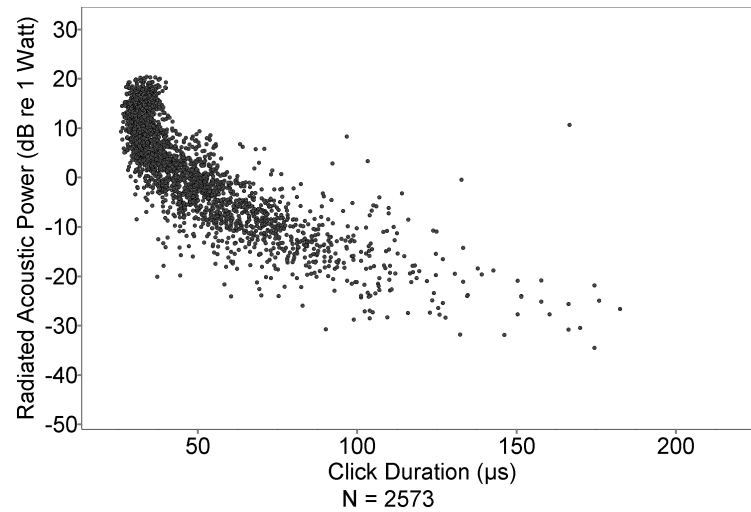


FIG. 78. Bivariate plot of radiated acoustic power (dB re 1 watt) vs. click duration (μs) (BUS).

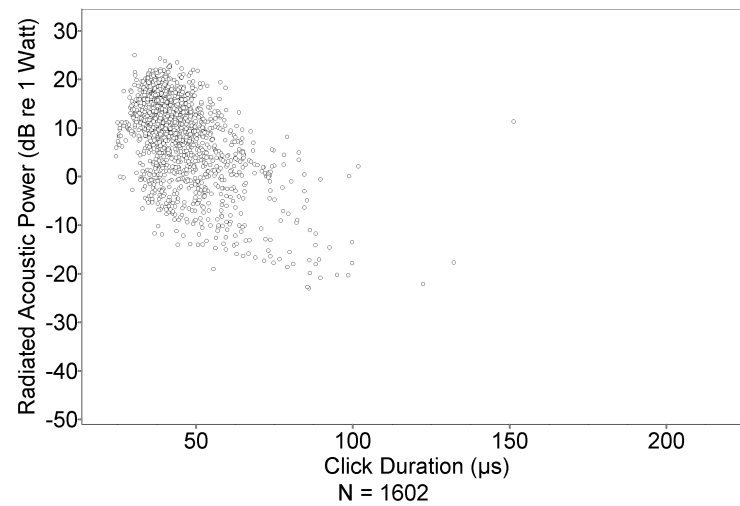


FIG. 79. Bivariate plot of radiated acoustic power (dB re 1 watt) vs. click duration (μs) (SAY).

TABLE XXVIII. Linear regression results for peak frequency (kHz) vs. click duration (μ s).

Subject	Count	X term	Intercept	R ²	t	p
BRT	10852	-0.7412	107.3	0.5725	-120.6	<0.0001
BUS	2573	-0.8686	101.4	0.4035	-41.70	<0.0001
SAY	1602	-0.7010	132.1	0.1866	-19.16	<0.0001
Pooled	15027	-0.7705	109.9	0.5250	-128.9	<0.0001

TABLE XXIX. Second order polynomial regression results for peak frequency (kHz) vs. click duration (μ s).

Subject	Count	X ²	X term	Intercept	R ²	s ²	F	p
BRT	10852	4.852	-1591	1.367e5	0.613	4.822e7	8576	<0.0001
BUS	2573	12.30	-26178	1.514e5	0.531	4.358e8	1454	<0.0001
SAY	1602	6.084	-1402	1.503e5	0.199	3.065e8	198.8	<0.0001
Pooled	15027	5.204	-1657	1.393e5	0.563	5.631e8	9691	<0.0001

The distribution of peak frequency values with respect to click duration is shown in Figures 80-83. Linear regression statistics are given in Table XXVIII. Second order polynomial regression statistics are given in Table XXIX.

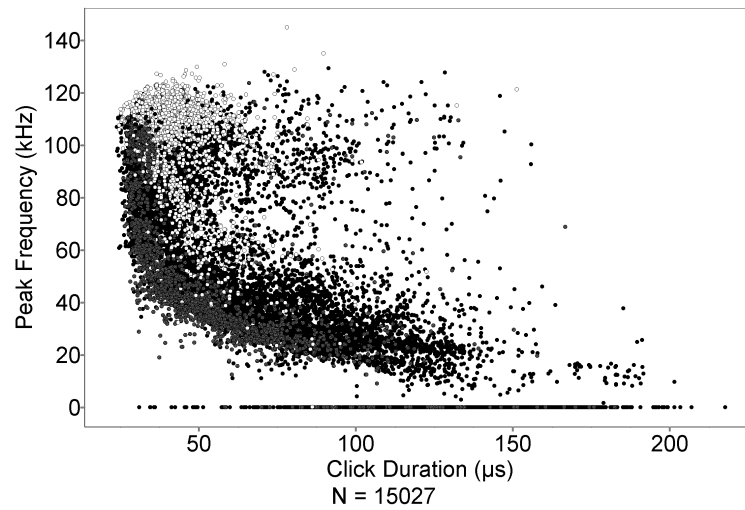


FIG. 80. Bivariate plot of peak frequency (kHz) vs. click duration (μs) (pooled).

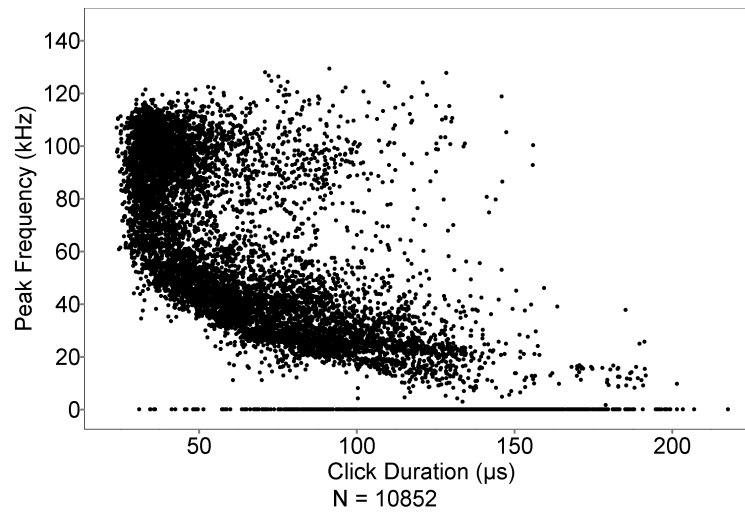


FIG. 81. Bivariate plot of peak frequency (kHz) vs. click duration (μs) (BRT).

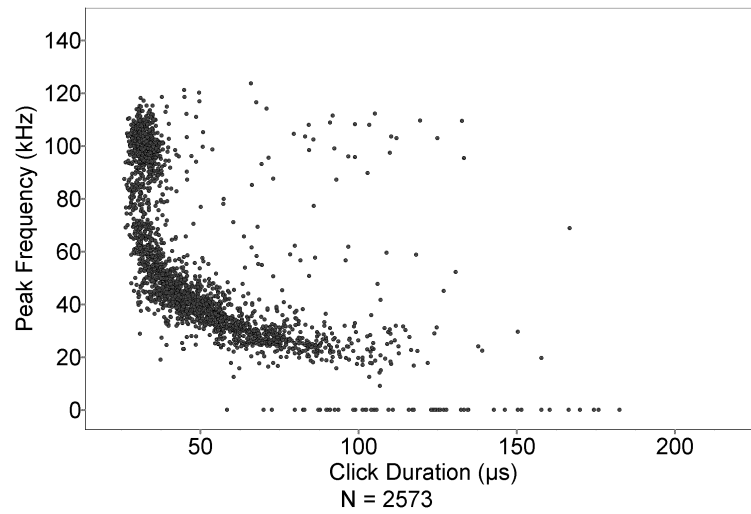


FIG. 82. Bivariate plot of peak frequency (kHz) vs. click duration (μs) (BUS).

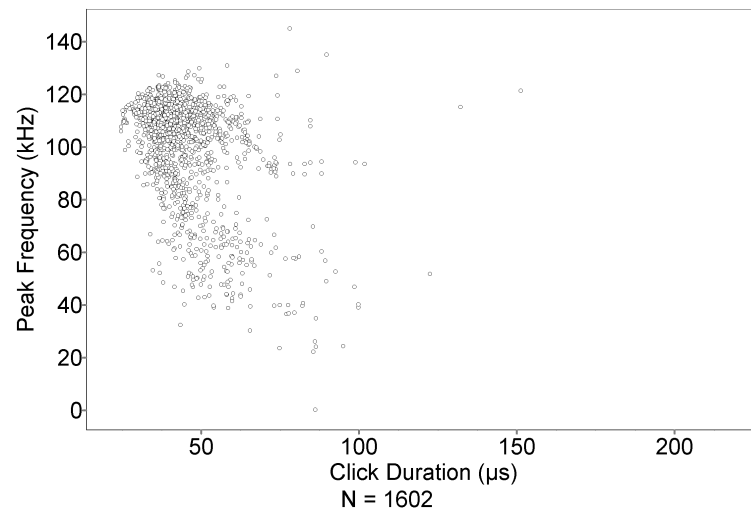


FIG. 83. Bivariate plot of peak frequency (kHz) vs. click duration (μs) (SAY).

TABLE XXX. Linear regression results for dominant frequency (kHz) vs. click duration (μ s).

Subject	Count	X term	Intercept	R ²	t	p
BRT	10852	-0.5148	96.49	0.5462	-114.3	<0.0001
BUS	2573	-0.6395	91.44	0.4396	-44.91	<0.0001
SAY	1602	-0.4762	117.4	0.1694	-18.06	<0.0001
Pooled	15027	-0.5391	98.55	0.4906	-120.3	<0.0001

TABLE XXXI. Second order polynomial regression results for dominant frequency (kHz) vs. click duration (μ s).

Subject	Count	X ²	X term	Intercept	R ²	s ²	F	p
BRT	10852	4.411	-1288	1.232e5	0.612	2.444e8	8543	<0.0001
BUS	2573	10.413	-2120	1.338e5	0.623	1.741e8	2126	<0.0001
SAY	1602	8.122	-1411	1.418e5	0.213	1.530e8	216.8	<0.0001
Pooled	15027	4.687	-1338	1.250e5	0.550	3.039e8	9182	<0.0001

The distribution of dominant frequency values with respect to click duration is shown in Figures 84-87. Linear regression statistics are given in Table XXX. Second order polynomial regression statistics are given in Table XXXI.

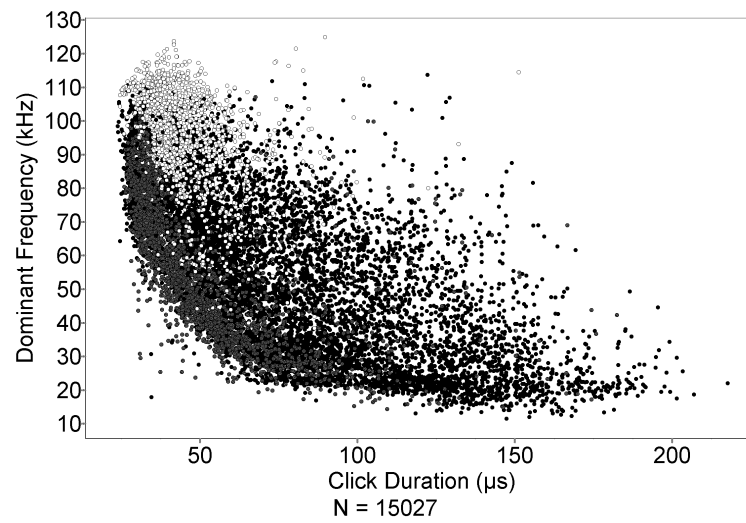


FIG. 84. Bivariate plot of dominant frequency (kHz) vs. click duration (μs) (pooled).

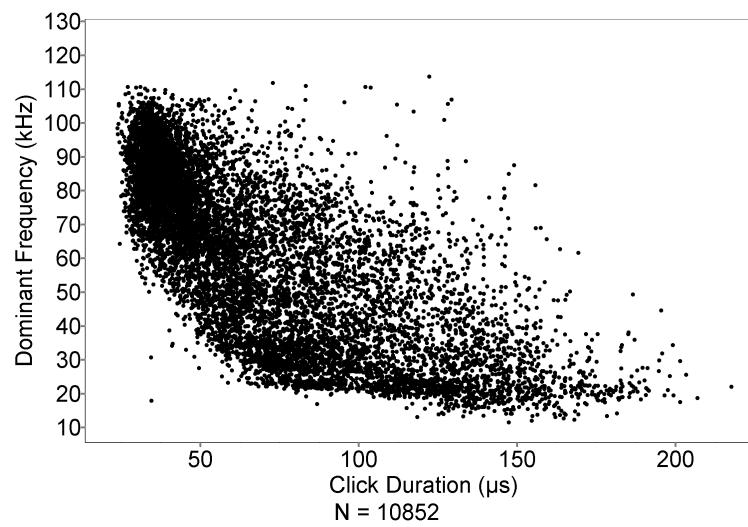


FIG. 85. Bivariate plot of dominant frequency (kHz) vs. click duration (μs) (BRT).

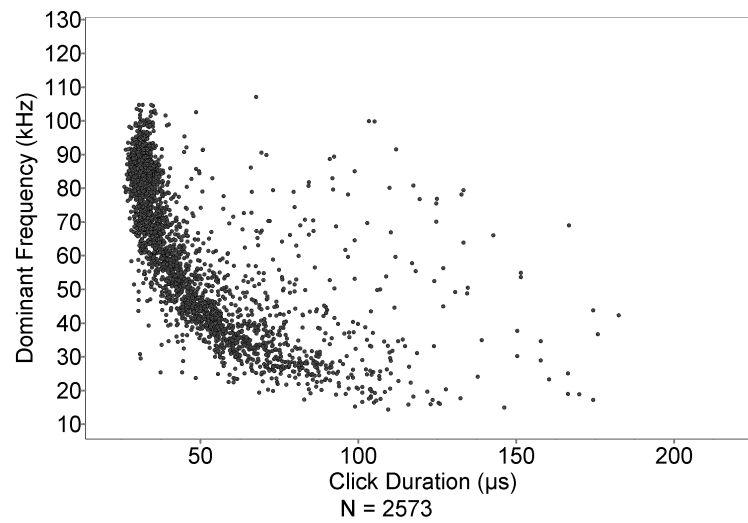


FIG. 86. Bivariate plot of dominant frequency (kHz) vs. click duration (μs) (BUS).

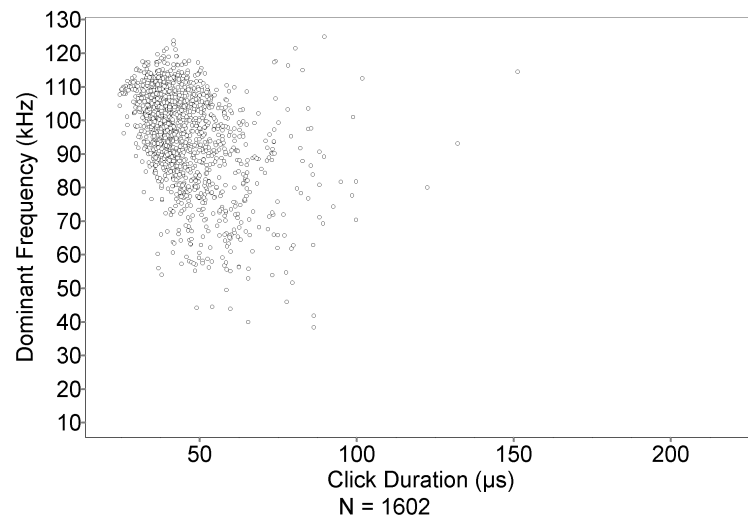


FIG. 87. Bivariate plot of dominant frequency (kHz) vs. click duration (μs) (SAY).

TABLE XXXII. Linear regression results for -3 dB bandwidth (kHz) vs. click duration (μs).

Subject	Count	X term	Intercept	R ²	t	p
BRT	10852	-0.4838	87.63	0.4847	-101.0	<0.0001
BUS	2573	-0.6118	87.25	0.4423	-45.16	<0.0001
SAY	1602	-0.3328	71.78	0.06636	-10.66	<0.0001
Pooled	15027	-0.4606	84.05	0.4380	-108.2	<0.0001

TABLE XXXIII. Second order polynomial regression results for -3dB Bandwidth (kHz) vs. click duration (μs).

Subject	Count	X ²	X term	Intercept	R ²	s ²	F	p
BRT	10852	1.163	-687.6	94676	0.489	3.199e8	5197	<0.0001
BUS	2573	6.627	-1554	114180	0.524	2.001e8	1415	<0.0001
SAY	1602	1.524	-508.2	76349	0.068	2.261e8	57.97	<0.0001
Pooled	15027	1.340	-688.9	91616	0.444	3.071e8	5998	<0.0001

The distribution of -3 dB bandwidth values with respect to click duration is shown in Figures 88-91. Linear regression statistics are given in Table XXXII. Second order polynomial regression statistics are given in Table XXXIII.

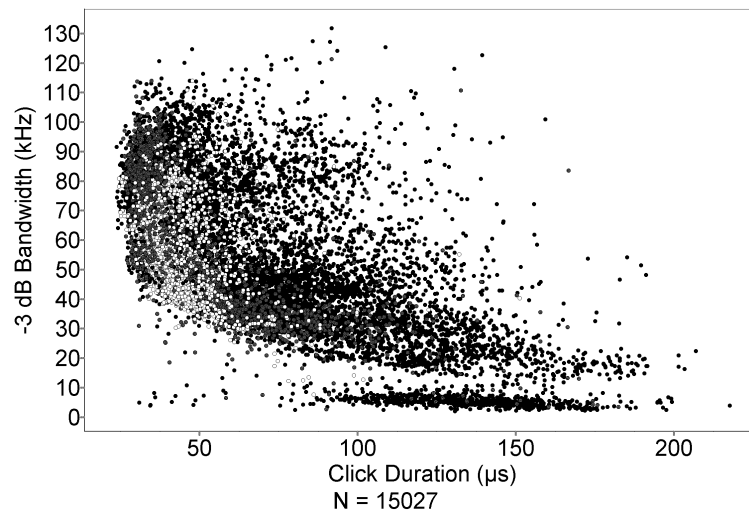


FIG. 88. Bivariate plot of -3dB bandwidth (kHz) vs. click duration (μs) (pooled).

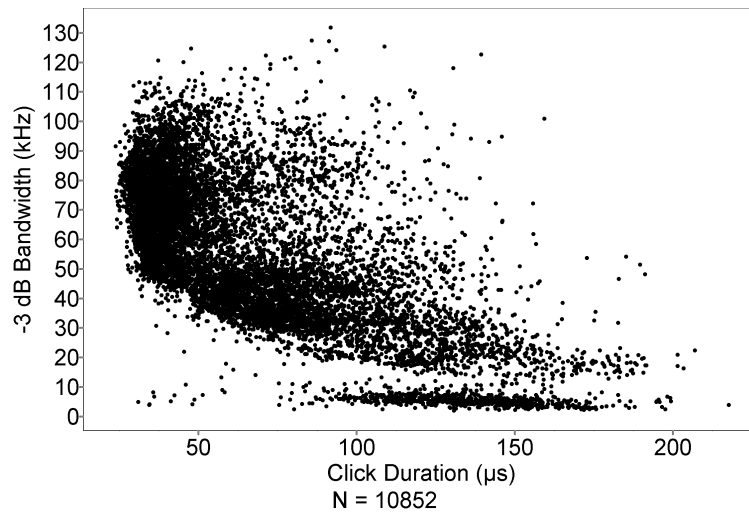


FIG. 89. Bivariate plot of -3dB bandwidth (kHz) vs. click duration (μs) (BRT).

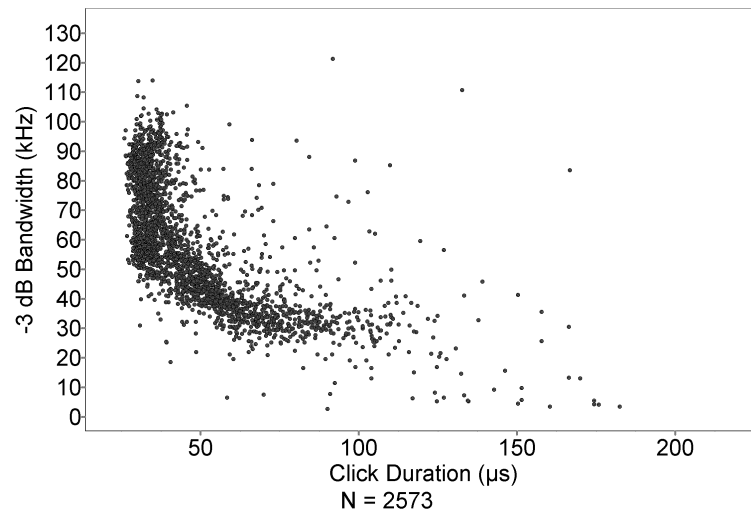


FIG. 90. Bivariate plot of -3dB bandwidth (kHz) vs. click duration (μs) (BUS).

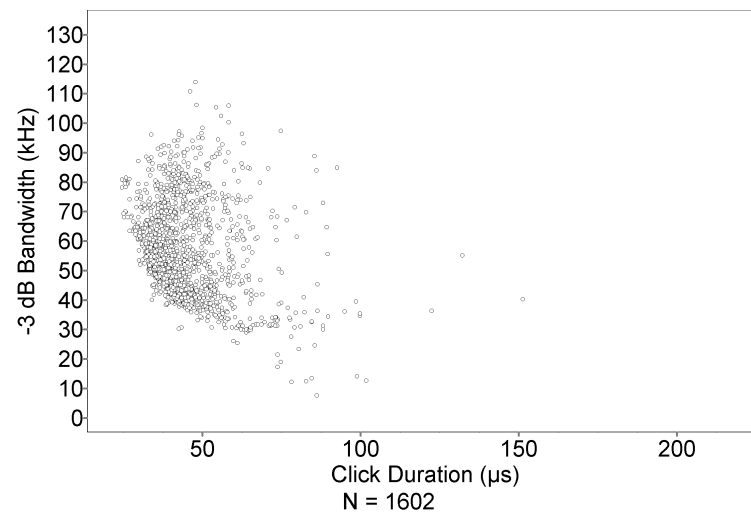


FIG. 91. Bivariate plot of -3dB bandwidth (kHz) vs. click duration (μs) (SAY).

TABLE XXXIV. Linear regression results for peak-to-peak source level (dB re 1 μ Pa) vs. radiated acoustic power (dB re 1 watt).

Subject	Count	X term	Intercept	R ²	t	p
BRT	10852	0.9942	187.2	0.9876	931.4	<0.0001
BUS	2573	0.9928	187.8	0.9933	616.4	<0.0001
SAY	1602	1.026	185.5	0.9921	447.8	<0.0001
Pooled	15027	0.9872	187.1	0.9891	1168	<0.0001

5. Radiated acoustic power treated as an independent variable

Peak-to-peak source level amplitudes plotted against radiated acoustic power are shown in Figures 92-95. Linear regression statistics are given in Table XXXIV.

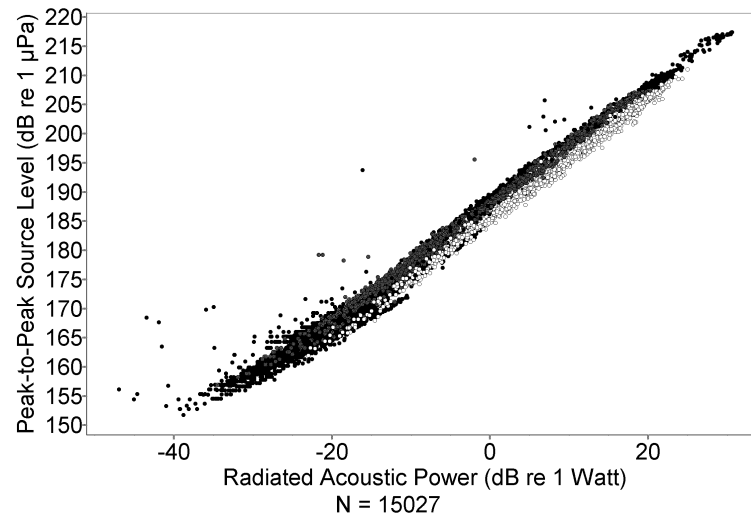


FIG. 92. Bivariate plot of peak-to-peak source level (dB re 1 μ Pa) vs. radiated acoustic power (dB re 1 watt) (pooled).

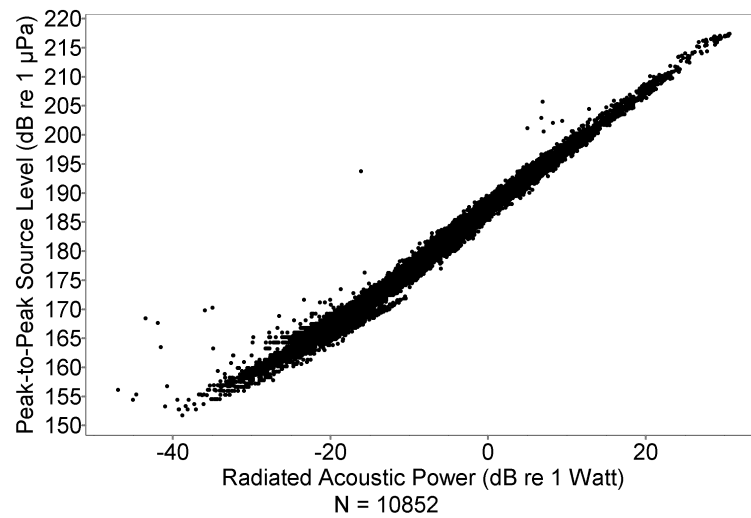


FIG. 93. Bivariate plot of peak-to-peak source level (dB re 1 μ Pa) vs. radiated acoustic power (dB re 1 watt) (BRT).

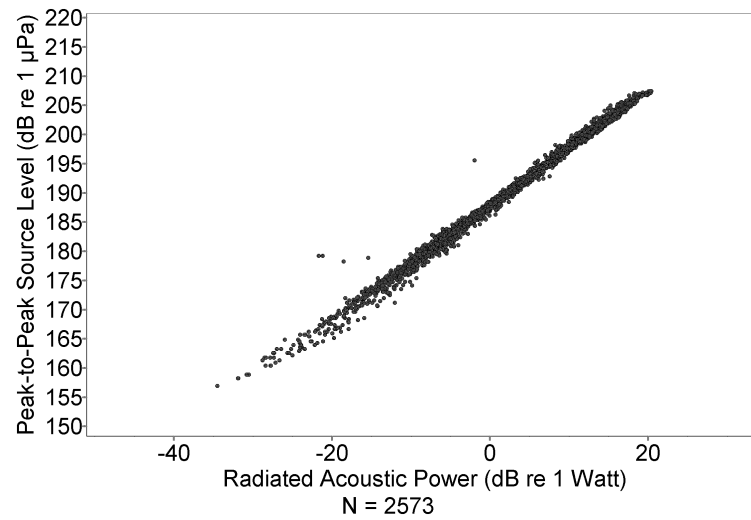


FIG. 94. Bivariate plot of peak-to-peak source level (dB re 1 μ Pa) vs. radiated acoustic power (dB re 1 watt) (BUS).

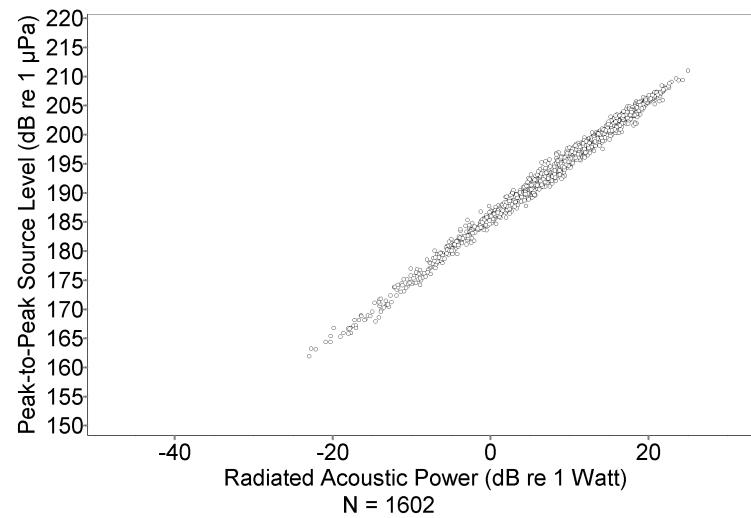


FIG. 95. Bivariate plot of peak-to-peak source level (dB re 1 μ Pa) vs. radiated acoustic power (dB re 1 watt) (SAY).

TABLE XXXV. Linear regression results for energy flux density (dB re 1 $\mu\text{Pa}^2\text{s}$) vs. radiated acoustic power (dB re 1 watt).

Subject	Count	X term	Intercept	R ²	t	p
BRT	10852	0.8409	127.5	0.9498	453.0	<0.0001
BUS	2573	0.8588	128.7	0.9764	326.0	<0.0001
SAY	1602	0.9847	126.8	0.9730	239.9	<0.0001
Pooled	15027	0.8609	127.9	0.9621	618.0	<0.0001

Energy flux density values plotted against radiated acoustic power are shown in Figures 96-99. Linear regression statistics are given in Table XXXV.

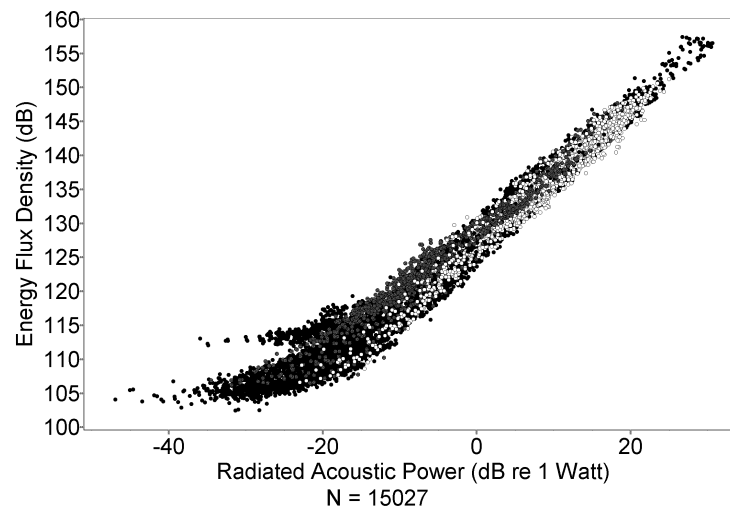


FIG. 96. Bivariate plot of energy flux density (dB re $1 \mu\text{Pa}^2\text{s}$) vs. radiated acoustic power (dB re 1 watt) (pooled).

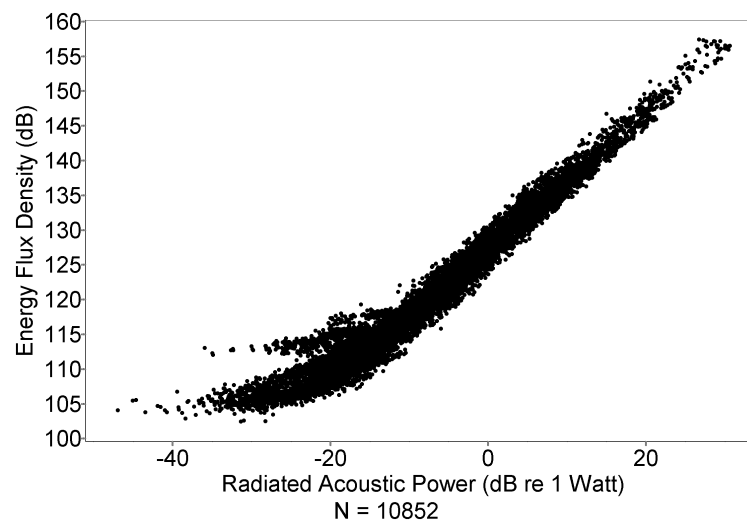


FIG. 97. Bivariate plot of energy flux density (dB re $1 \mu\text{Pa}^2\text{s}$) vs. radiated acoustic power (dB re 1 watt) (BRT).

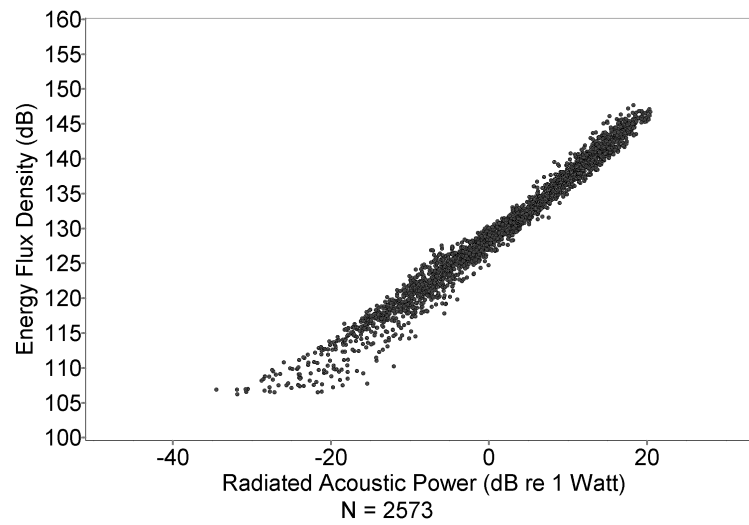


FIG. 98. Bivariate plot of energy flux density (dB re $1 \mu\text{Pa}^2\text{s}$) vs. radiated acoustic power (dB re 1 watt) (BUS).

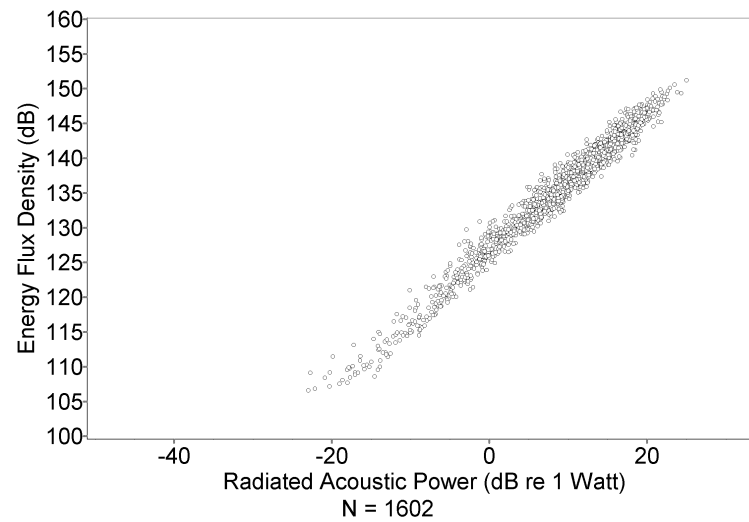


FIG. 99. Bivariate plot of energy flux density (dB re $1 \mu\text{Pa}^2\text{s}$) vs. radiated acoustic power (dB re 1 watt) (SAY).

TABLE XXXVI. Linear regression results for peak frequency (kHz) vs. radiated acoustic power (dB re 1 watt).

Subject	Count	X term	Intercept	R ²	t	p
BRT	10852	2.187	73.14	0.5827	123.1	<0.0001
BUS	2573	2.384	54.91	0.6557	69.97	<0.0001
SAY	1602	1.388	89.23	0.3780	31.18	<0.0001
Pooled	15027	2.133	70.83	0.5964	149.0	<0.0001

The distribution of peak frequency values with respect to radiated acoustic power is shown in Figures 100-103. Linear regression statistics are given in Table XXXVI.

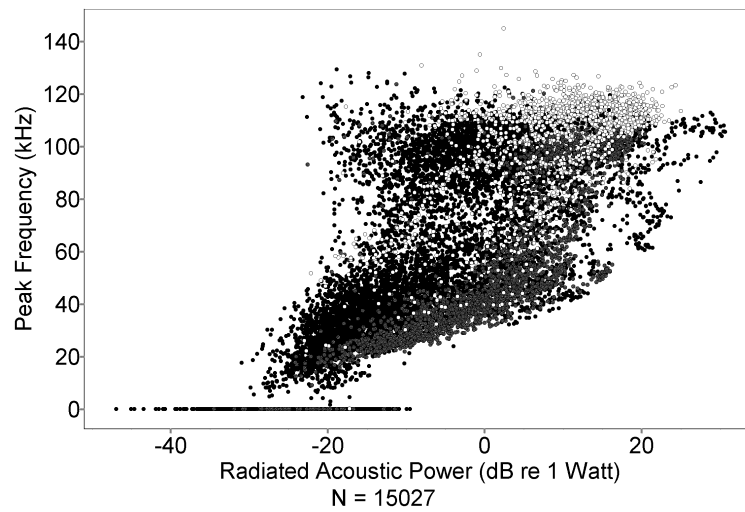


FIG. 100. Bivariate plot of peak frequency (kHz) vs. radiated acoustic power (dB re 1 watt) (pooled).

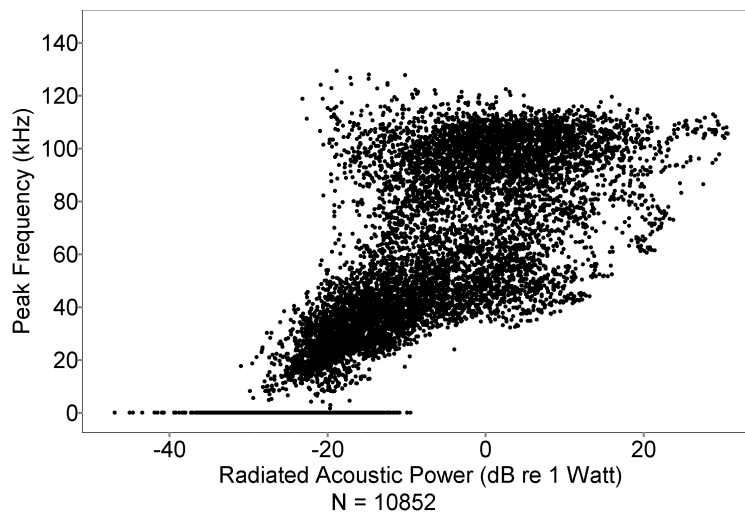


FIG. 101. Bivariate plot of peak frequency (kHz) vs. radiated acoustic power (dB re 1 watt) (BRT).

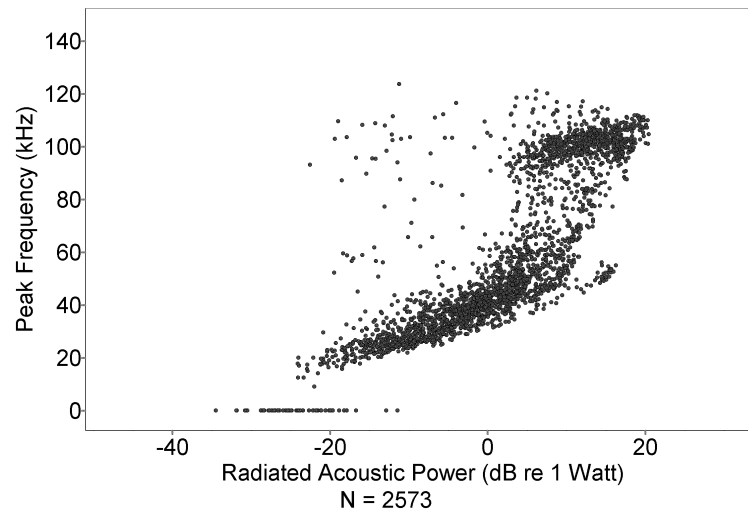


FIG. 102. Bivariate plot of peak frequency (kHz) vs. radiated acoustic power (dB re 1 watt) (BUS).

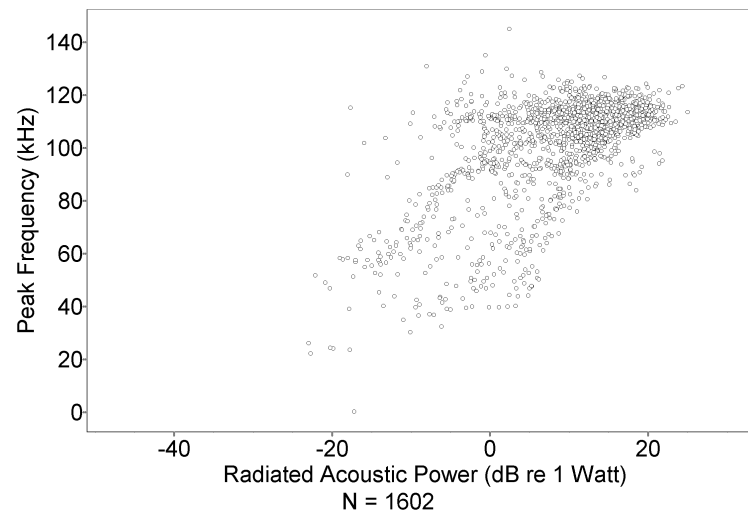


FIG. 103. Bivariate plot of peak frequency (kHz) vs. radiated acoustic power (dB re 1 watt) (SAY).

TABLE XXXVII. Linear regression results for dominant frequency (kHz) vs. radiated acoustic power (dB re 1 watt).

Subject	Count	X term	Intercept	R ²	t	p
BRT	10852	1.567	73.16	0.5920	125.5	<0.0001
BUS	2573	1.735	57.26	0.6983	77.13	<0.0001
SAY	1602	0.9691	88.10	0.3625	30.16	<0.0001
Pooled	15027	1.538	71.42	0.5924	147.8	<0.0001

The distribution of dominant frequency values with respect to radiated acoustic power is shown in Figure 104-107. Linear regression statistics are given in Table XXXVII.

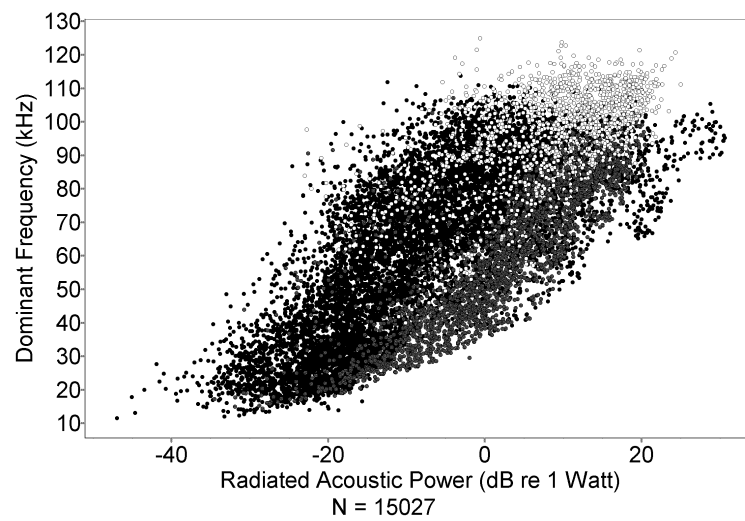


FIG. 104. Bivariate plot of dominant frequency (kHz) vs. radiated acoustic power (dB re 1 watt) (pooled).

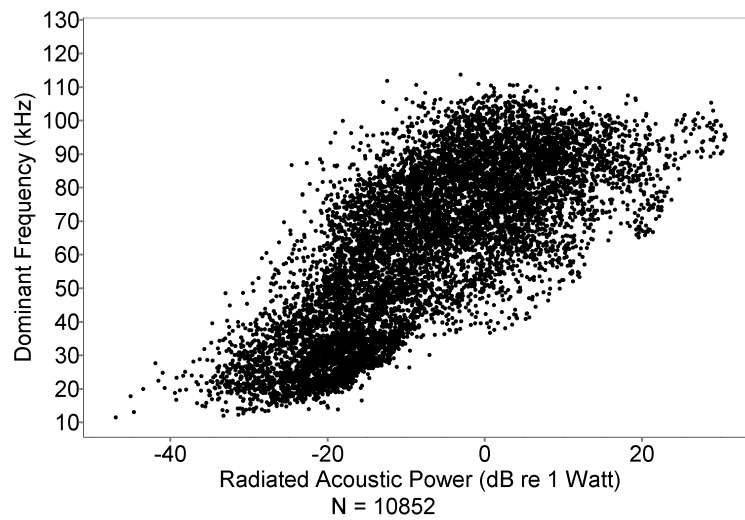


FIG. 105. Bivariate plot of dominant frequency (kHz) vs. radiated acoustic power (dB re 1 watt) (BRT).

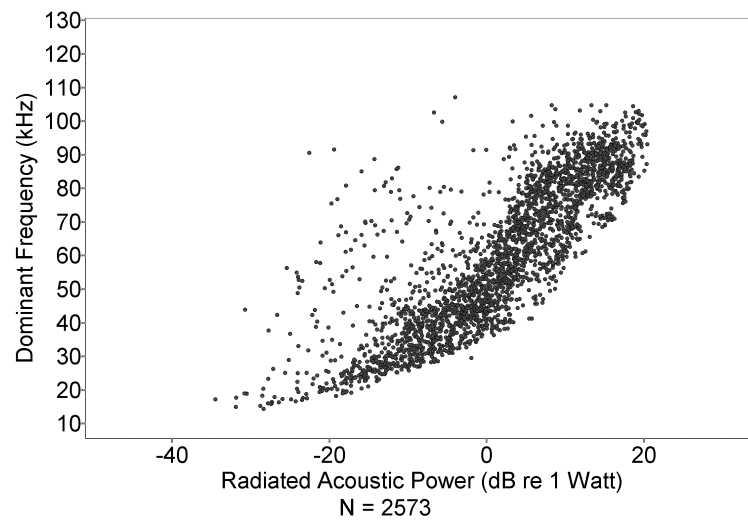


FIG. 106. Bivariate plot of dominant frequency (kHz) vs. radiated acoustic power (dB re 1 watt) (BUS).

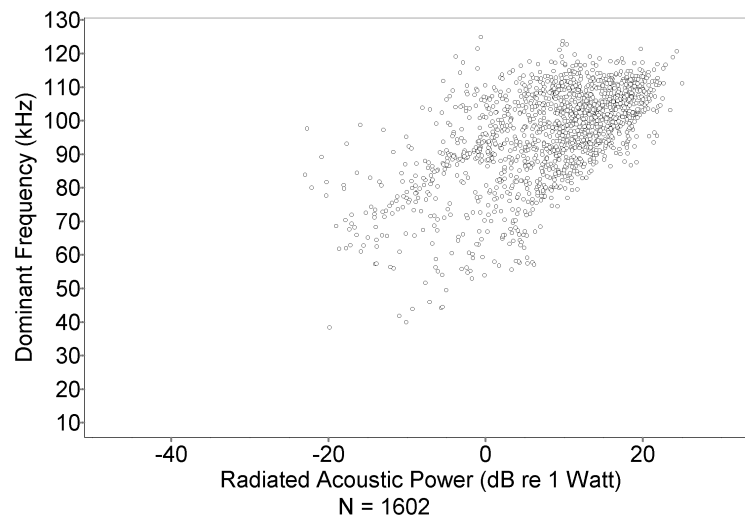


FIG. 107. Bivariate plot of dominant frequency (kHz) vs. radiated acoustic power (dB re 1 watt) (SAY).

TABLE XXXVIII. Linear regression results for -3 dB bandwidth (kHz) vs. radiated acoustic power (dB re 1 watt).

Subject	Count	X term	Intercept	R ²	t	p
BRT	10852	1.209	63.59	0.3539	77.10	<0.0001
BUS	2573	1.340	55.10	0.4575	46.56	<0.0001
SAY	1602	-0.2722	59.23	0.02293	-6.128	<0.0001
Pooled	15027	0.9630	59.26	0.2839	77.18	<0.0001

The distribution of -3 dB bandwidth values with respect to radiated acoustic power is shown in Figures 108-111. Linear regression statistics are given in Table XXXVIII.

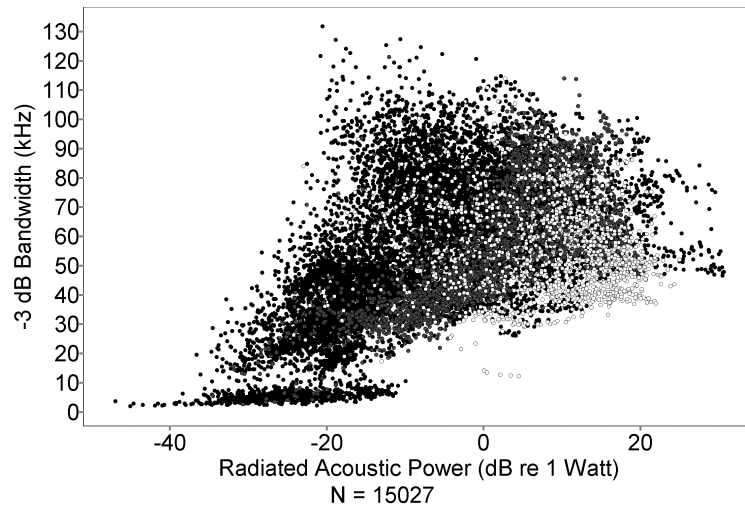


FIG. 108. Bivariate plot of -3dB bandwidth (kHz) vs. radiated acoustic power (dB re 1 watt) (pooled).

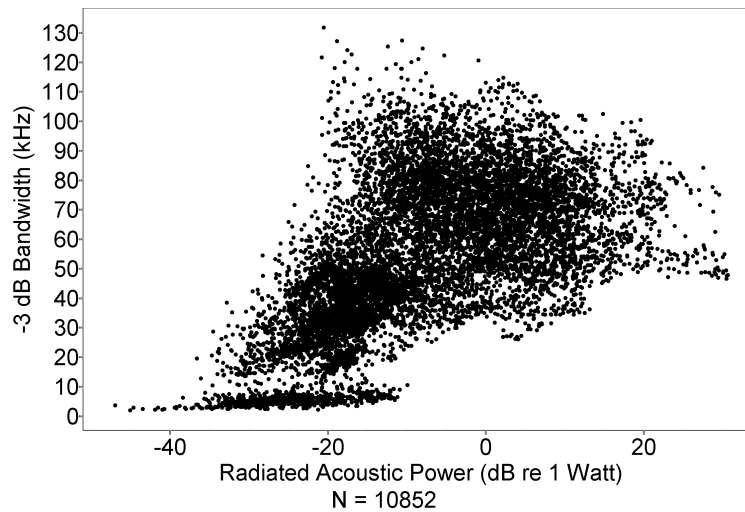


FIG. 109. Bivariate plot of -3dB bandwidth (kHz) vs. radiated acoustic power (dB re 1 watt) (BRT).

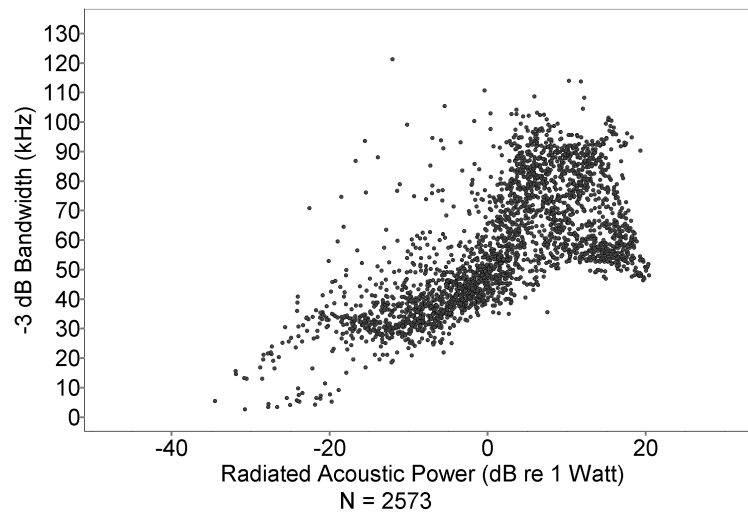


FIG. 110. Bivariate plot of -3dB bandwidth (kHz) vs. radiated acoustic power (dB re 1 watt) (BUS).

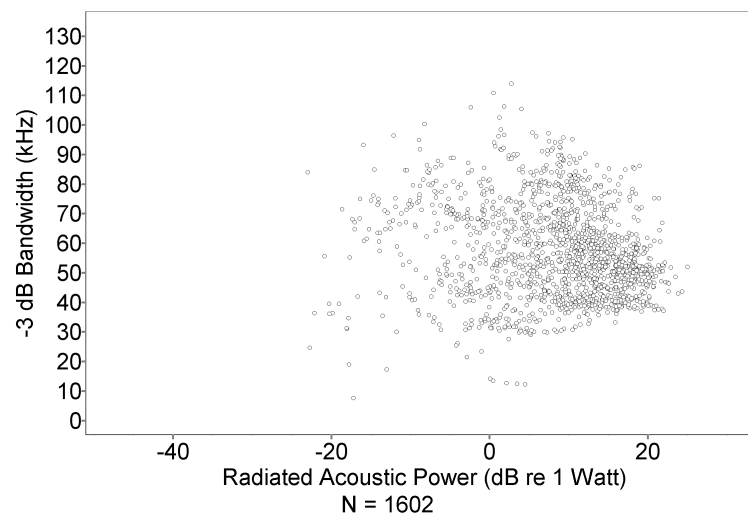


FIG. 111. Bivariate plot of -3dB bandwidth (kHz) vs. radiated acoustic power (dB re 1 watt) (SAY).

6. Classification of clicks

Houser *et al.* (1999) proposed a method of classifying bottlenose dolphin biosonar clicks based upon the frequency domain representation of each click. Table XXXIX lists the results of applying the Houser et alia classification procedure to the click data set of this study. Figure 112 shows a histogram of the percentage of clicks in each category split by the subjects. The categories proposed by Houser et alia are as follows:

A: Unimodal Low, a click with peak frequency less than 70 kHz.

B: Low Dominant, a click with peak frequency less than 70 kHz and a secondary peak greater than 70 kHz between -3 and -10 dB down.

C: Bimodal, a click with two peak frequencies, one less than 70 kHz and one greater than 70 kHz, that are within 3 dB of each other.

D: High Dominant, a click with peak frequency greater than 70 kHz and a secondary peak less than 70 kHz between -3 and -10 dB down.

E: Unimodal High, a click with peak frequency greater than 70 kHz.

W: Wideband, a click with a -3 db bandwidth greater than 85 kHz.

M: Multiple, a click with 3 or more distinct peak frequencies within 3 db of one another.

D. Discussion

Peak-to-peak source level amplitude values (Figures 20-23) show signs of individual variation. The distribution for BRT is weighted toward relatively low-amplitude clicks around 170 dB re 1 μ Pa, while many of the clicks for both BUS and SAY are of an amplitude between 190 and 200 dB re 1 μ Pa. The significant differences found between subjects on this property indicate that a considerable amount of variation

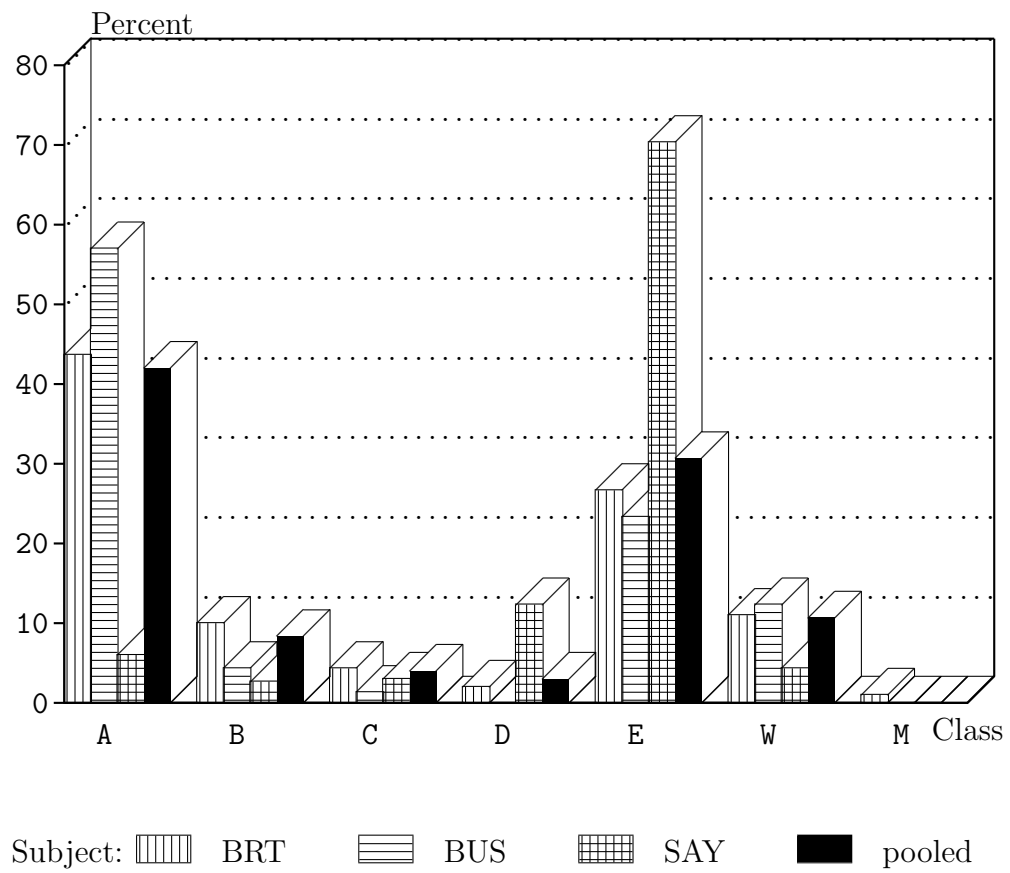


FIG. 112. Histogram of percentages of clicks in classes.

TABLE XXXIX. Classifications of clicks based upon spectral shape.

Class	Subject			
	BRT	BUS	SAY	Pooled
A: Unimodal Low	4,751 (44%)	1,470 (57%)	99 (6%)	6,320 (42%)
B: Low Dominant	1,122 (10%)	112 (4%)	46 (3%)	1,280 (8%)
C: Bimodal	504 (5%)	40 (2%)	52 (3%)	596 (4%)
D: High Dominant	248 (2%)	25 (1%)	201 (13%)	474 (3%)
E: Unimodal High	2,897 (27%)	602 (23%)	1,129 (70%)	4,628 (31%)
W: Wideband	1,214 (11%)	322 (12%)	72 (4%)	1,608 (11%)
M: Multiple	116 (1%)	2 (0.08%)	3 (0.2%)	121 (1%)
Total	10,852	2,573	1,602	15,027

may occur without reducing the efficacy of biosonar use for the target recognition task studied here.

1. Click duration

The click duration is skewed and is reminiscent of a Poisson distribution (Figures 24-27). For all subjects, the bin with the largest number of clicks within it lies in the range 35 to 45 μ s. This agrees closely with a typical figure reported by Au *et al.* (1974). Again, significant differences are noted between all three subjects on this property. The common click duration values below 50 μ s, though, fall below published figures by Au (1993, Table 7.2) of a range of 50 to 80 μ s. This may be due in part to the difference in calculation of click duration. Interestingly, the mean value of 63.5 μ s time duration is quite close to the value published by Wiersma (1982) of 59.7 μ s,

although Wiersma's number of clicks examined was 10, and in this study some 15,027 clicks were examined.

The clicks with the highest peak-to-peak amplitudes and radiated acoustic power values also have the shortest click durations. Because bottlenose dolphin biosonar signals are impulsive transients, the statistical method of determining click duration will find shorter durations for higher amplitude clicks. The signal-to-noise ratio (SNR) is much higher for high amplitude clicks than for low amplitude clicks. As the SNR decreases, the click duration necessarily increases.

2. Peak-to-peak amplitude

Au reported the largest amplitude click measured (at 230 dB re 1 μ Pascal) as having an acoustic power of 59 watts (Au, 1993, p.130). The largest amplitude observed within the data set of this study was 217 dB re 1 μ Pascal, a bit less than one-quarter the amplitude of the highest amplitude click reported by Au. The experimental conditions differed, the primary difference being distance to target. In Au's study, the distance was 70 meters, while in this study it was always less than 5 meters. Because target detection and recognition depends upon receipt of echoes and two-way travel introduces attenuation and spreading loss, at a given signal-to-noise ratio longer distances require higher amplitude clicks to achieve the same perceived loudness in the return echo.

The calculation of click duration is sensitive to the signal-to-noise ratio, as is detection and discrimination. The longer-duration clicks tend to be those with lower amplitudes and thus lower signal-to-noise ratios. Higher amplitude clicks are associated with shorter click durations. Linear regression showed a significant relationship between peak-to-peak amplitude and click duration, with some six-tenths of the variation in peak-to-peak amplitude in the pooled data being explained by the click du-

ration (see Table XXII). A higher order model, second-order polynomial regression, improves the coefficient of determination from about six-tenths to about seven-tenths (see Table XXIII). The plots of various properties taken against click duration demonstrate a similar trend, reminiscent of exponential decay. Zar (1984) warns, however, of taking transformations of variables (such as the log transformation) without regard for the *homoscedasticity* of the data. Log transformation is warranted in cases where variance in measurement increases with increasing values of the independent variable, but this does not appear to be the case for the current data set. Second-order polynomial regressions have been applied to data where click duration is taken as the independent variable in order to show the kind of improvement in fit values that may be achieved by a non-linear model.

Indications of considerable variability have appeared previously in the literature. The wide variability of ensond production was noted in Diercks *et al.* (1971). Kamminga and Beitsma (1990) published results from six bottlenose dolphins, where their subjects included both animals in the care of man and in the wild. In plots of frequency and bandwidth, the individuals tended to produce clicks in distinct, and in some cases non-overlapping, portions of the plot space. Au (1993) reviewed the properties of clicks, and noted substantial variability in some of these, including peak amplitude, peak frequency, and -3 dB bandwidth.

3. Bimodality

Discussion of *bimodality* takes two distinct forms. The first describes two peaks in the spectral representation of a single click. The second concerns the appearance of two distinct peak frequencies observed when considering an ensemble of clicks. For ease of reference, *spectral bimodality* will be used to refer to the former and *ensemble bimodality* will be used to refer to the latter.

An early publication of a click with spectral bimodality can be seen in Figure 1 of Evans (1973), where a click from *Inia geoffrensis* is shown. Discussion later in the paper concerned adaptive beam-forming, and observations were related to a series of clicks with different peak frequencies for components of the same click in *Tursiops truncatus*. Evans concludes that this is evidence for a “multiple element transmitting array” in *Tursiops truncatus*. Poché *et al.* (1982) presented waveforms and spectral plots of clicks from *Tursiops truncatus* that showed spectral bimodality.

An early publication of evidence indicating ensemble bimodality is seen in Kellogg (1961, Plate VII). A graphical display is shown there that includes peak frequencies from a series of clicks, where the peak frequencies range from 25 kHz up to 170 kHz. The bimodal distribution of biosonar clicks, or ensemble bimodality, seen in each subject in this study accords with results reported by Moore and Pawloski (1990) but not directly with the results reported by Au (1980). Au characterized the peak frequency and bandwidths of clicks produced by several bottlenose dolphins in a biosonar task in Kaneohe Bay, Oahu. In his work, Au reported histograms of peak frequencies showing a unimodal distribution with peaks in the range of 110 to 125 kHz across four subjects. There are several possible explanations for the differences between Au’s study and this one. First, the ambient noise in Kaneohe Bay is higher than the ambient noise in San Diego Bay (Au, 1993). This may have led the subjects in Kaneohe Bay to preferentially produce high-amplitude and high-frequency clicks. Second, the differences between our methods may have resulted in a greater proportion of lower-amplitude and lower-frequency clicks being part of this dataset. With a gap of almost two decades between our studies, the technology readily available now made it considerably easier to obtain a wider dynamic range, extending the useful range of recordings such that low-amplitude clicks can be analyzed. Third, the biosonar task in Au’s experiment involved targets at ranges over 70m, which

would render low-amplitude clicks less effective. By comparison, targets in this study were at ranges closer than 5m. Further, Moore and Pawloski (1990) showed that it is possible to put several characteristics of clicks under stimulus control. This suggests that training to task where these characteristics are not examined could result in superstitious behavior affecting the relative likelihood of the dolphin emitting clicks with particular characteristics. Averaging techniques in Au's study make it less likely for low-frequency clicks to be represented in the dataset. These considerations, either separately or in combination, might render it less likely for Au's study to reflect the lower-frequency mode clicks that were reported in this study.

Au (1980) did not address spectral bimodality directly; clicks with bimodal spectra were given only as being off-axis. This leads to an implication of spectral bimodality as an artifact of hydrophone placement in the acoustic field. In the dataset analyzed here, though, spectral bimodality cannot be considered an artifact of equipment placement. The hydrophone was placed on the main acoustic axis of the subject, and the subject's position was enforced by use of a bite plate, although internal beam steering might have produced this effect. Movement of the dolphin on the bite plate contributes to variation, possible spectral changes, and changes in estimates of radiated acoustic power.

Moore and Pawloski (1990) note that stimulus control of frequency by dolphins appears to be a difficult task, and speculate that this might be due to the mechanics of click production. They note a general tendency toward emission of spectrally bimodal clicks at higher click amplitudes.

4. Classification

The classification scheme for clicks based upon the frequency domain representation devised by Houser *et al.* (1999) is used here for comparative purposes. Certain features

of this classification are based upon arbitrary choices, such as the demarcation of 75 kHz as the boundary between low frequency and high frequency modes. However, the arbitrary nature of these choices is ameliorated by the fact that these selections were made with respect to a very large data set. The values in the data thus inform the choices.

The PSD plots of click ensonds can also reveal the presence of a significant secondary peak. Clicks having this property are called bimodal, and may represent the contribution of multiple sound sources to the ensond.

While the “Multiple” category was well-represented in the Houser et alia data set, relatively few clicks were so classified in this study. There are two reasons that may account for this occurrence. First, the specifications for obtaining discrete Fourier transforms differed. Houser et alia used a 256 point FFT with a rectangular window where all 256 points in the FFT came from around the click. In this study, a 2048 point FFT was employed with a Hamming window, and only the points calculated as being within the click duration were used, while the remainder of the 2048 points were filled with zeroes. This difference in analytical technique results in the frequency representations of this study being on the whole smoother in the outlines of the PSD plots. The frequency representations in the Houser dataset thus reflect more of the ambient noise. Because their classification system uses features in the PSD of a click, anything that changes the PSD, such as choice of windowing function, the definition of the relevant signal, and window size, can lead to a different distribution of classifications.

An interesting example of how classification can change with changes in spectral analysis is illustrated in Figures 113-116. Figure 113 shows the time series of a biosonar click. Figure 114 shows the PSD for the click when processed as in this study, with a 2048 point FFT, Hamming window applied over the points computed to be

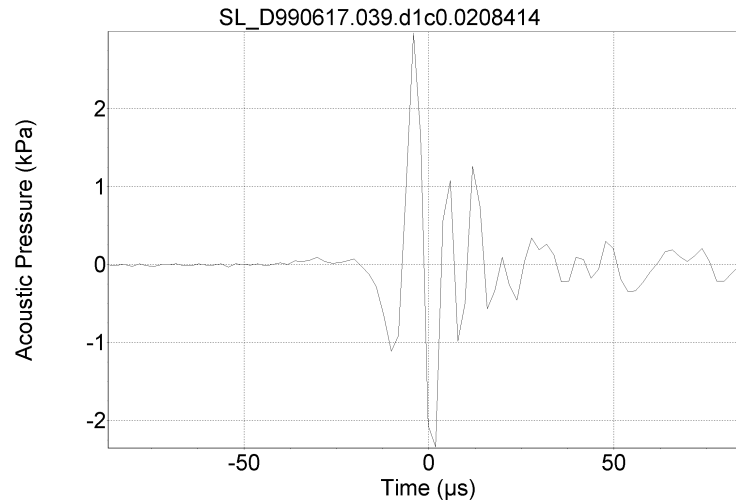


FIG. 113. Time series representation of a dolphin click.

within the click duration, and zero-padding of the remaining points. The classification found for that PSD is “E: Unimodal High.” Figure 115 shows the PSD for the click when processed with a 2048 point FFT, a rectangular window applied over the points computed to be within the click duration, and zero-padding of the remaining points. The classification found for that PSD is “C: Bimodal.” Figure 116 shows the PSD for the click when processed as in Houser *et al.* (1999) with a 256 point FFT and a rectangular window applied over the sample points. The classification found for that PSD is “M: Multiple.”

The choice of a window (other than a rectangular window) for use with the discrete Fourier transform represents a compromise where reducing sidelobes is desirable, but also affects other properties of the transform. For this study, the Hamming window was selected as a reasonable compromise. Marc Olivieri (personal communication) notes that use of the Hamming window reduces the contribution of low frequency components that occur early in the signal.

It is noticeable in the histograms of dominant frequency (44–47) the distribution

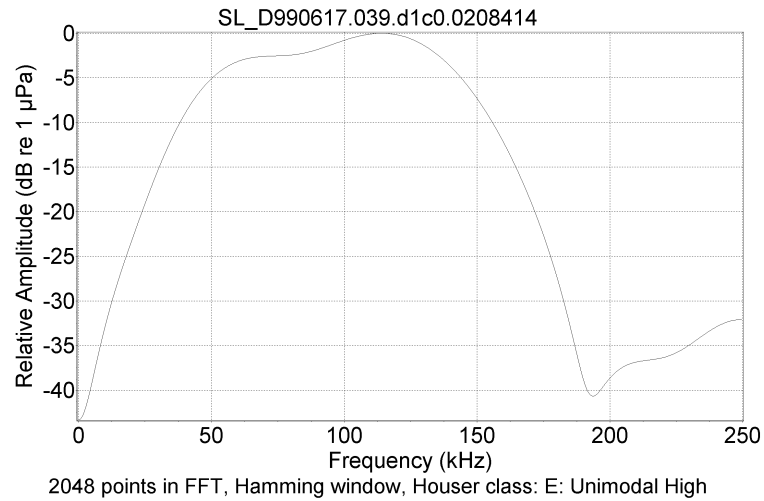


FIG. 114. PSD of click using 2048 points and a Hamming window as processed in this study.

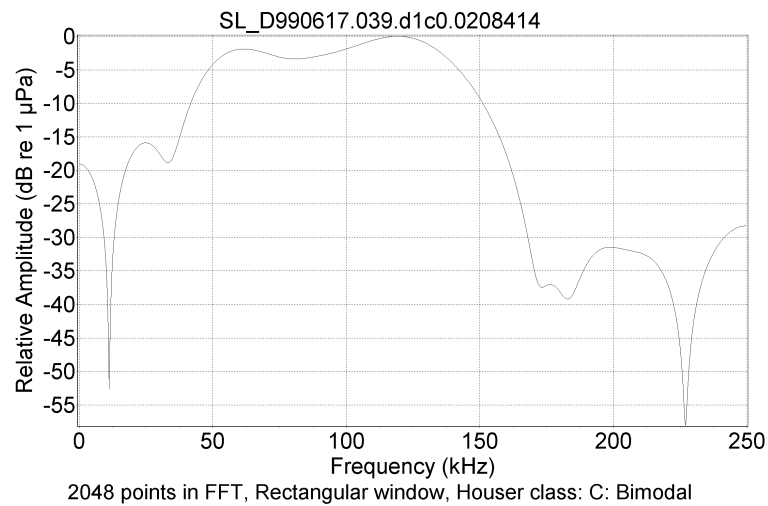


FIG. 115. PSD of click using 2048 points and a rectangular window.

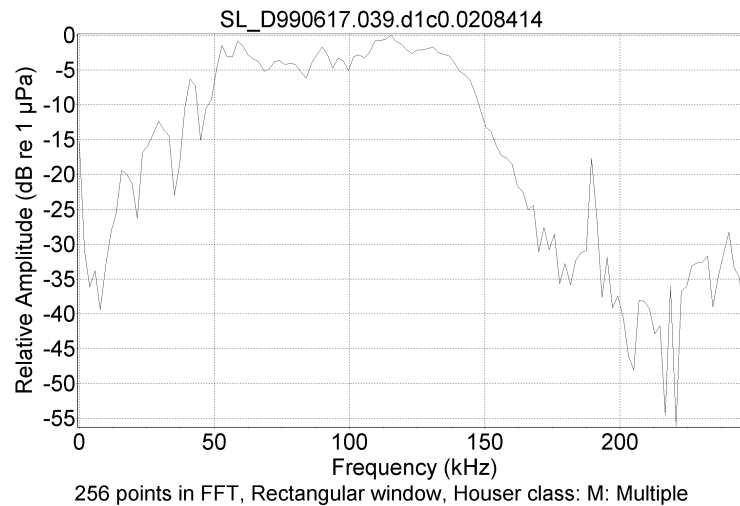


FIG. 116. PSD of click using 256 points and a rectangular window as processed in Houser *et al.* (1999).

of values does not show as sharp a distinction between low and high frequency peaks as seen in the histograms of peak frequency (40–43). The statistical nature of the determination of dominant frequency contributes to this spreading of values. In cases of clicks classified as “B: Low Dominant” or “D: High Dominant”, significant energy occurs in high and low frequencies, respectively. The determination of dominant frequency is likely to return a value somewhere in between the two regions where most peak frequencies are observed to occur.

It can be seen in 112 that there are apparent differences between subjects in the distribution of clicks in the Houser *et al.* (1999) classification scheme. SAY utilized primarily “E: Unimodal High” type clicks, while the predominant click class utilized by both BRT and BUS was “A: Unimodal Low”. This inter-subject variability in utilization of classes of clicks may be evidence for different *strategies* in the use of biosonar for target recognition. It should be noted that BRT and BUS were captured from the wild, while SAY was born at the Navy facility. The different use of types of clicks may derive ontologically from the differing environmental and functional con-

ditions during upbringing. Alternatively, both BRT and BUS are older than SAY, and differences in SAY's biosonar usage may stem from age-related changes in hearing. That hearing in dolphins may change with age was documented by Ridgway and Carder (1997). Examination of a greater number of subjects will be necessary to examine such issues. Since comparison is sensitive not only to the selection of digital signal processing parameters but also to the relation between alignment of the subject and placement of the hydrophone, casual recording of signals that does not give information about alignment will not be as useful as recordings where alignment information is available. Lammers and Au (2001) reported the use of a multi-element recording system that provides such alignment data for recording unrestrained subjects in open waters.

5. Interrelationships with intranarial pressure

The interrelationships between the various characteristics of biosonar clicks with the intranarial pressure difference from basal pressure show that there is no simple determination of those characteristics based upon that pressure. This is an intriguing result, since our current best account of the production of clicks implicates a pneumatic mechanism for click production, and the bony nares is the indicated reservoir of pressurized gas driving click production. The observations relevant to the mechanism of click production confirm the same result seen in previous studies (Ridgway *et al.*, 1980; Amundin and Andersen, 1983; Ridgway and Carder, 1988). This indicates that the intranarial pressure difference provides the energy for click production while regulatory and control functions of the anatomy between the bony nares and the phonic lips mostly determine the characteristics of biosonar clicks.

In two of the three subjects in this study, a significant regression result links increasing radiated acoustic power values to those for increasing intranarial pressure

difference. This effect is slight and probably is resolved because of the large number of observations available for analysis. High intranarial pressures occur concomitant with whistle onsets. The subjects sometimes ramp up intranarial pressure in preparation for emitting a whistle onset while still emitting clicks.

In other analyses, though, significant relationships are found where the slope of the regression differs between positive and negative for different subjects. It is hard to argue for a particular relationship when the available data do not show a consistent trend. This is the case for all the frequency domain characteristics examined here (peak frequency, dominant frequency, and -3dB bandwidth). Instead, it could be argued that these results show that biosonar click production may be subject to widespread individual variation in the mode of production. Biosonar click production is apparently a learned behavior (Reiss, 1988) with many parameters. Individuals may settle upon different combinations of parameters which produce effective biosonar clicks.

Substantial intranarial pressure is necessary for click production (Ridgway *et al.*, 1980; Amundin and Andersen, 1983; Ridgway and Carder, 1988; Cranford *et al.*, 2000). A minimum intranarial pressure difference of about 11 kPa was observed in the current study when clicks were produced. This is distinctly lower than the minimum figure of 25 kPa observed by Amundin and Andersen (1983). However, Evans and Prescott (1962) found that click-like sounds were produced in the nasal passages of a dead *Tursiops truncatus* specimen when air at 10.3 kPa and 10 liters per minute flow rate was passed through them.

E. Conclusion

Intranarial pressure provides the energy driving the click production system in the bottlenose dolphin (Ridgway *et al.*, 1980; Amundin and Andersen, 1983; Ridgway and Carder, 1988; Cranford *et al.*, 2000). But intranarial pressure does not explain most of the variation seen in the various click characteristics examined here. While statistical analysis of the results of this study show a significant correlation, it remains a weak correlation. Most of the variability seen in the production of clicks must derive from other causes within the click production process; this yields a situation where the interrelationships between intranarial pressure and the properties of emitted clicks are complex. The control structures which allow pressurized intranarial gas to flow or which cut off that flow and the motor systems which enervate them obviously play a crucial role in the click production process. The mechanical properties of the structures at the site of click production also appear to be variable under motor control of the dolphin, providing another set of factors contributing to determination of emitted click properties.

The minimum intranarial pressure difference seen in the three subjects of this study is just over 11 kPa. Given the large number of observed clicks, this value likely approaches the minimum intranarial pressure difference needed to produce clicks.

The variation observed in the click properties examined in this study is not an artifact. Considerable variation exists, whether one examines the pooled data or compares distributions between individuals. The variation in some cases casts a new light on previous descriptions of particular properties where such variation may not have been appreciated. This may be seen in the case of the bimodal distribution of peak and dominant frequencies. Simple characterization of some value as “typical” for clicks produced by bottlenose dolphins should be avoided. In a number of cases, a

“typical” value based upon a mean would be highly misleading, as again in the case of peak frequencies, where the mean value obtained falls into a region of the histogram where relatively few exemplars were found (Figure 40).

As indicated by the comparison of classification of a click under the Houser *et al.* (1999) procedure and the procedure used in this study, the manner in which analysis is conducted plays a large role in what results are found. A consistent approach is necessary to even allow comparison of results across research studies. There are many possible approaches; a combinatorial analysis of the free parameters would undoubtedly result in a very large number of permutations. The parameters selected as the basis of analysis for this study may form a starting point for discussion and possible improvement. The goal should be to establish, by consensus or by convention, the widespread use of a single set of consistent and reasonable parameters in performing click analysis. The desirable effects of such a standard would include better communication, greater comparability of results, and eventually better participation from researchers who otherwise might not attempt to utilize click analysis.

CHAPTER V

BIOENERGETICS OF INDIVIDUAL BIOSONAR CLICK TRAINS

A. Introduction

Consider an analogy between how biological organisms interact with the world and human economics. Instead of the money that underlies human economy, we can discuss energy as the coin of the realm in biological action. Each organism takes in energy and converts it, whether autotrophically or heterotrophically. As humans have budgets for their money, so we can think of organisms having a metabolic budget. Humans have income and debts measured in monetary terms, and animals have metabolic intake and demands. The societal environment of humans may impose taxes that reduce the monetary budget available, and the environment of organisms may impose costs in some places that add to metabolic demands. This research is about determining what kind of costs biosonar click sound production requires in the Atlantic bottlenose dolphin, *Tursiops truncatus*. In order to estimate this, a variety of measurements is necessary. Along the way, certain relationships between physiologic and acoustic phenomena will be elucidated.

Having an understanding of the relationship between the metabolic demand imposed by sound production and relevant parameters of the acoustic environment will aid in our understanding of bottlenose dolphin biology and ecology and also inform policy decisions that impact how humans change those environments. The biosonar signals of odontocete species may be adapted to environmental conditions (Evans, 1980). Bottlenose dolphin biosonar is based upon the active emission of high-amplitude transient sounds called clicks. Although data from studies in the wild is generally lacking (Evans *et al.*, 1998), biosonar is commonly assumed to play a sig-

nificant role in the ability of bottlenose dolphins to navigate and find food in turbid waters. Bottlenose dolphins are believed to communicate via both clicks and tonal ensonds called whistles. This communication is widely considered to be crucial to the normal social structure and function of bottlenose dolphin groups (Herman and Tavolga, 1980; Norris and Dohl, 1980). There is wide variation in the environmental parameters in which bottlenose dolphins are commonly found. There are both inshore and open ocean ecotypes. In inshore environments, there are wide differences in parameters such as depth, sound speed profile, bottom type, and surface conditions (Richardson *et al.*, 1995). Understanding something of how much it may cost bottlenose dolphins to produce their ensonds will help us understand the apparent choices that individuals and groups make in remaining in a particular environment or migrating to a different environment. When human agency causes a change in environmental parameters affecting acoustics, such as adding anthropogenic noise sources, having an understanding of how this may affect the metabolic budget of bottlenose dolphins also can provide valuable information about how such changes may influence the behavior of bottlenose dolphins.

The addition of noise to a marine environment imposes additional costs upon organisms who produce and perceive sound within that environment. The crucial question is, “How much does it cost?” If the cost is insignificant in the overall metabolic energy budget of bottlenose dolphins, we can rationally justify policy decisions that are different from the case that obtains if that cost is significant. This question has been difficult to answer for a variety of technical and ethical reasons. Unlike questions in human economics where one can directly interrogate persons concerning their budgets, we cannot simply inquire of the organism how much of its metabolic budget goes into sound production. Because the essential question involves both the acoustic product (the produced ensond) and the underlying process (the physiological

mechanism of sound production), the technical demands involve both acoustics and physiology being considered simultaneously. The acoustic problem is one that has been faced before: transduce a wide-bandwidth signal accurately and record it reliably in a marine environment (Diercks *et al.*, 1971). The physiological problem has also been faced before: transduce physiological measurements accurately and store them reliably in a marine environment (Ridgway *et al.*, 1980; Amundin and Andersen, 1983; Ridgway and Carder, 1988). In each case, the task is challenging. When putting these together to acquire simultaneous recordings, the difficulty level is not merely additive. A significant logistical burden is added. In the research reported here, this burden was met and the various difficulties overcome to yield a unique data set of simultaneous acoustic and physiological recordings taken of bottlenose dolphins in a biosonar task (Elsberry *et al.*, 1999; Cranford *et al.*, 2000).

The results from this study of bottlenose dolphins can be applied more generally to other odontocete species where obtaining similar data is impractical or infeasible. The bottlenose dolphin can be considered a model species in these cases by similarity of morphology.

The process of producing biosonar clicks requires a portion of the energy budget of the dolphin. There are two broad categories of approach in determining estimates of energy which biosonar click production uses. The first approach, which characterizes most past research efforts, seeks to define and delimit this amount by starting with the total energy budget or the basal metabolic rate and attempt to infer the amount which is involved in biosonar click production. These yield a systemic measure. The second approach attempts to model the underlying physics and apply measured parameters from the process in order to calculate an estimate of energy used in the process. This approach yields measures for particular phenomena. Both are useful, as the systemic measure provides an upper bound for energy costs produced via models of particular

processes, and measures of individual processes gives an indication of the relative significance of those processes in the systemic budget.

To estimate the work of sound production, both acoustic and physiologic data are necessary. For the acoustic part, the pressure the sound field can be measured over time. Given certain other data and assumptions, an estimate of acoustic power in watts can be derived. On the physiological side, there is a further complication in that attempting to estimate watts from some directly measurable physiological quantity requires that a particular model of sound production be adopted. In this instance, the relevant physiological measurement is taken to be intranarial pressure, the pressure of the gas inside the bony nasal passages of the bottlenose dolphin measured simultaneously with the produced sound. The hypothesized mode of sound production adopted here for the purpose of deriving the estimate of watts is that of sound production via passing pressurized gas through the phonic lips. The physical model used to produce the estimate of power is that of a simple piston and cylinder.

Having established the need for acoustic pressure measurements, physiological pressure measurements, and a relevant physiological model of sound production, the background information for each of these items should now be considered. The first step is to take up models of sound production and justify a selection for a relevant sound production model. Then, the means of determining various characteristics of bottlenose dolphin ensonds will be examined. Finally, some prior work on bioenergetics as it applies to bottlenose dolphin ensonds will be considered.

1. Overview of research on dolphin sound production

For decades, we have had more information about how bottlenose dolphins employ acoustic ensonds than how they produce those ensonds. A variety of factors combine to make localization of the sound source or sources in dolphins a challenging task. Un-

til recently the question of how they produce their ensonds was a matter of contentious debate. The difficulties in localizing the sound source or sources used by bottlenose dolphins are numerous. First, simply making good measurements of these sounds is technically demanding. The ultrasonic range utilized by bottlenose dolphins (20-200 kHz, broadly) is one that is not covered by conventional audio recording equipment, nor is it a range commonly utilized in radio and test equipment. This means that the equipment employed in making recordings of bottlenose dolphin ensonds either is fabricated specifically for this purpose or is optimized for some other purpose, but used in this fashion anyway. Fabrication is an expensive proposition and raises questions concerning how comparable the results obtained are to results found using other equipment. Using commercially available equipment designed for other purposes has often meant accepting bandwidth limitations that are not biologically justified. A common misconception is that even when using audio range gear, a bottlenose dolphin click ensond contains enough of a low-frequency component that such gear can reliably record the timing if not the frequency content of such clicks. As reported by Evans *et al.* (1998), bottlenose dolphins can and do emit click ensonds that may be entirely missed by audio range recording equipment. Commercial equipment designed for very high sampling rates, as for radio test equipment, may restrict dynamic range. This introduces quantization error and can affect spectral analysis, as well as making it difficult to adjust amplification to utilize as much of the available dynamic range as possible without clipping the signal.

One idea of dolphin click generation proposes that clicks are laryngeal in origin (Purves and Pilleri, 1983). Initial development of this concept probably stemmed from assumed similarity of morphology and function in most mammals, including the bats as terrestrial users of active biosonar. Further work also advanced laryngeal production as an alternative to other views which made counter-factual predictions

(Purves and Pilleri, 1983).

Evans (1973) discussed various hypotheses of sound production. He noted several criteria that any successful theory must meet. These criteria were derived from observations of sound production in dolphins. The criteria cited were: the ability to produce up to 600 pulses per second of 10-100 μ s in duration and 160-180 dB re 1 μ Pa source level; the ability to produce whistles for up to 3 s in the frequency range of 2 to 30 kHz; the ability to produce clicks and whistles simultaneously; and the ability to produce beam patterns corresponding to observed beam patterns from dolphins. These were derived from observed characteristics of sounds produced by delphinids.

Bel'kovich and Dubrovskiy (1976) give a fairly detailed hypothesis of sound generation at the lateral margins of the nasal plugs. They assert that there are similarities in this mechanism to that of the human vocal cords. They conclude that the internal nasal plugs can operate independently, simultaneously and can produce both whistles and clicks.

Dormer (1979) used high-speed cineradiographic techniques to observe movements of musculature in three species, including *Tursiops truncatus*. His results excluded laryngeal production of clicks, whistles, and miscellaneous other sounds, and he concluded that the match of movement activity and timing of click onsets implicated the nasal plugs as contributing to sound production. Dormer also offered a mechanical model of sound production in the porpoise. He relegated the role of the larynx to that of a valve controlling air flow from the lungs into the naso-pharyngeal air space (what is referred to here as the *intranarial space*).

2. Experimental work involving pressure measurements

There have been four published prior studies that measured intranarial pressure in odontocetes (Ridgway *et al.*, 1980; Amundin and Andersen, 1983; Ridgway and

Carder, 1988; Cranford *et al.*, 2000). No attempt to estimate bioenergetic cost of ensonds was made in these previous studies.

3. Metabolic estimation of biosonar cost

Bioenergetic costs in odontocete species have been approached in the past utilizing energy budgets (discussed in Richardson *et al.* (1995)) and analysis of oxygen consumption (Cole, 1995).

The bioenergetic cost of biosonar activities has been approached by Cole (1995), who used analysis of respiratory gases to estimate basal metabolic rates and metabolic rates during the performance of a biosonar task. The difference between these two rates provides an estimate of the energy requirements needed for biosonar use. Cole utilized four *Tursiops truncatus* subjects in her work, and found a pooled estimate of 1.95 x basal metabolic rate as a cost of echolocation use at a 100% duty cycle. The actual increase in metabolic costs will obviously depend upon the proportion of time spent in actual echolocation activity, but Cole's figure places an upper bound on the likely cost to a subject engaged in an echolocation task.

By using a model based upon the relevant anatomy and measurements of physiological parameters in the subject performing a biosonar task, it is possible to estimate a lower bound on the cost of sound production for biosonar. The estimate is a lower bound because there may be work performed by musculature not associated with elements of the model, and thus not included in producing the estimate of cost.

Knowing the pressure in the intranarial space is insufficient on its own to derive an estimate of work, and thus bioenergetics, but by coupling measured pressure with a model of intranarial dynamics, estimates of work can be derived. Work is by definition force applied over a distance, and power is the rate at which work is performed. A simple model of intranarial dynamics produces conservative estimates

of work and power. The intranarial space is a volume which is divided between two lateral passages running between the premaxillary bone anteriorly and the frontal bone posteriorly. A complex of three muscles can close off the space anteroventrally, and the nasal plug can close off the space posteriodorsally. The model is an equivalent piston-cylinder, which simplifies the calculations needed for deriving work and power estimates. The parameters of the piston-cylinder model were derived from available anatomical information and a set of volume measurements taken from *Tursiops truncatus* skulls. This information was not taken from the particular subjects used in this study. The total area of the musculature at the anteroventral end of the intranarial space yields the value of the area of the model piston face. The volume of the intranarial space in a series of skull preparations of bottlenose dolphins yields the information for initial volume before pressurization, and thus the height of the cylinder at the initial volume in the model.

4. Necessity of pressure data to produce estimates

It is only with respect to a particular mechanism of sound production that one can assess the effort which goes into making the sound, and from that the efficiency with which physiologic effort is converted into acoustic energy. In this work the theory of sound production at the *museau de singe* or monkey lips, now referred to as the phonic lips (Cranford *et al.*, 1996), was adopted. Under this view, the dolphin produces pressure in the bony nares and manipulates the dorsal bursae and associated phonic lips to produce both clicks and whistles. Because pressurization of gas in the bony nares requires work on the part of the dolphin to initiate and maintain, such pressurization events impose energetic costs on the dolphin that must be paid out of its metabolic energy budget. This budget places a hard limit upon what can be considered feasible energy expenditures. However, energy budgets and

examination of oxygen consumption are systemic measures which cannot directly provide information concerning the processes of click production for individual click trains. Modelling the physics of click sound production can produce estimates of mechanical work for individual pressurization events. Mechanical work is the work done in the classical physics definition of work: force applied over a distance. There are two concerns which estimating mechanical work only indirectly addresses, which are the amount of physiological effort that underlies the perceived mechanical work, and the amount of physiological effort which is ignored by finding mechanical work.

B. Methods

Seven skulls of *Tursiops truncatus* were measured for volume of the intranarial spaces. The technique involved closing off the dorsal apertures of the nasal passages with a 1/4" thick neoprene pad, pouring small metal balls (Daisy BBs, steel shot with zinc plating, 4.37mm diameter) into one or both side passages to fill, then measuring the balls in a graduated cylinder to obtain the volume. Packing of these balls was quite good even without agitation; volume observed before and after agitation in the graduated cylinder was within the limit of resolution of the cylinder (2ml). To obtain volumes for the right and left sides, balls were added until the volume filled was level with the ventral edge of the septum dividing the right and left passages. A volume measure based upon the space enclosed by the ventral extension of the pterygoid bones was made by use of modeling clay applied to close off the characteristic gaps on each lateral side, and filling the space defined within the pterygoid bones and as far caudally as the suture of the sphenoid and basioccipital bones.

A set of computed tomography (CT) sections in one specimen of *Tursiops truncatus* was also measured. The CT sections were provided by Dr. Ted W. Cranford.

Measurements were taken using the NIH JIMAGE software package. Measurements of the area filled with gas in each section were made. An estimate of total gas volume was made by numerically integrating the area in each section times the slice thickness over all the sections. An estimate of the area of the surface of the palatopharyngeal muscle complex was made by measuring the distance across the bony nares just ventral of the septum and numerically integrating the product of that distance with slice thickness over all the sections.

1. Calculations of work and power based on model

A *pressurization event* (PE) is a period of time in which the *intranarial pressure* rises above the resting state pressure (termed *basal pressure* here), and then returns to the resting state pressure. Emitted clicks reliably occur only in association with PEs.

The amount of work associated with a PE can be estimated on the basis of a model of click sound production. The model has certain assumptions which are reasonable, but which if violated could lead to inaccuracy of the derived estimate. A piston-cylinder model of the underlying physics is adopted. The area of the piston face is taken as the cross-sectional area of the palatopharyngeal muscle complex as it enters the ventral portion of the bony nasal passages. The initial volume of the cylinder is taken from measurements of the volume of the right and left bony nasal passages in prepared skulls of *Tursiops truncatus* and data from computed tomography. Intranarial pressure at a given time is taken from pressure catheter readings in the bony nares. The model assumptions are that the volume of gas leaving the pressurized reservoir per click ensound is negligible, and that pressure changes in the reservoir are adiabatic (over the time course of interest, there is negligible thermal interchange between the pressurized gas and the surrounding tissues) (Coulombe *et al.*, 1965). Given these measurements, model, and assumptions, the derivation of an

equation yielding an estimate of work in Joules follows.

$$Work = Force \bullet distance \quad (5.1)$$

$$Joules = Newtons \bullet Displacement \quad (5.2)$$

$$Joules = [Pascals * Area] \bullet Displacement \quad (5.3)$$

$$Volume_t = \frac{Volume_0}{\left(\frac{P_0}{P_t}\right)^{\frac{1}{\gamma}}} \quad (5.4)$$

$$|\Delta Volume| = |Volume_0 - Volume_t| \quad (5.5)$$

$$Displacement = \Delta height = \frac{|\Delta Volume|}{Area} \quad (5.6)$$

where γ is the adiabatic exponent for air, 1.40.

The work performed over the course of a PE is derived by numerical integration, based upon the discussion of "work performed against a variable force" in Miller, Jr. (1977, p. 120). The initial volume, V_0 , is taken as the sum of the volumes of the right and left nasal passages adjusted for displacement of tissues lining those passages. The pressure values are taken from the average of digitized values within each 1 ms period of time within the PE. The algorithm to do this can be expressed as a summation based upon the equations given above.

$$Joules = \sum_{i=1}^{n-1} \left(\frac{P_i + P_{i+1}}{2} * A \right) \bullet \frac{|V_i - V_{i+1}|}{A} \quad (5.7)$$

$$Joules = \sum_{i=1}^{n-1} (\bar{P} * A) \bullet \frac{|\Delta V|}{A} \quad (5.8)$$

where A is the area of the piston face, \bar{P} is the mean of the i th and $(i + 1)$ th measured pressures, and $|\Delta V|$ is the absolute value of the difference in volume between the i th and $(i + 1)$ th samples, as calculated by considering the pressure change observed to occur under adiabatic conditions.

Numerical integration to find mechanical work estimates was performed only on pressurization events classed as *complete* (see Methods section of Chapter 2).

The effect of increasing depth on mechanical work was estimated using the results from the mechanical work estimate found for the conditions of our study, that is, with the subject stationed at 0.5m depth. First, the basal pressure was adjusted to reflect the ambient pressure at depth as well as the basal pressure seen at 0.5m. Second, the numerical integration was re-run with the adjusted pressure figures. This process was repeated for pressures up to 10 atmospheres, corresponding to a depth of 100m.

C. Results

The measurements taken from *Tursiops truncatus* skulls are given in Table XL, where CBL is condylar-basal length, PW is parietal width, LPM is left premaxillary width (at the anterior border of the left bony naris), RPM is right premaxillary width (at the anterior border of the right bony naris), LNP is left nasal passage, RNP is right nasal passage, and PNV is pressurized nasal volume.

A linear regression of total length with LNP volume yields a regression line of $Y = -41.91 + 0.479 * X$ and an R^2 value of 0.65. This means that total length explains almost two-thirds of the variation seen in LNP volume. The complementary linear

TABLE XL. Physical measurements of *Tursiops truncatus* skulls.

Specimen	CBL	PW	LPM	RPM	LNP	RNP	PNV	Sex	Length
	(cm)	(cm)	(cm)	(cm)	(ml)	(ml)	(ml)		(cm)
084248	47.9	21.0	3.6	5.4	72	72	310	M	242.0
084250	50.8	20.5	3.8	5.5	80	86	288	F	250.0
084242	48.2	19.4	3.8	5.3	82	84	274	F	263.0
084271	51.9	19.8	3.8	5.4	88	88	292	F	285.0
084285	50.5	20.9	4.3	6.0	89	86	278	F	267.5
084036	52.2	20.0	3.6	5.6	100	92	366	M	277.0
084065	49.3	20.5	4.2	5.8	82	84	314	M	266.0

regression for RNP yields a regression line of $Y = -2.358 + 0.329 * X$ and an R^2 value of 0.615.

1. Computed tomography

Computed tomography (CT) measurements of a *Tursiops truncatus* (dolphin #3 scanned by Ted W. Cranford on June 12, 1986) gave the following results. Nasal passage muscle inclusion volume was $6.74e-5 \text{ m}^3$. Excluded nasal passage muscle volume was $1.86e-5 \text{ m}^3$. Left nasal passage air volume was $2.83e-5 \text{ m}^3$. Right nasal passage air volume was $2.50e-5 \text{ m}^3$. Total nasal passage air volume was $5.33e-5 \text{ m}^3$. Total muscle and air volume was $1.39e-4 \text{ m}^3$. The cross-sectional area just inferior to the nasal septum was $2.20e-3 \text{ m}^2$.

Complete pressurization events (PEs) in which a biosonar click train occurred were analyzed. For 306 PEs, a mean value of 10.3 joules was found, with a standard deviation of 4.155. Of those 306 PEs, 225 PEs had no whistle ensounds. These 225

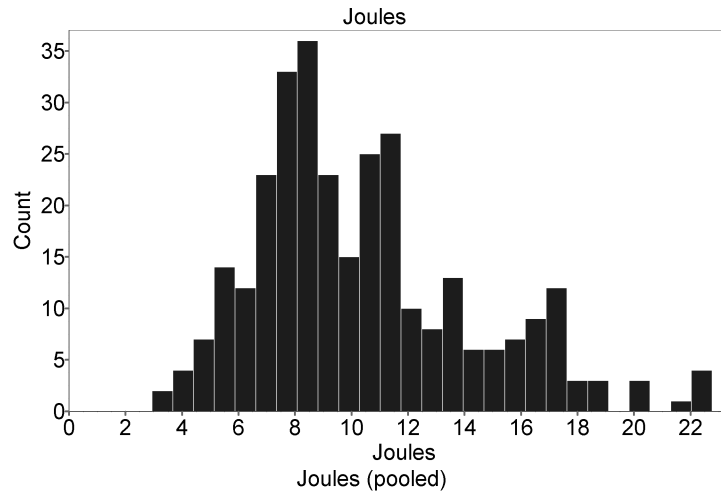


FIG. 117. Histogram of joules in complete pressurization events (pooled).

PEs had a mean of 8.5 joules and a standard deviation of 2.49 joules. The remaining 81 PEs had associated whistle ensonds. These 81 PEs had a mean of 15.4 joules and a standard deviation of 3.66 joules.

Figures 117-119 show histograms of joules in pressurization events for all three subjects. Figure 118 and figure 119 compare the distribution of values for those pressurization events that do not include a whistle ensond and those that do, respectively.

Complete pressurization events (PEs) in which a biosonar click train occurred were analyzed. For 306 PEs, a mean value of 5.49 watts was found, with a standard deviation of 2.77. Of those 306 PEs, 225 PEs had no whistle ensonds. These 225 PEs had a mean of 4.48 watts and a standard deviation of 2.07 watts. The remaining 81 PEs had associated whistle ensonds. These 81 PEs had a mean of 8.28 watts and a standard deviation of 2.54 watts.

Figures 120-122 show histograms of watts in pressurization events for all three subjects. Figure 121 and figure 122 compare the distribution of values for those pres-

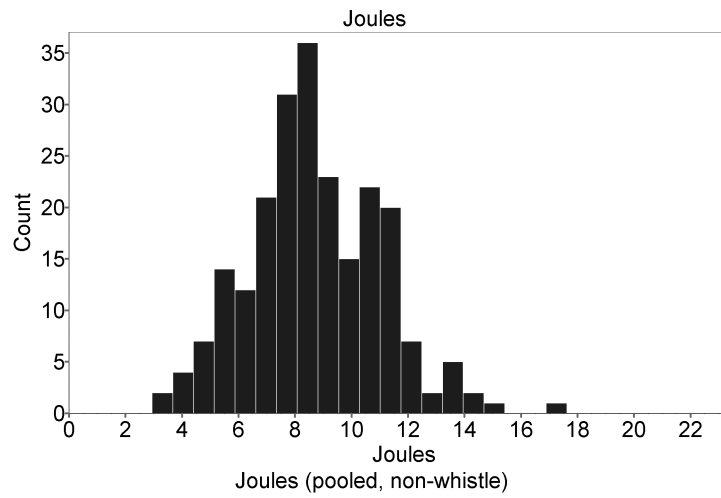


FIG. 118. Histogram of joules in complete pressurization events where no whistle ensounds occur (pooled).

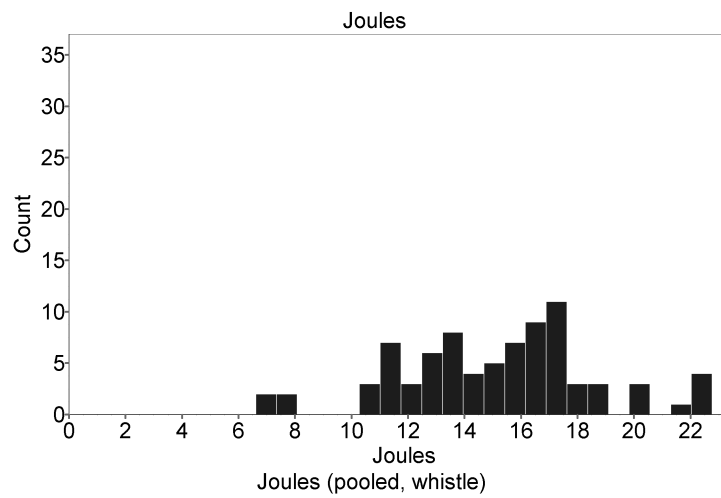


FIG. 119. Histogram of joules in complete pressurization events where whistle ensounds occur (pooled).

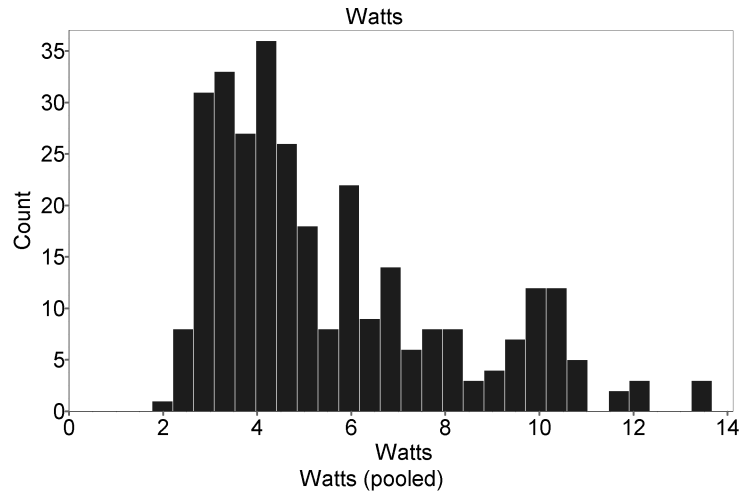


FIG. 120. Histogram of watts in complete pressurization events (pooled).

surization events that do not include a whistle ensound and those that do, respectively.

Analysis of a complete pressurization event with a value of mechanical work near the average value of 10.5 Joules shows the change in work with depth seen in Figure 123. The value for one atmosphere of pressure is what is observed; the remaining values are based upon re-computing the numerical integration with changes to the basal pressure as needed for each depth.

D. Discussion

1. Physics of click production and energy

Anthony Sloss worked from physical principles and previously reported click parameters to derive an estimate of energy requirements in the bottlenose dolphin (Sloss, 1984). Sloss derived a maximum power output value of 1,740 watts to account for a click of 228.1 dB re 1 μ Pascal peak-to-peak amplitude. Sloss references Au for

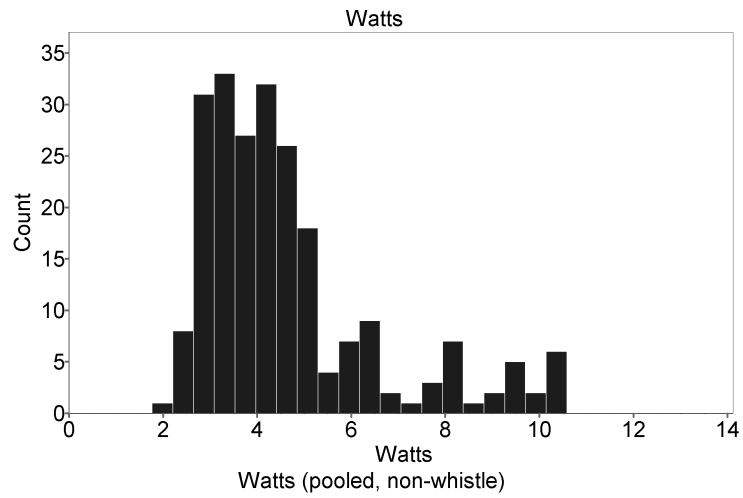


FIG. 121. Histogram of watts in complete pressurization events where no whistle ensounds occur (pooled).

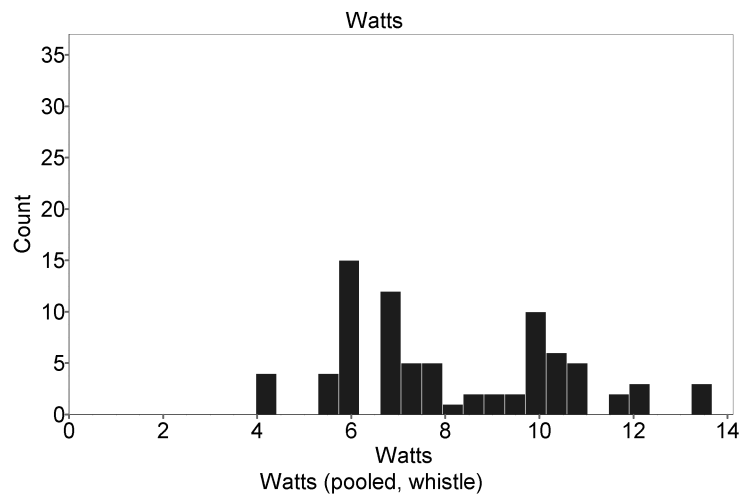


FIG. 122. Histogram of watts in complete pressurization events where whistle ensounds occur (pooled).

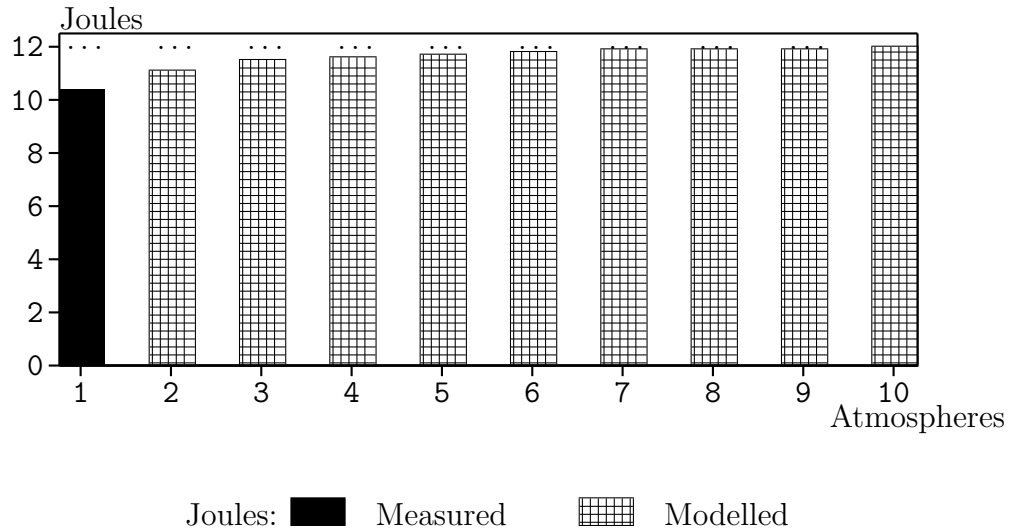


FIG. 123. Effect of depth on work required to achieve the same intranarial pressure difference.

both the figure for click amplitude and the equation for conversion to watts, which incorporates an adjustment for directivity index. A more recent treatment by Au (1993) uses a different constant term that significantly changes the estimate. When the more recent procedure is applied to Sloss's numbers, the maximum power figure drops to 43 watts, which fits better with previous bioenergetic work studies (Cole, 1995) and the present study. Cole's figure of about 150 watts power expenditure during biosonar would handily accommodate this revised power estimate. Given the duty cycle calculated by Sloss, even very low efficiencies of conversion of energy into radiated acoustic power are consistent with the estimates of work found in this study.

2. Time scales

Previous bioenergetic estimates for energy used for biosonar have been derived from dietary energy budgets and analysis of respiratory gases (Cole, 1995). The time scales at which these analyses operate are days or weeks in the case of dietary energy budgets, and a few minutes in the case of analyzing respiratory gases. One advantage

of the approach taken in this study is that the time-scale of analysis is down to a fraction of a second to several seconds.

A daily dietary budget for bottlenose dolphins in the care of man usually may be near 12,000 kilocalories. This gives a value of 50,160 kilojoules per day. The average energy dissipation is thus 580 watts. The average power during pressurization events of about 5 watts is a small fraction of the total energy dissipation. If we assume a 20% efficiency of muscular conversion of physiologic work to mechanical work (Purves and Pilleri, 1983), this would yield about 25 watts due to compressing intranarial gas, which is still a small fraction of the total energy dissipation.

3. Work and depth

The result concerning the relation of mechanical work and depth has implications for our understanding of the ecology and evolution of dolphins. By the analysis performed here, it appears that the mechanical work necessary to achieve a particular intranarial pressure difference increases modestly as depth increases. Resources found at depth thus should not impose a large bioenergetic penalty on the use of biosonar associated with locating or discriminating those resources.

The types and mechanisms of sound production in a likely terrestrial ancestor of odontocete cetaceans may be inferred by identification of features which occur widely in extant mammalian groups and avoiding derived and specialized mechanisms of sound production (Norris, 1968). Laryngeal sound production is such a mechanism, as is the production of some sounds in the nasal passages or lips. Laryngeal sound production is based upon a pneumatic mechanism. The source of pressurized gas for laryngeal sound production in terrestrial mammals is the lungs. In order to compress gas in the lungs, it is necessary to move the diaphragm anteriorly or to contract the pleural space or both. These options require that force is applied over a relatively

large surface area and a relatively long displacement in order to effect a particular change in pressure. These combine to indicate that using such a laryngeal sound source is bioenergetically more costly than what is seen in the use of the monkey lips/dorsal bursae complex.

An additional consideration is that as depth increases, lung volume decreases due to the ambient pressure. Decreased lung volume reduces the range of motion available for compressing the remaining gas. By 50 meters depth, the lung gas volume is about one-fifth of what it was at the surface. The transition to primarily nasal rather than laryngeal sound production was likely a key adaptation allowing odontocete cetaceans to utilize resources at depth.

4. Model-based estimation relies upon assumptions of model

Since at least part of the analysis of the data is based on a model of click sound production, it is apparent that the results depend upon the accuracy of the assumptions of the model and the applicability of the model to the biological system.

The use of a piston-cylinder model is suggested by the observed motion of the palatopharyngeal muscle complex, which moves antero-dorsally during a pressurization event, compressing gas within the intranarial space. The intranarial space is curved, divided by a septum, and its cross-section varies. The variation in cross-sectional area, though, nowhere approaches an order of magnitude difference throughout.

The estimation of mechanical work should be taken as a lower bound on the amount of work needed for production of a pressurization event. The physiological work required to keep the nasal plug in place is ignored, since the nasal plug does not act in the piston-like fashion that is seen for the palatopharyngeal muscle complex. Mechanical work is the result of expenditure of a greater amount of physiological

work. The efficiency of conversion of physiological work into mechanical work in this particular system is unknown. The piston-cylinder model estimates mechanical work required for compression of the gas in the intranarial space, but it does not account for work required in the muscular control of the nasal plugs, monkey lip/dorsal bur-sae complex, the various sacs and sinuses, and neurological energetic demands for perceiving and processing biosonar information. At the time scale of analysis in this study, however, the mechanical work associated with pressurizing the intranarial gas is likely the largest component of the overall bioenergetic cost.

5. Clicks and whistles in context

Lammers and Au (2001) studies of the Hawaiian spinner dolphin (*Stenella lon-girostris*) indicate that the frequency content of whistles may vary in predictable ways with changes in angular separation from the direction of the animal, and that these cues may be important in the social cohesion of groups of dolphins. This role for whistles in maintaining group cohesion could not easily be subsumed by much more directional clicks. The cost of sound production for the purpose of group cohesion, if premised primarily upon whistles, could well exceed that for biosonar use.

One concept that arises from consideration of Lammers and Au (2001) is that the *signature whistle hypothesis* of Caldwell and Caldwell may have more to do with *orientation* in social groups than with *identification* of individuals. If familiarity with the characteristics of often-repeated whistles in the group improves estimation of relative directions to other members of the group, this would provide a simple explanation for favoring the repetition of some particular whistle for each individual.

E. Conclusion

By using a simple piston-cylinder model of click sound production, an estimate of mechanical work needed for individual pressurization events associated with biosonar sound production was made. The average mechanical work for 306 complete pressurization events examined was 10.3 joules. This should be considered a lower bound on energy expenditure in the production of biosonar click trains. By examining a physical model of the pressurization process, the time scale of analysis is reduced to that of some fraction of a second to several seconds in duration. The average value of work obtained indicates that the most obviously energy-intensive part of biosonar use, the production of high intranarial pressures for the pneumatic mechanism of click production, does not place a high metabolic demand on the dolphin. When compared to systematic values obtained for metabolic demands of biosonar use (Cole, 1995), there appears to be considerable work done outside of the process examined here.

Both work and power were found to be higher for those pressurization events associated with whistle ensonds. Whistle ensonds are thus more costly in terms of metabolic budget for dolphins to produce. This finding has implications for the relative roles of click and whistle ensonds in dolphin ecology and social structure and perhaps explains why whistles are not utilized by dolphins for biosonar.

Modelling the effect of depth upon work performed indicates that work should increase modestly as depth increases. The effect is greater at lesser depths. A change from 1 atmosphere of pressure to 10 atmospheres of pressure increases work by about 20%. The pneumatic mechanism of click production utilized as the basis for this analysis indicates that the intranarial pressure difference is the critical value for being able to produce clicks. As depth increases, the distance over which muscles must act to produce a fixed intranarial pressure difference decreases, while the pressure (and

thus force) against which they must act increases. These countervailing physical conditions yield the result of modestly increasing work required with increases in depth.

CHAPTER VI

CONCLUSION

A. Measurement of intranarial pressure and biosonar signals

The measurement of intranarial pressure during a biosonar task links physiologic data to the functional context of biosonar use. The characterization of *pressurization events* in a quantifiable manner permitted statistical confirmation of previous qualitative observations. The average intranarial pressure was significantly higher for those pressurization events during which a whistle vocalization occurs. This confirmed observations made by Ridgway *et al.* (1980); Amundin and Andersen (1983); Ridgway and Carder (1988).

All three subjects displayed a minimal intranarial pressure difference to produce biosonar clicks in the interval of 11.26 to 12.24 kPa. Because of the large number of clicks examined, these values probably closely approach the minimum intranarial pressure difference needed for the production of biosonar clicks.

Higher intranarial pressure implies higher bioenergetic demands, and thus yields the inference that whistle vocalizations are relatively more costly to produce than are click vocalizations. This has implications for the ecology, evolution, and social structure of odontocete species.

B. Biosonar click characteristics

There were several interesting results found from the data examined here. While pneumatic production of clicks and whistles at the *monkey lips/dorsal bursae* complex is supported by several lines of evidence (Cranford *et al.*, 2000), intranarial pressure was essential for click production but was not found to be the primary determinant

of most characteristics of biosonar clicks. In the case of *radiated acoustic power*, a significant regression links it to intranarial pressure, but with a weak coefficient of regression. For frequency domain characteristics, there were cases of significant regression results with trends going in the positive direction in one subject while in another subject a significant trend was noted going in the negative direction. These findings indicate that the interrelationships of intranarial pressure with biosonar click characteristics are complex.

An exploration of three different methods of determining click duration was done. The statistical procedure developed by Wiersma (1982) performed better on the test data than an algorithm based on a description by Au or the alternate method described by Kamminga. While the determination of click duration is crucial to further analysis of both time domain and frequency domain characteristics, there is no general agreement between researchers on which method should be used, and which method was used to determine click duration is rarely reported in the literature.

The classification scheme proposed by Houser *et al.* (1999) was used here for comparison. There were some notable differences in distribution of biosonar clicks in categories between the data analyzed here and those originally examined by Houser *et alia.* These differences appear to be largely due to differences in the selected parameters of signal analysis. This indicates that classification methods are sensitive to choices made in analysis, and that if comparisons are to be made between data sets, the same parameters should be deployed in the analyses undertaken in each case. This also indicates that whenever characteristics of biosonar clicks are reported, the parameters of analysis should also be reported. The relevant parameters include the method of determination of click duration, whether peak-to-peak or RMS amplitude is utilized, and the details of transforming a click time series to the frequency domain. Transformation to the frequency domain via a discrete Fourier transform will require

reporting the window size, whether zero-padding is utilized, whether and which windowing function is applied, and to which points the windowing function is applied.

C. Bioenergetics of individual pressurization events

Combining physiologic data on intranarial pressure with a model of biosonar click production permitted an estimation of mechanical work within individual pressurization events. An average value of 10.3 joules per pressurization event was obtained. Further modelling of the effect of depth on mechanical work required to produce a particular intranarial pressure difference indicates that the amount of work required increases modestly as depth increases. The use of a nasal mechanism for biosonar sound production keeps the bioenergetic cost of biosonar sound production at depth similar to that near the surface. This contrasts with the situation that would obtain for use of the lungs as a pressurized gas reservoir and laryngeal sound production.

The bioenergetics of biosonar sound production in the Atlantic bottlenose dolphin indicate that individual pressurization events are a small fraction of the overall energy budget, at least for clicks of the amplitudes observed in this study. There is no dataset of intranarial pressure correlated with production of very high amplitude clicks. Such a dataset would resolve whether there are non-linearities in the mechanism of biosonar click sound production that would affect the relative costliness of biosonar click production and many other questions.

REFERENCES

- Amundin, M. and Andersen, S. H. (1983). "Bony nares air pressure and nasal plug muscle activity during click production in the harbour porpoise, *Phocoena*, and the bottlenosed dolphin, *Tursiops truncatus*". J. Exp. Biol. **105**, 275–282.
- Au, W. W. L. (1980). "Echolocation signals of the Atlantic bottlenose dolphin (*Tursiops truncatus*) in open waters", in *Animal Sonar Systems*, edited by R. G. Busnel and J. F. Fish (Plenum Press, New York), pp. 251–282.
- Au, W. W. L. (1993). *The Sonar of Dolphins* (Springer-Verlag, New York).
- Au, W. W. L., Floyd, R. W., Penner, R. H., and Murchison, A. E. (1974). "Measurement of echolocation signals of the Atlantic bottlenose dolphin, *Tursiops truncatus* Montagu, in open waters". J. Acoust. Soc. Am. **56**(4), 1280–1290.
- Au, W. W. L., Moore, P. W. B., and Haun, J. E. (1978). "Propagation of Atlantic bottlenose dolphin echolocation signals". J. Acoust. Soc. Am. **64**, 411–422.
- Au, W. W. L., Moore, P. W. B., and Pawloski, D. (1986). "Echolocation transmitting beam of the Atlantic bottlenose dolphin". J. Acoust. Soc. Am. **80**, 688–691.
- Bel'kovich, V. M. and Dubrovskiy, N. A. (1976). *Sensory Bases of Cetacean Orientation (Sensonyye Osnovy Orientatsii Kitoobraznykh)* (Izdatel'stvo Nauka, Leningrad, USSR). Translated to English by the Joint Publications Research Service, Arlington, VA.
- Blackwood, D. J. (1991). "Analysis of motion and EMG during mastication in subcondylar fracture patients". M.S. thesis, University of Texas at Arlington.

- Cole, K. R. (1995). “Energetics in the Atlantic bottlenose dolphin *Tursiops truncatus* Montagu”. Ph.D. thesis, University of Aberdeen, Aberdeen, Scotland.
- Cooley, J. and Tukey, J. (1965). “An algorithm for the machine calculation of complex Fourier series”. *Math. Computation* **19**(90), 297–301.
- Coulombe, H. N., Ridgway, S. H., and Evans, W. E. (1965). “Respiratory water exchange in two species of porpoise”. *Science* **149**, 86–88.
- Cranford, T. and Amundin, M. (2003). “Biosonar pulse production in odontocetes: The state of our knowledge”, in *Advances in the Study of Echolocation in Bats and Dolphins*, edited by J. Thomas, C. Moss, and M. Vater (The University of Chicago Press, Chicago), pp. 27–35.
- Cranford, T., Elsberry, W., Van Bonn, W., Carr, J., Blackwood, D., Carder, D., Kamolnick, T., Todd, M., Decker, E., Bozlinski, D., and Ridgway, S. (2000). “Physiologic evidence for two independent sonar signal generators in the bottlenose dolphin”. *J. Acoust. Soc. Am.* **108**(5(1)), 2613.
- Cranford, T. W. (1992). “Functional morphology of the odontocete forehead: implications for sound generation”. Ph.D. thesis, University of California at Santa Cruz.
- Cranford, T. W. (2000). “In search of impulse sound sources in odontocetes”, in *Hearing by Whales and Dolphins*, edited by W. Au, A. Popper, and R. Fay (Springer-Verlag, New York), pp. 109–156.
- Cranford, T. W., Amundin, M., and Norris, K. S. (1996). “Functional morphology and homology in the odontocete nasal complex: Implications for sound generation”. *J. Morph.* **228**, 223–285.

Cranford, T. W., Van Bonn, W. G., Chaplin, M. S., Carr, J. A., Kamolnick, T. A., Carder, D. A., and Ridgway, S. H. (1997). “Visualizing dolphin sonar signal generation using high-speed video endoscopy”. *J. Acoust. Soc. Am.* **102**(5, Pt. 2), 3123.

Diercks, K., Trochta, R., and Evans, W. (1973). “Delphinid sonar: measurement and analysis”. *J. Acoust. Soc. Am.* **54**(1), 200–204.

Diercks, K., Trochta, R., Greenlaw, C., and Evans, W. (1971). “Recording and analysis of dolphin echolocation signals”. *J. Acoust. Soc. Am.* **49**(6, Pt. 1), 1729–1732.

Dormer, K. (1979). “Mechanism of sound production and air recycling in delphinids: Cineradiographic evidence”. *J. Acoust. Soc. Am.* **65**(1), 229–239.

Elsberry, W., Carder, D., Cranford, T., Carr, J., and Ridgway, S. (1999). “Multi-channel digital acquisition methods applied to simultaneous physiological and acoustic events”, in *13th Biennial Conference on the Biology of Marine Mammals*, (Society for Marine Mammalogy, Wailea, HI), p. 53.

Evans, W. (1973). “Echolocation by marine delphinids and one species of freshwater dolphin”. *J. Acoust. Soc. Am.* **54**(1), 191–199.

Evans, W., Blackwood, D., Norris, J., and Stienessen, S. (1998). “Ecology and biosonar of dolphins”, in *Conference on the Biosonar of Animals* (North Atlantic Treaty Organization, Carvoeiro, Portugal).

Evans, W. and Dreher, J. (1962). “Observations on scouting behavior and associated sound production by the Pacific bottlenosed porpoise (*Tursiops gilli* Dall)”. *Bull. S. Cal. Acad. Sci.* **61**(4), 217–226.

Evans, W. and Maderson, P. (1973). "Mechanisms of sound production in delphinid cetaceans: A review and some anatomical considerations". *Am. Zoologist* **13**, 1205–1213.

Evans, W. and Prescott, J. (1962). "Observations of the sound production capabilities of the bottlenose porpoise: A study of whistles and clicks". *Zoologica* **47**, 121–128.

Evans, W. E. (1980). "Dolphins and their mysterious sixth sense". *Oceanus* **23**(3), 69–75.

Fristrup, K. and Watkins, W. (1992). "Characterizing acoustic features of marine mammal sounds". Technical Report 92-04, Woods Hole Oceanographic Institution, Woods Hole, MA.

Green, R. F., Ridgway, S. H., and Evans, W. E. (1980). "Functional and descriptive anatomy of the bottlenosed dolphin nasolaryngeal system with special reference to the musculature associated with sound production", in *Animal Sonar Systems*, edited by R.-G. Busnel and J. F. Fish (Plenum, New York), pp. 199–238.

Herman, L. M. and Tavolga, W. N. (1980). "The communication systems of cetaceans", in *Cetacean Behavior: Mechanisms & Functions*, edited by L. M. Herman, (John Wiley & Sons, New York), pp. 149–210.

Houser, D. S., Helweg, D. A., and Moore, P. W. (1999). "Classification of dolphin echolocation clicks by energy and frequency distributions". *J. Acoust. Soc. Am.* **106**(3, Pt. 1), 1579–1585.

Kamminga, C. and Beitsma, G. R. (1990). "Investigations on cetacean sonar

IX: remarks on dominant sonar frequencies from *Tursiops truncatus*". Aquatic Mammals **16**(1), 14–20.

Kamminga, C. and Cohen Stuart, A. B. (1995). "Wave shape estimation of delphinid sonar signals, a parametric model approach". Acoust. Letters **19**(4), 70–76.

Kamminga, C., Cohen Stuart, A. B., and de Bruin, M. G. (1998). "A time-frequency entropy measure of uncertainty applied to dolphin echolocation signals". Acoust. Letters **21**(8), 155–160.

Kamminga, C., Cohen Stuart, A. B., and Silber, G. K. (1996). "Investigations on cetacean sonar XI: intrinsic comparison of the wave shapes of some members of the *Phocoenidae* family". Aquatic Mammals **22**(1), 45–55.

Kamminga, C., Engelsma, F. J., and Terry, R. P. (1999). "An adult-like sonar wave shape from a rehabilitated orphaned harbour porpoise (*Phocoena phocoena*)". Ophelia **50**(1), 35–42.

Kamminga, C., van Howe, M. T., Engelsma, F. J., and Terry, R. P. (1993). "Investigations on cetacean sonar X: a comparative analysis of underwater echolocation clicks of *Inia* spp. and *Sotalia* spp.". Aquatic Mammals **19**(1), 31–43.

Kellogg, W. N. (1961). *Porpoises and Sonar* (University of Chicago Press, Chicago).

Lammers, M. O. and Au, W. W. L. (2001). "Directionality and the occurrence of social acoustic signals in traveling pods of Hawaiian spinner dolphins (*Stenella longirostris*)", in *14th Biennial Conference on the Biology of Marine Mammals*, (Society for Marine Mammalogy, Vancouver, BC), pp. 121–122.

- Lawrence, B. and Schevill, W. E. (1956). "The Functional Anatomy of the Delphinid Nose". *Bull. Mus. Comp. Zool.* **114**(4), 103–151.
- Lilly, J. C. (1978). *Communication Between Man and Dolphin* (Crown Publishers, Inc., New York).
- Lyons, R. G. (1997). *Understanding Digital Signal Processing* (Addison-Wesley, Reading, MA).
- Miller, Jr., F. (1977). *College Physics*. Fourth edition (Harcourt Brace Jovanovich, New York).
- Moore, P. W. B. and Pawloski, D. A. (1990). "Investigations on the control of echolocation pulses in the dolphin (*Tursiops truncatus*)", in *Sensory Abilities of Cetaceans: Laboratory and Field Evidence*, edited by J. A. Thomas and R. A. Kastlein (Plenum Press, New York), pp. 305–316.
- Nichols, R. H., Diercks, K. J., Trochta, R. T., Greenlaw, C. F., and Evans, W. E. (1971). "Recording and analysis of dolphin echolocation signals". *J. Acoust. Soc. Am.* **49**(6 Pt. 1), 1729–1732.
- Norris, K. S. (1964). "Some problems of echolocation in cetaceans", in *Marine Bio-Acoustics*, edited by W. N. Tavolga (Pergamon Press, New York), pp. 317–336.
- Norris, K. S. (1968). "The evolution of acoustic mechanisms in odontocete cetaceans", in *Evolution and Environment*, edited by E. Drake (Yale University Press, New Haven), pp. 298–323.
- Norris, K. S. (1969). "The echolocation of marine mammals", in *The Biology of Marine Mammals*, edited by H. T. Andersen (Academic Press, New York), pp.

391–423.

Norris, K. S. (1975). “Cetacean biosonar: Part 1 - Anatomical and behavioral studies”, in *Biochemical and biophysical perspectives in marine biology*, edited by D. C. Malins and J. R. Sargent (Academic Press, New York), pp. 215–234.

Norris, K. S. and Dohl, T. P. (1980). “The structure and function of cetacean schools”, in *Cetacean Behavior: Mechanisms & Functions*, edited by L. M. Herman, (John Wiley & Sons, New York), pp. 211–262.

Norris, K. S., Dormer, K. J., Pegg, J., and Liese, G. J. (1971). “The mechanism of sound production and air recycling in porpoises: a preliminary report”, in *Proceedings of the Annual Conference on Biological Sonar (Fremont, CA)*, volume 8, pp. 1–11.

Norris, K. S. and Harvey, G. W. (1972). “A theory for the function of the spermaceti organ of the sperm whale (*Physeter catodon* L.)”, in *Animal Orientation and Navigation*, edited by S. R. Galler, K. Schmidt-Koenig, G. J. Jacobs, and R. E. Belleville (NASA Scientific and Technical Office, Washington, D.C.), pp. 397–417.

Norris, K. S., Prescott, J. H., Asa-Dorian, P. V., and Perkins, P. (1961). “An experimental demonstration of echolocation behavior in the porpoise, *Tursiops truncatus* (Montagu)”. *Biol. Bull.* **120**(2), 163–176.

Poché, L. B., Luker, L. D., and Rogers, P. H. (1982). “Some observation of echolocation clicks from free-swimming dolphins in a tank”. *J. Acoust. Soc. Am.* **71**(4), 1036–1038.

Purves, P. (1966). “Anatomical and experimental observations on the cetacean

sonar system”, in *Animal Sonar Systems: Biology and Bionics*, edited by R.-G. Busnel (NATO Advanced Study Institute, Plenum Press, New York), volume 1, pp. 197–270.

Purves, P. E. and Pilleri, G. E. (1983). *Echolocation in Whales and Dolphins* (Academic Press Inc., London).

Reiss, D. (1988). “Observations on the development of echolocation in young bottlenose dolphins”, in *Animal Sonar Processes and Performance*, edited by P. E. Nachtigall and P. W. B. Moore (Plenum Press, New York), pp. 121–127.

Richardson, W. J., Greene, Jr., C. R., Malme, C. I., and Thomson, D. H. (1995). *Marine Mammals and Noise* (Academic Press, San Diego).

Ridgway, S. H. (1983). “Dolphin hearing and sound production in health and illness”, in *Hearing and Other Senses: Presentations in Honor of E. G. Wever*, edited by R. R. Fay and G. Gourevitch, (The Amphora Press, Groton, CT), pp. 247–296.

Ridgway, S. H. and Carder, D. A. (1988). “Nasal pressure and sound production in an echolocating white whale, *Delphinapterus leucas*”, in *Animal Sonar*, edited by P. E. Nachtigall and P. W. B. Moore (Plenum, New York), pp. 53–60.

Ridgway, S. H. and Carder, D. A. (1997). “Hearing deficits measured in some *Tursiops truncatus*, and discovery of a deaf/mute dolphin”. *J. Acoust. Soc. Am.* **101**, 590–594.

Ridgway, S. H., Carder, D. A., Green, R. F., Gaunt, A. S., Gaunt, S. L., and Evans, W. E. (1980). “Electromyographic and pressure events in the nasolaryngeal system of dolphins during sound production”, in *Animal Sonar Systems*,

- edited by R. G. Busnel and J. F. Fish (Plenum, New York), pp. 239–249.
- Ridgway, S. H. and Howard, R. (1979). “Dolphin lung collapse and intramuscular circulation during free diving: Evidence from nitrogen washout”. *Science* **206**, 1182–1183.
- Scammon, C. M. (1968). *The Marine Mammals of the North-western Coast of North America* (Dover Publications, Inc., New York).
- Slijper, E. J. (1979). *Whales*. Second edition (Cornell University Press, Ithaca, NY).
- Sloss, A. (1984). “The physics of high intensity sound production in delphinids”. B.S. thesis, University of California at Santa Cruz.
- Wiersma, H. (1982). “Investigations on cetacean sonar IV: a comparison of wave shapes of odontocete sonar signals”. *Aquatic Mammals* **9**(2), 57–66.
- Wood, F. G. (1973). *Marine Mammals and Man* (Robert B. Luce, Washington, D.C.).
- Wood, F. G. and Evans, W. E. (1980). “Adaptiveness and ecology of echolocation in toothed whales”, in *Animal Sonar Systems*, edited by R.-G. Busnel and J. F. Fish (Plenum Press, New York), pp. 381–426.
- Zar, J. H. (1984). *Biostatistical Analysis*. Second edition (Prentice Hall, Englewood Cliffs, NJ).

VITA

Wesley Royce Elsberry, 2911 Lawrence, Irving, TX 75065

Wesley Royce Elsberry is a biologist with an eclectic educational and work background. Wesley is a graduate of the University of Florida where he earned a B.S. in zoology in 1982, the University of Texas at Arlington where he earned an M.S.C.S. (computer science) in 1989, and a Ph.D. in Wildlife and Fisheries Sciences at Texas A&M University in 2003. He has taught as adjunct faculty at Washington State University Tri-Cities. His work experience includes anesthesiology research, veterinary research, software design and production for military aircraft and logistics, and programming, electronics design, and data analysis in behavioral research. During his graduate studies at Texas A&M, he produced the first versions of web sites for the Department of Wildlife and Fisheries Sciences, the Department of Marine Biology, and the Texas Marine Mammal Stranding Network. His most recent area of research is dolphin biosonar sound production and bioenergetics. He is a co-author on peer-reviewed papers in the "Journal of Experimental Biology" and in "Biology and Philosophy". He has given invited talks for the "Center for Theology and Natural Sciences" (2001), the "Committee for Scientific Investigation of Claims of the Paranormal" (2002), and the "San Diego Association for Rational Inquiry" (2003). He received the Society for Marine Mammalogy's "Fairfield Memorial Award for Innovation in Marine Mammal Research" in 2001.